REPUBLIC OF TÜRKİYE
ERCİYES UNIVERSITY
GRADUATE SCHOOL OF NATURAL AND APPLIED SCIENCES
DEPARTMENT OF AGRICULTURAL SCIENCE AND TECHNOLOGY

ALTERNATIVE METHODS TO CONTROL *Fusarium* spp. AND MYCOTOXINS PRODUCED IN STORED GRAINS IN IRAQ

Prepared by
HUSSEIN ALI SALMAN AL-SAHHO

Supervisor
Assoc. Prof. Dr. Sümer HORUZ
Second Supervisor
Assoc. Prof. Dr. Kevser KARAMAN

Phd. Thesis

March 2026
KAYSERİ

REPUBLIC OF TÜRKİYE
ERCİYES UNIVERSITY
GRADUATE SCHOOL OF NATURAL AND APPLIED SCIENCES
DEPARTMENT OF AGRICULTURAL SCIENCE AND TECHNOLOGIES

ALTERNATIVE METHODS TO CONTROL *Fusarium* spp. AND MYCOTOXINS PRODUCED IN STORED GRAINS IN IRAQ

(PhdThesis)

Prepared by
HUSSEIN ALI SALMAN AL-SAHHO

Supervisor
Assoc. Prof. Dr. Sümer HORUZ
Second Supervisor
Assoc. Prof. Dr. Kevser KARAMAN

March 2026
KAYSERİ

COMPLIANCE WITH SCIENTIFIC ETHICS

I hereby declare that all the information presented in this study has been obtained in accordance with academic and ethical principles. I also affirm that, as these principles require, all materials and results that do not originally belong to this study have been fully and accurately cited and referenced.

Hussein Ali Salman AL-SAHHO

"Alternative Methods to Control *Fusarium* spp. and Mycotoxins Produced in Stored Grains in Iraq" titled Ph.D. Thesis has been prepared in accordance with the Erciyes University Graduate School Thesis Proposal and Thesis Writing Guidelines.

Prepared by
Hussein Ali Salman AL-SAHHO
Signature

Supervisor
Assoc. Prof. Dr. Sümer HORUZ
Signature

Second Supervisor
Assoc. Prof. Dr. Kevser KARAMAN
Signature

Head of the Department

Prof. Dr. Mehmet ARSLAN
Signature

ACKNOWLEDGEMENTS

Praise and thanks be to God, and my success is only through God. I would like to extend my sincere thanks and appreciation to Assoc. Prof. Dr. Sümer HORUZ and Assoc. Prof. Dr. Kevser KARAMAN I am honored to be one of their students, as they provided me with great help, guidance and support throughout my studies, and completely edited and improved the writing of the manuscript. I would like to express my sincere gratitude to the members of the Department of Agricultural Sciences and Technology, College of Agriculture, and Erciyes University with all its departments and professors. I would like to extend my sincere thanks to the Turkish government and people for everything they have provided us to complete our studies with ease. I would also like to extend my sincere thanks to professor Halima HUSSEIN and my colleagues in Iraq at the Agriculture College. University of Baghdad, Ministry of Agriculture, Plant Protection Department, Ministry of Science and Technology, University of Fallujah and Al-Basrah University. I would also like to thank all my friends in the Quality Control Department and Dr. Saif KHATTAWI, I appreciate everyone who supported me and stood by me throughout my studies. I dedicate this effort and success to the souls of my mother, father, and brother Saad AL-SAHOO. I thank all my family members, my brothers and sisters, for their support and assistance. My thanks to my wife, my study and travel companion, and everyone who was the reason for me obtaining this degree and who has always been by my side. My love and appreciation to everyone I have mentioned.

Hussein Ali Salman AL-SAHHO

2026, KAYSERİ

ALTERNATIVE METHODS TO CONTROL *Fusarium* spp. AND MYCOTOXINS PRODUCED IN STORED GRAINS IN IRAQ

Hussein Ali Salman AL-SAHHO

Erciyes University, Graduate School of Natural and Applied Sciences
Ph. D. Thesis, March 2026
Supervisor: Assoc. Prof. Dr. Sümer HORUZ
Second Supervisor: Assoc. Prof. Dr. Kevser KARAMAN

ABSTRACT

Fusarium spp. are one of the most important fungi that attack plants and cause significant crop losses, especially in wheat. This study was conducted to detect *Fusarium* spp. in wheat samples collected from Iraqi silos and to find natural alternatives to chemical fungicides in inhibiting toxin production. We tested the efficacy of *Dodonaea viscosa* plant extract (DVE) at concentrations of 0.5%, 1.0%, and 1.5%, nanoparticles (chitosan nanoparticles loaded with DVE) at a concentration of 0.75, ozone gas at a flow rate of 2.4 L/min for 30-60 minutes, and sea salt (regular or nano) at four concentrations (1, 2, 2.5, and 3%) to inhibit the growth of *Fusarium* spp. strains and the production of deoxynivalenol (DON) and moniliformin (MON) toxins. After the strains were phenotypically identified, seven strains were then characterized belonging to three *Fusarium* species: *F. oxysporum, F. pseudograminearum,* and *F. chlamydosporum*. The above-mentioned treatments were statistically significant and showed a clear effect in reducing the growth of all *Fusarium* spp. strains. The results indicated that the greatest inhibitory effect was achieved by nano-salt, chitosan nanoparticles loaded with DVE, DVE and ozone treatments, respectively. Nano-sea salt contributed to the inhibition of mycotoxin production. The highest inhibition rate for DON toxin in nano-sea salt was recorded in *F. pseudograminearum* strain 3 at a rate of 83.38%, while the highest inhibition rate for MON toxin production was 87.69% in *F. chlamydosporum* strain 8.

Key words: *Dodonaea viscosa*, *Fusarium* spp., DON, MON, Ozone, Sea Salt

IRAK'TA DEPOLANAN BUĞDAYDA GÖRÜLEN *Fusarium* TÜRLERİNİN VE ÜRETTİKLERİ MİKOTOKSİNLERİN KONTROLÜNE YÖNELİK ALTERNATİF YÖNTEMLER

Hussein Ali Salman AL-SAHHO

Erciyes Üniversitesi, Fen Bilimleri Enstitüsü
Doktora Tezi, Mart 2026
Danışman: Doç. Dr. Sümer HORUZ
İkinci Danışman Doç. Dr. Kevser KARAMAN

ÖZET

Fusarium spp., bitkilere önemli zararlar veren ve özellikle buğdayda önemli ürün kayıplarına yol açan en önemli fungus cinslerinden biridir. Bu çalışma, kimyasal fungisitlere doğal alternatifler bulmak amacıyla yapılmıştır. Bu çalışmada, *Fusarium* spp. suşlarının büyümesini ve deoxynivalenol (DON) ve moniliformin (MON) toksinlerinin üretimini engellemek için *Dodonaea viscosa* etanol ekstraktı (DVE) %0.5, %1.0 ve %1.5 konsantrasyonlarında, nanopartiküller (DVE yüklü kitosan nanopartikülleri) %0.75 konsantrasyonunda, 30 ve 60 dakika boyunca 2.4 L/dakika akış hızında ozon gazı ve dört farklı konsantrasyonda (1, 2, 2.5 ve 3%) deniz tuzunun (normal veya nano) etkinliği test edilmiştir. İzolatlar fenotipik olarak tanılandıktan sonra, polimeraz zincir reaksiyonu (PCR) teknolojisi kullanılarak yedi izolat üç *Fusarium* türüne ait *F. oxysporum, F. pseudograminearum ve F. chlamydosporum* olarak karakterize edilmiştir. Yukarıda anılan işlemler *Fusarium* spp. izolatlarına uygulanmış ve işlemler istatistiksel olarak anlamlı bulunarak tüm *Fusarium* spp. izolatlarının büyüme hızlarını azaltmada belirgin bir etki göstermiştir. Sonuçlara bakıldığında, en büyük etki sırasıyla nano tuz, DVE yüklü kitosan nanopartikülleri, etanol ekstraktı ve ozon gazı ile elde edilmiştir. Deniz tuzu, nano ölçekte işlendiğinde, mikotoksin üretiminin inhibisyonuna katkıda bulunmuştur. DON toksini için en yüksek inhibisyon oranı %83.38 ile *F. pseudograminearum* 3'te, MON toksini üretimi için en yüksek inhibisyon oranı %87.69 ile *F. chlamydosporum* 8'de kaydedilmiştir.

Anahtar Kelimeler: *Dodonaea viscosa*, *Fusarium* spp., DON, MON, Ozon, Deniz Tuzu

TABLE OF CONTENTS

ALTERNATIVE METHODS TO CONTROL *Fusarium* spp. AND MYCOTOXINS PRODUCED IN STORED GRAINS IN IRAQ

COMPLIANCE WITH SCIENTIFIC ETHICS ii
COMPLIANCE WITH THE GUIDELINES iii
ACCEPTANCE AND APPROVAL iv
ACKNOWLEDGEMENTS v
ABSTRACT vi
ÖZET vii
TABLE OF CONTENTS viii
ABBREVIATIONS xii
LIST OF TABLES xiii
LIST OF FIGURES xv
INTRODUCTION 1

CHAPTER 1

GENERAL INFORMATION AND LITERATURE STUDY

1.1. Problem Statement 4
1.2. Purpose of the Research 4
1.3. Significance of the Research 4
1.4. Literature Review 5
1.4.1. Wheat (*Triticum aestivum*) 5
1.4.2. Fungi Associated with Wheat 6
1.5. *Fusarium* 6
1.5.1. Factors Affecting the Growth of *Fusarium* spp. 8
1.5.2. Major Diseases Caused by *Fusarium* spp. 8
1.6. Mycotoxin 10
1.6.1. Factors Affecting Mycotoxin Production 11
1.6.2. Major Mycotoxins 12
1.6.2.1. Fumonisins 12
1.6.2.2. Deoxynivalenol (DON) 13
1.6.2.3. Moniliformin MON 14

1.7. Methods of Controlling and Reducing Fungi and Their Mycotoxins 15
1.7.1. Physical Control 16
1.7.1.1. Ozone application 16
1.7.2. Biological Control 18
1.7.3. Chemical Control 19
1.7.3.1. Effect of sea salt on fungi 20
1.7.4. Plant Extracts 21
1.7.4.1. Dodonaea viscosa plant 23
1.7.5. Nanotechnology 24
1.7.5.1. Chitosan and nanotechnology 25

CHAPTER 2

MATERIAL AND METHODS

2.1. Material 28
2.1.1. Equipment and Tools Used in the Study 28
2.2. Methods 29
2.2.1. Wheat Sampling and Isolation of *Fusarium* spp. Strains from Seeds 29
2.2.2. Morphological identification of the *Fusarium* spp. strains 30
2.2.3. Molecular identification of *Fusarium* spp. strains 30
2.2.4. Sequencing and data analysis 31
2.2.5 Pathogenicity test of *Fusarium* spp. strains 31
2.2.6. Preparation of ethanolic Extract for *Dodonaea viscosa* (DVE) 32
2.2.7. Identification of the Major Components of DVE Using GC-MS System 32
2.2.8. Biosynthesis of Chitosan Nanoparticles Loaded DVE 33
2.2.9. Measurement and Characterization of Nanoparticles 33
2.2.9.1. UV-Visible spectroscopy 33
2.2.9.2. Fourier-Transform infrared spectroscopy (FT-IR) 33
2.2.9.3. Atomic Force Microscopy (AFM) 34
2.2.9.4. Field-Emission Scanning Electron Microscopy (FE-SEM) 34
2.2.9.5. X-ray Diffraction (XRD) 34
2.2.9.6. Energy-dispersive X-ray spectroscopy 34
2.2.10. *In Vitro* Efficacy of DVE and Chitosan NPs Loaded with DVE in Inhibiting the Growth of *Fusarium* spp. 35
2.2.11. Ozone Gas Application and Its Effects on *Fusarium* spp. Strains on PDA 36

2.2.12. Efficiency of Sea Salt and Nano Sea Salt in inhibiting *Fusarium* spp. strains 36
2.2.13. Testing the DON and MON Mycotoxins production from *Fusarium* spp. strains after treatments 37
2.2.14. Statistical Analysis 38

CHAPTER 3

RESULTS

3.1. Wheat Sampling 39
3.1.1. Wheat Sampling for *Fusarium* spp. Strains 39
3.1.2. Morphological identificatication of *Fusarium* spp. strains 40
3.1.3. Molecular identificatication of *Fusarium* spp. strains 41
3.1.3. Pathogenicity test of *Fusarium* spp. Strains 43
3.1.4. Testing the Effect of DVE on the Growth of *Fusarium* spp. Strains 44
3.1.5. Identification of the components of DVE by using a GC-MS system 45
3.1.7. Conformational and morphological analysis of chitosan NPs loaded with DVE 47
3.1.7.1. UV-Visible Spectroscopy 47
3.1.7.2. Fourier transform infrared spectroscopy (FT-IR) 48
3.1.7.3. Atomic Force Spectroscopy (AFM) 51
3.1.7.4. Field Emission Scanning Electron Microscopy (FESEM) 52
3.1.7.5. Energy-dispersive X-ray spectroscopy (EDX) 53
3.1.7.6. X-ray Diffraction (XRD) 54
3.1.8. Effect of chitosan NPs loaded with DVE on *Fusarium* spp. strains 55
3.1.9. Effect of DVE and Chitosan NPs Loaded with DVE on the Production of DON and MON Mycotoxins 56
3.1.10. Evaluation of the effect of ozone gas on the growth of *Fusarium* spp. strains 59
3.1.11. The Effect of Ozone Gas on Mycotoxins Production 61
3.1.12. The Efficiency of normal and nano sea salt on inhibiting *Fusarium* spp. Strains 63
3.1.13. The Effect of Nano Sea Salt on the Production of Mycotoxins 67
3.1.14. Evaluation of the Best Four Treatments Applied to *Fusarium* spp. Strains ... 68

CHAPTER 4
DISCUSSION, CONCLUSION, FUTURE STUDIES

4.1. Discussion **71**
4.1.1. Identification of *Fusarium* spp. strains isolated from local wheat samples 71
4.1.2. The Pathogenicity Test of *Fusarium* spp. strains 72
4.1.3. Effect of DVE on the growth of *Fusarium* spp. strains 72
4.1.4. Effect of DVE-loaded chitosan NPs on *Fusarium* spp. strains 74
4.1.4.1. UV-Vis spectroscopy 75
4.1.4.2. Fourier transform infrared spectroscopy (FTIR) 75
4.1.4.3. Atomic Force Microscopy 76
4.1.4.4. Field-emission scanning electron microscope (FESEM) 76
4.1.4.5. Energy-dispersive X-ray spectroscopy (EDX) 77
4.1.4.6. X-ray diffraction (XRD) 78
4.1.5. Effect of The Treatments on the Growth and Mycotoxin Production of *Fusarium* spp. Strains 79
4.1.5.1. Effect of ethanolic DVE and DVE-loaded Chitosan NPs on Production of Mycotoxin by Fusarium spp. 80
4.1.5.2. Effect of Ozone Gas on the Growth of Fusarium spp. Strains and Its Mycotoxins Production 82
4.1.5.3. Effect of The Sea Salt on The Normal and Nano-Particle Scale on Fusarium spp. Strains and Their Mycotoxins Production 84
4.2. Conclusions **86**
4.3. Future Studies **87**
REFERENCES **89**
APPENDICES **112**
CURRICULUM VITAE **122**

ABBREVIATIONS

°C	: Centigrade degree
µL	: Microliter
AFM	: Atomic Force Microscopy
bp	: Base pair
DNA	: Deoxyribonucleic Acid
DON	: Deoxynivalenol
DVE	: *Dodonaea viscosa* extract
FAO	: Food and Agriculture Organization
FE-SEM	: Field-Emission Scanning Electron Microscopy
FTIR	: Fourier-Transform Infrared Spectroscopy
GC-MS	: Gas Chromatography-Mass Spectrometry
HPLC	: High-performance liquid chromatography
mL	: Milliliter
mm	: Millimeter
MON	: Moniliformin
NIV	: Nivalenol
nm	: Nanometer
NPs	: Nanoparticles
PCR	: Polymerase Chain Reaction
ZEN	: Zearalenone

LIST OF TABLES

Table 1. Instruments and equipment used in the study 28

Table 2. Analysis conditions of energy-dispersive X-ray spectroscopy 35

Table 3. Wheat sampling from different Governorates of Iraq 39

Table 4. *Fusarium* spp. strains gen bank accession numbers 41

Table 5. Pathogenicity test for *Fusarium* strains shows the effect of the fungus on seed germination on PDA in *vitro* 43

Table 6. Mean inhibition percentage (%) of *Fusarium* spp. strains treated with different concentrations of *D. viscosa* extract (DVE) 45

Table 7. Identified components of ethanolic leaf extract of *D. viscosa* using GC-MS system 47

Table 8. Results the FTIR analysis of DVE, chitosan NPs loaded with DVE 50

Table 9. Inhibition percentage (%) of *Fusarium* spp. strains treated with the chitosan NPs loaded with DVE 56

Table 10. Deoxynivalenol (µg/L) concentrations of *Fusarium* spp. strains after treatment with the DVE and chitosan NPs loaded with DVE and inhibition ratios 58

Table 11. Moniliformin (µg/L) concentrations of *Fusarium* spp. strains after treatment with the DVE and chitosan NPs loaded with DVE and inhibition ratios 59

Table 12. The effect of ozone gas on the growth of *Fusarium* spp. strains on PDA at different concentrations and different exposure periods 60

Table 13. The inhibition ratio (%) values of ozone gas on the growth of *Fusarium* spp. strains at different concentrations and different exposure periods 61

Table 14. Deoxynivalenol (DON) concentrations (µg/L) and inhibition ratio (%) of *Fusarium* spp. strains before and after ozone treatment 62

Table 15. Moniliformin (MON) concentrations (µg/L) and inhibition ratio (%) of *Fusarium* spp. strains before and after ozone treatment 62

Table 16. The effect of normal and nano sea salt at different concentrations on the growth of seven *Fusarium* spp. strains 66

Table 17. Deoxynivalenol (DON) concentrations (µg/L) and inhibition ratio (%) of *Fusarium* spp. strains before and after nano sea salt treatment NS: Non-Significant. 67
Table 18. Moniliformin (MON) concentrations (µg/L) and inhibition ratio (%) of *Fusarium* spp. strains before and after nano sea salt treatment 67
Table 19. Difference in inhibition values (%) of DON production between four different treatments estimated by HPLC 68
Table 20. Difference in percentage of inhibition of MON production between four treatments estimated by HPLC 69

LIST OF FIGURES

Figure 1. Chitosan nanoparticles and their applications in various fields.....26
Figure 2. Iraq Administrative map 30
Figure 3. A) D. viscosa tree and leaves, B) Grinding the leaves into powder, C: Extraction of ethanolic extract for D. viscosa (DVE) process.....32
Figure 4. The ozone gas treatment of Fusarium spp. strains.....36
Figure 5. Morphological characteristics of three Fusarium spp. on PDA. a: Fusarium oxysporum strain 4, b: Fusarium pseudograminearum strain 7 and c: Fusarium chlamydosporum strain 8 40
Figure 6. The microscopic examination of Fusarium strains distinguished by their morphological characteristics; A) Fusarium oxysporum growing on a PDA, B) macroconidia of Fusarium, C) Conidiophores of Fusarium oxysporum, and D) Spore-forming stimuli in Fusarium species 40
Figure 7. A phylogenetic tree was constructed for three isolates belonging to three Fusarium spp. strains from wheat stored in Iraq. a) F. oxysporum (PQ721292.1 Iraq), b) F. pseudograminearum (PQ721291.1 Iraq), c) F. chlamydosporum (PQ721294.1 Iraq) 42
Figure 8. Pathogenicity test for Fusarium spp. strains on PDA; F. pseudograminearum strain 2, F. pseudograminearum strain 3, F. oxysporum strain 4, F. oxysporum strain 5, F. pseudograminearum strain 6, F. pseudograminearum strain 7 and F. chlamydosporum strain 8. The plates numbered in yellow at the bottom represent the control group, and the others are the replicates.....43
Figure 9. The effect of the ethanolic extract of D. viscosa leaves (DVE) in inhibiting the growth of Fusarium spp. strains, (a): F. pseudograminearum strain 2, (b): F. pseudograminearum strain 3, (c): F. oxysporum strain 4, (d): F. oxysporum strain 5, (e): F. pseudograminearum strain 6, (f): F. pseudograminearum strain 7, and (g): F. chlamydosporum strain 8 44
Figure 10. Gas chromatography-mass spectrometry (GC-MS) chromatogram of the ethanolic D. viscosa extract 46

Figure 11. UV–Visible spectrophotometer test: a) DVE, b) Chitosan NPs loaded with DVE 48
Figure 12. FTIR spectra, A) DVE, B) chitosan NPs loaded with DVE 49
Figure 13. AFM surface morphology and particle size distribution of chitosan NPs loaded with DVE 52
Figure 14. SEM micrographs of chitosan NPs loaded with DVE: (A) primary nanoparticles (100,000×), B) secondary agglomerates after drying (50,000×), and C) irregular surface morphology with apparent porosity (30,000×)..... 53
Figure 15. EDX analysis of chitosan NPs loaded with DVE 54
Figure 16. XRD spectrums of chitosan NPs loaded with DVE 55
Figure 17. The efficiency of the DVE loaded chitosan NPs on Fusarium spp. strains on PDA, (A) control group for seven strains (B) strains growth after DVE-loaded chitosan NPs. (Fusarium pseudograminearum strain 2, Fusarium pseudograminearum strain 3, Fusarium oxysporum strain 4, Fusarium oxysporum strain 5, Fusarium pseudograminearum strain 6, Fusarium pseudograminearum strain 7 and Fusarium chlamydosporum strain 8) 56
Figure 18. Deoxynivalenol and Moniliformin standard chromatogram by HPLC analysis, a) DON standard, b) MON standard 57
Figure 19. Ozone gas treatment on Fusarium spp. strains (4 liters/minute for 60 minutes) on seven Fusarium spp. strains (F. pseudograminearum strain 2, F. pseudograminearum strain 3, F. oxysporum strain 4, F. oxysporum strain 5, F. pseudograminearum strain 6, F. pseudograminearum strain 7, F. chlamydosporum strain 8) 60
Figure 20. Effect of four concentrations (1, 2, 2.5 and 3 %) of normal sea salt on seven Fusarium spp. strains on PDA in vitro, the plates numbered in red color at the bottom of the figure represent the control group. The plates in the rows above represent the application of sea salt at four different concentrations, as recorded on plates (1, 2, 2.5 and 3 %) on Fusarium strains: (Fusarium pseudograminearum strain 2, Fusarium pseudograminearum strain 3, Fusarium oxysporum strain 4, Fusarium oxysporum strain 5, Fusarium pseudograminearum strain 6, Fusarium pseudograminearum strain 7 and Fusarium chlamydosporum strain 8) 63

Figure 21. AFM surface morphology and particle size distribution of nano sea salt . 64
Figure 22. Effect of four concentrations (1, 2, 2.5 and 3 %) of nano sea salt on seven Fusarium spp. strains on PDA in vitro, the plates numbered in red color at the top row of the figure represent the control group. The plates in the rows under represent the application of nano sea salt at four different concentrations, as recorded on plates (1, 2, 2.5 and 3 %) on Fusarium strains: Fusarium pseudograminearum strain 2, Fusarium pseudograminearum strain 3, Fusarium oxysporum strain 4, Fusarium oxysporum strain 5, Fusarium pseudograminearum strain 6, Fusarium pseudograminearum strain 7 and Fusarium chlamydosporum strain 8 65
Figure 23. Comparison of inhibition rates of DON toxin production after the four treatments 69
Figure 24. Comparison of inhibition rates of MON toxin production after the four treatments 70

INTRODUCTION

The ancient world and its civilizations recognized wheat as an essential part of human food. Mesopotamia, the Nile Valley, Anatolia, and Greece were the primary homes for its cultivation. It belongs to the genus *Triticum* spp. in the *Poaceae* (grass) family (Ahmed, 2005). Wheat cultivation has spread to wide areas of the world, including tropical, subtropical, and even high-altitude regions (Shewry, 2009). Wheat flour is an important source of carbohydrates, protein, fats, and minerals. (Iqbal et al., 2022). The world is heading towards greater wheat production due to population growth and increased consumption of flour as a staple on the table. Hard wheat produces bread, while pastries are made from soft wheat. In addition, flour, one of the products of the milling process, is a secondary product that contains a high percentage of vitamins and fiber (Ahmed, 2005). It requires preserving grains and preventing their damage, the presence of regular warehouses with high efficiency in grain storage, and grain types and sizes that vary according to need. In storing wheat, ideal conditions are required to prevent insect and microorganism infestations, such as fungi and bacteria, and to ensure grain preservation for an extended period. Several processes must be carried out before storage, such as removing all impurities, stones, minerals, and plant materials other than wheat. This process is essential for achieving high-quality yields, reducing pollution, and lowering drying and equipment maintenance costs (Inamdar and Suresh, 2014).

Chemical pesticides have caused severe damage to workers, grains and the environment, despite their limited effectiveness. Therefore, it was necessary to search for alternative materials that are safer for the environment, workers and crops and that do not leave any residues (Khader et al., 2001).

Fungal diseases are important causes of wheat crop damage, and their transmission may occur through soil or seeds. Many plant diseases can infect wheat and cause damage during growth, including rot, seed diseases, and seedling drop (Ishtiaq et al., 2019). Fungi

are no less dangerous than other pests on grains, in addition to the fact that this effect may be transmitted to humans and animals through the secretion of mycotoxins. Studies and research have proven that there are more than 400 types of mycotoxins that are dangerous to human health and sometimes lead to cancer (Oadi, 2020). Numerous studies support the presence of *Fusarium* spp. in wheat in the field, but research supporting the study of stored grains and their infection with *Fusarium* spp. are limited (Chehri et al., 2010). *Fusarium* spp. are crucial fungi that can infect grains before and during harvest, and the infection is then transmitted to storage and causes grain damage (Lacey et al., 1999). The most important of these toxins that pose a risk to humans and animals are: aflatoxins (AFs), ochratoxins (OTs), trichothecenes, zearalenone (ZEN), and ergot alkaloids, in addition to deoxynivalenol, nivalenol (NIV), and HT-2 toxins (HT-2), deoxynivalenol, nivalenol and fumonisin B1 (Eskola et al., 2001; Ji et al., 2019).

Deoxynivalenol (DON) is a mycotoxin, a type of trichothecene, and is known as a vomiting toxin. It is one of the toxins secreted by *F. pseudograminearum* (Cui et al., 2022). Moniliformin (MON) is also a mycotoxin produced by *Fusarium* spp., and there are approximately 40 species fungi that can produce this toxin (Ivić et al., 2009; Radić et al., 2019). In addition to *Fusarium* spp., *Penicillium* spp., and *Aspergillus* spp., some fungi infect cereals. *Penicillium* spp. causes damage to cereals and often infects cereals in temperate regions. They are storage fungi and produce mycotoxins (Eskola et al., 2001; Ji et al., 2019).

The use of extracts and natural materials as alternatives to chemical pesticides is a goal of many researchers seeking to avoid the problems these pesticides can cause. They have found that these materials can be suitable alternatives because they are harmless, naturally decompose, and are environmentally friendly (Kim et al., 2005). Many plants have been used to produce plant extracts. In this study, *Dodonaea viscosa* a plant native to tropical and subtropical regions of the Americas, Africa, and Australia, was used. This plant has different species which may vary in leaf size and shape. Its leaves are also considered an effective treatment for wounds and other ailments, such as rheumatism, digestive problems, and skin diseases (Beshah et al., 2020). Nanotechnology was used in this study to increase the efficiency of the ethanolic extract of *D. viscosa* and sea salt, and to enhance the materials used, such as their large surface area and chemical and physical properties. Nanotechnology can be defined as the process of producing materials with one or more

dimensions on a scale of 100 nanometers or less (Peters et al., 2014). The ethanolic extract was converted into nanoparticles by binding it to nano chitosan, which has been used in agricultural applications due to its important properties, such as biodegradability and environmental friendliness when used in fertilizers and seed coatings (Ibrahim and Thalaj, 1998). In addition, it is used as a nanomaterial due to the combination of pesticides or chemicals with chitosan through ionic or covalent bonds, or encapsulating these materials with chitosan matrices due to its homogeneous and stable encapsulation property (Kashyap et al., 2015). Some studies have confirmed the effectiveness of ozone gas in preserving and storing rice without any damage for 12 months when exposed to ozone for 180 minutes (Nur et al., 2015). Exposure of barley to ozone also helped to affect the growth of *Fusarium* spp. and mycotoxins produced, and maintain the quality of barley (Dodd et al., 2011). Due to the need to search for other and many alternatives, to traditional and chemical methods, and to apply low-cost and effective treatments as well as alternatives against pathogens, including fungi, sea salt was also used in this study as one of the means to affect the *Fusarium* spp. and test its effectiveness in inhibiting growth and production of mycotoxins.

In this study, the ethanolic extract of *D. viscosa* (DVE) in its normal and nano formulation, ozone gas at different concentrations and exposure times, and sea salt in its normal and nano formulation were used to detect the ability of these treatments to inhibit the growth of *Fusarium* spp. strains and their ability to inhibit the production of toxins (DON and MON).

CHAPTER 1

GENERAL INFORMATION AND LITERATURE STUDY

1.1. Problem Statement

The research aimed to verify the presence of *Fusarium* spp. in stored grains in Iraq and to assess the effects of alternative chemical fumigation methods used to control *Fusarium* spp. in stored wheat. The potential of these materials and treatments to reduce the production of mycotoxins associated with the growth of *Fusarium* spp.

1.2. Purpose of the Research

Chemical pesticides and insecticides have long been used to control insects and fungi in grain stores. This poses a risk to the environment and workers in this field, as it also leaves behind waste after fumigation, in addition to its high cost. This research aims to demonstrate the effects of alternative methods and materials that are cheaper, derived from nature, do not affect workers or the environment, do not generate waste, and do not affect food. The effect of these methods and materials was studied on seven *Fusarium* spp. isolates, which were phenotypically and genetically identified. The effects of ethanolic and nano extracts of *D. viscosa*, as well as sea salt and ozone gas, on strains isolated from grain stores across different governorates in Iraq, were also studied. The effect of these materials and methods on the production of DON and MON mycotoxins was revealed.

1.3. Significance of the Research

Fungal infections and the associated production of mycotoxins pose a significant threat to human and animal health. This fungal infection may be transmitted from the field to silos and grow further in grain stores when suitable conditions are present. *Fusarium* spp. are one of the important fungi that infect grains and cause diseases in wheat fields. It

produces different types of mycotoxins. In this study, *Fusarium* spp. species were isolated and treatments were applied to them. The effect of the chemical alternative treatments on the growth of these isolates and their potential to produce toxins were revealed. Modern techniques, such as nanotechnology, were used to achieve maximum effectiveness by converting the alcoholic extract of *D. viscosa* into nanoparticles using chitosan. Sea salt was also converted into nanoparticles by grinding it in specialized mills and treating it with ozone gas at varying concentrations.

1.4. Literature Review

1.4.1. Wheat (*Triticum aestivum*)

People rely primarily on grains for their diet, most notably rice and wheat (Mrema et al., 2012). They have noted that wheat cultivation and its presence in ancient civilizations are very old, and archaeologists have established that Mesopotamia is its original home. The Sumerian civilization in southern Iraq, specifically the city of Kish, 65 miles south of Baghdad, is believed to be the birthplace of bread-making. It is thought that the first wheat seeds were used around 3500 BCE, and archaeologists have found wheat seeds in parts of Türkiye, Egypt, Syria, and Ethiopia (Cooper, 2015; Kayhan, 2014). The wheat grain has a unique structure that gives it distinctive properties. One of these parts is the endosperm, which contains between 81-84 % starch (Rajendran, 2003). The germ also constitutes 3% of the wheat grain and contains vitamins, enzymes, minerals, antioxidants, and fats (Khaled et al., 2023). Wheat provides a high calorie content due to its carbohydrate content and is also a rich source of minerals, vitamins, and proteins (Al-Sharmani et al., 2019). China and India are the world's largest wheat producers (Pon & Bhalla, 2013). Global wheat production in 2024 reached approximately 798 million tons and wheat production of Iraq was 5.23 million tons (FAO, 2024). After the crops mature and at the appropriate time, they are harvested, which is the first step in the process by which wheat is obtained, and then transported by specialized carriers to warehouses prepared for this purpose until they are consumed (Yousef et al., 2016). The process of cleaning grains before storage plays a key role in extending their shelf life, as eliminating microorganisms present in wheat is crucial to preventing further spoilage (Bevan et al., 1997). Non-wheat materials, minerals, foreign matter, stones, clay clumps, soil, other grain seeds, and damaged or diseased wheat are removed (Miller, 2019; Maheshwari,

2018). The moisture content of grains ranges between 10% and 14%, which plays a key role in their storage safety. There are several methods to reduce the moisture content of grains after harvest, such as exposing them to sunlight to limit fungal growth and activity (Yousef et al., 2016). Various chemicals are used to eliminate pests that harm wheat, such as insects, fungi, rodents, and others, through a process called fumigation. However, the use of chemicals can pose environmental and health hazards to workers, affect the quality and properties of the food, and leave residues (FAO, 2014). Countries strive to stabilize their wheat stocks to meet their populations' needs and control the quantity and price in local markets, given the variation in production rates from one season to another. Therefore, providing adequate storage facilities for the crop is crucial to controlling this variability (Bevan et al., 1997).

1.4.2. Fungi Associated with Wheat

Many fungal diseases can infect plants and crops, and they are divided into two main groups that are considered the most important and most common:

Obligate fungal diseases: Loose smut, Wheat leaf rust or brown rust, wheat stem rust or black rust, striped rust or yellow rust, powdery mildew, karnal Punt, flag smut, and common bunt. Non-obligate fungal diseases: *Fusarium* head blight, tan spots, septoria disease, common root rot, crown root rot, and black point (Kayim et al., 2022).

Field fungi, storage fungi, and rot fungi are three groups of fungi that can attack grains at different stages. The genera *Fusarium* spp., *Alternaria*, *Helminthosporium*, and *Cladosporium* are the most common species that can infect grains before harvest in the field. The second group includes species from the genera *Aspergillus* and *Penicillium.* In contrast, the third group grows and feeds on crop and plant residues, including *Chaetomium* spp., Papulospora spp., *Fusarium graminearum*, and *Sordaria* spp. (Christensen & Kaufmann, 1965).

1.5. *Fusarium*

Fusarium spp. are a type of filamentous fungi, and it is a large genus within it. Filamentous fungi, which come from the Latin fusus, meaning spindle, are closely related to plants and spread in the soil (Desjardins and Proctor, 2007). *Fusarium* spp. comprises

approximately 300 phylogenetically distinct species. Research has identified 20 species groups and 9 monophyletic strains. Soil is the ideal environment for many *Fusarium* spp., and it can be considered a parasite and has the ability to transform into necrotic fungi. *Fusarium* spp. has been responsible for significant economic losses in many crops, causing vascular wilt, root rot, and stem rot (Rampersad, 2020).

Fusarium spp. are a controversial fungus with significant variation in its morphological characteristics, although similar morphologies may differ in other ways. Since its discovery by Heinrich Friedrich Link in 1809, no unified taxonomic system has been established for *Fusarium* spp., as their classification has been chaotic. *Fusarium* spp. includes over 1,000 species (Stakheev et al., 2016). *Fusarium* spp. are a pathogen group and a significant source of many plant diseases that can affect plants, particularly grains. Controlling it before harvest is crucial, and even during storage, conditions must be provided to prevent the growth of this fungus, in turn, is a source of numerous mycotoxins, including trichothecenes of types A and B, zearalenone (ZEA), and fusarium ergot (FBs). Group A includes T-2 toxin, HT-2 toxin, neosolaniol (NEO), and 4,15-diacetoxyscoprinol (DAS). Group B includes nivalenol (NIV), deoxynivalenol (DON), and its derivatives 3-acetyl (3-AcDON) and 15-acetyl (15-AcDON), and fusarenone-X (Topi et al., 2020). *Fusarium* spp. have two life cycles: *Fusarium* spp is characterized by having two types of life cycles, sexual and asexual. Some types of *Fusarium* spp. produce sexual spores (meiotic), which are produced in airborne spores that cause plant pollution (Dweba et al., 2017). Approximately 20% of *Fusarium* spp. reproduce sexually, known Conidia major and minor are the mode of reproduction of *Fusarium* spp., an asexual Deutromycota (Deacon, 2005).

Scientific classification of *Fusarium* spp. Kingdom: *Fungi* , Division : *Ascomycota ,* Class : *Sordariomycetes ,* Order : *Hypocreales ,* Family : *Nectriaceae ,* Genus : *Fusarium* .

Studies indicate that there are large numbers of species in the classification of *Fusarium* spp. that may reach a thousand species. The classification process for the genus is complex; different methods, various schemas and tables are used for classification. Selected species include*; F. avenaceum, F. bubigeum, F. culmorum, F. graminearum, F. langsethiae, F. oxysporum, F. poae, F. solani, F. sporotrichioides, F. tricinctum, F. verticillioides, F. virguliforme* (Moretti, 2009).

1.5.1. Factors Affecting the Growth of *Fusarium* spp.

The *Fusarium* spp. fungus spreads across different environments, especially in the soil (Burgess et al., 1987) or plant residues (Rheeder et al., 1990) in a reconstituted form or within the plant tissue (Zeller et al., 2003). *Fusarium* spp. fungus causes many plant diseases, including seedling damping-off disease, *Fusarium* wilt disease, and head blight of wheat. It is the most effective fungal disease in grain crops (Burgess et al., 1987). Some factors affect the growth of *Fusarium* spp., such as temperature, light, pH, and the type of nutrient medium. Some studies mentioned that fungi grow in a wide range of temperatures, such as *F. oxysporum*, it grows between 10-35 °C, although the optimum growth temperature is 27-28°C (Gordon, 2017; Kraft, 1994; Fravel et al., 1996). *Fusarium* spp. tends to grow better in an acidic medium, the highest level of growth was recorded at pH 5-6 (Cochrane, 1958). The optimum pH for growth of *F. oxysporum* and *F. solani* ranged from 4.5 to 6.0, while this range varied when compared to *F. graminearum* and *F. equiseti*, which grew at pHs of 3.5 and 6.5, respectively. Light intensity also affects fungal growth, with *F. solani* reaching its highest growth rate in 12 hours of light and 12 hours of darkness (Kumar et al., 2010).

1.5.2. Major Diseases Caused by *Fusarium* spp.

Many fungal pathogenic infections are caused by *Fusarium* spp., which result in infections that reduce crops and have an economic impact, in addition to crop losses and damage. *Fusarium head blight* (FHB) is considered one of the most important and dangerous diseases that affect grains, and the leading cause of this disease is the *Fusarium graminearum* fungus (Beccari et al., 2022). *Fusarium graminearum* is one of the types of *Fusarium* spp. that infects grains, especially wheat, and causes *Fusarium* head blight (FHB), which is a devastating disease affecting wheat in different regions of the world, and the mycotoxins such as deoxynivalenol (DON) that it produces affect the quality of grains and the impact on animal health (AlTaweel et al., 2017). Researchers stated that FHB, in addition to its seriousness, is that the plant may be infected with this disease due to more than 17 species of *Fusarium* spp. The most common and proven species are *Fusarium graminearum*, *Fusarium poae*, *Fusarium avenaceum*, and *Fusarium culmorum*, which are among the most important species to contract this disease (Beccari et al., 2018). When humidity reaches 80–92% and temperatures between 20 and 30°C,

the release of ascospores and macrospores is stimulated, and infection occurs via wind and rain (Bolanos, 2018). There are many types of mycotoxins produced by *F. graminearum*. It has a significant toxic effect on humans and animals, including nivalenone, zearalenone, deoxynivalenol, and moniliformin, the external symptoms of this disease can be distinguished by the color of infected ears, which change to pink and orange (healthy ears are green). Cold and humid weather is an ideal environment for producing these germs; disease symptoms appear on the heads, stalks, and ears of grains (Kayim et al, 2022). Some studies have indicated that other types of *Fusarium* spp. because of this disease, such as *Bipolaris sorokiniana*, *Cephaliosporium gramineum*, *Fusarium graminarium* and *Fusarium culmorum*, wheat root rot occurs, with an infection rate of 34.32% in rain-fed areas. Soil fungi are more than 30 species and may be present on seeds; these fungi increase the infection rate of crops. These fungi include: *Alternaria* spp., *Rhizoctonia* spp., *Fusarium* spp., and *Bipolaris* spp., and replanting wheat simultaneously with planted varieties' sensitivity to the fungi that cause root rot disease (Muhammed & Hussein, 2022). *F. culmorum, F. pseudograminearum, F. equiseti*, *F. solani*, and *Drechslera halodes* caused root and crown rot of common and durum wheat and barley (Fernandez & Conner, 2011; Moubark, & Abdel-Monaim, 2011). The infection of a plant with the common root rot disease causes symptoms on the roots, including necrotic lesions, dry and warm areas are considered the most common areas for the growth of this disease. The common root rot and crown root rot may infect many fields and farms in India, Australia, Europe, and China, and the percentage of losses was as high as 75%. Some *Fusarium* species are responsible for infecting *Zea mays* L. with certain types of fungal diseases. *Fusarium* species are common fungal pathogens in maize, causing diseases such as seedling blight, stem rot, and ear rot. *Fusarium gramminerum*, *Fusarium fugicurii* (FFSC), and *Fusarium proliferatum* are among the dominant species causing ear rot in maize (Del Palacio et al., 2023). The fungus *Fusarium oxysporum* schlickend. *FR.* f. species *lycopersici* (Sac.) (FOL) may infect tomato crops with *Fusarium* wilt disease (Pandey et al., 2024).

Depending on the interaction between plants and fungi, fungi may obtain food from plants as decomposers or live with plants as beneficial symbionts (Eskola et al, 2001; Ji et al., 2019). Many plants are susceptible to *Fusarium* spp. infection, which is important for human and animal nutrition, and the infection varies from one plant to another, as it can

infect seedlings, roots, stems, and heads. The infection leads to a noticeable loss in the material value and quality of the crop. Crown rot (CR) is among the major diseases caused by *Fusarium* head blight (FHB) and root rot (RR). It may cause wilting, stunting, and necrosis of the plant, which varies according to the severity of the infection, two of the most dangerous wheat diseases worldwide are *Fusarium* CR and *Fusarium* FHB (Askun, 2018).

1.6. Mycotoxin

Mycotoxins (MTs) are toxic secondary metabolites produced by many fungal genera, such as *Aspergillus* spp., *Penicillium* spp., *Alternaria* spp., *Fusarium* spp. Furthermore, the origin of mycotoxins dates back to ancient Greece, consisting of two syllables: the first, mykes, meaning fungus, and the second, toxium, meaning poison. The different studies and research have proven that over 400 types of mycotoxins exist (Oadi, 2020). The most significant importance was placed on 12 mycotoxins due to their dangerous effects on humans, animals, and plants (WHO, 2018). Mycotoxicosis is the term used for poisoning associated with exposure to mycotoxins. Mycotoxicosis symptoms depend on the type of mycotoxin, the concentration and length of exposure, and the age, health, and sex of the exposed individual (Bennett and Clich, 2003). Mycotoxins play a significant role in affecting plant condition, and studies have shown that they weaken plants by inhibiting protein synthesis and cell division. One of the most important factors that lead to a plant becoming infected with fungi is the plant's genetic predisposition to infection, manufacturing practices, and environmental conditions such as temperature, humidity, and climate in general overall climate (Bryła et al., 2022). Research and studies in this field indicate that about 25% of global grain production worldwide has been contaminated with mycotoxins (Pal, 2017). The minimum concentrations of mycotoxins in food must not exceed specified international standards. It has not been proven that eating foods containing fungal toxins does not affect public health, and such foods are not without risk. There is evidence that aflatoxin B1 is a major cause of liver cancer in humans (Alkadri, 2012). Contamination of crops with mycotoxins caused significant losses, leading to decreased crop productivity and losses amounting to more than one billion five hundred million dollars due to only three types of mycotoxins: aflatoxins and *Fusarium* spp. toxins, and trichotoxins (Oadi, 2020; Bhatnagar et al., 2006). Aflatoxins, ochratoxin A,

fumonisins, tricothecins, and zearalenone are most important toxins that can be found in foods and have a significant impact on human health (Pitt, 2000).

1.6.1. Factors Affecting Mycotoxin Production

Many different factors affect the production of mycotoxins, such as the type of crop, climatic factors, like humidity and temperature, harvesting process, storage conditions. Studies have confirmed that insect infestation of grains contributes to the development of the fungal condition and the intensity of its growth (Gnonlonfin et al., 2013). Climatic conditions may not directly affect fungi, but they do affect plants, which in turn affect toxin-producing fungi, thereby encouraging or inhibiting toxin production in that environment. Areas with only arid or hot climates are less likely to experience fungal infections than areas with both arid and hot climates. Aflatoxin production was lower than under normal conditions in the presence of low-oxygen environments (Popovski & Celar ,2013). *Fusarium graminearum* is one of the types of *Fusarium* spp. that infects grains, especially wheat, and causes *Fusarium* head blight (FHB), which is a devastating disease affecting wheat in different regions of the world, and the mycotoxins such as deoxynivalenol (DON) that it produces affect the quality of grains and the impact on animal health (AlTaweel et al., 2017). Grain damage due to *Fusarium* has become a standard indicator of the presence of dioxynevalinol (DON) toxins, and also indicates infection of the grain by the fungus *Fusarium graminearum*. Furthermore, the variation in (DON) concentrations in field trials was related to the effect of environmental factors and the relationship between (DON) concentration and disease severity (Palazzini et al., 2015). In addition to temperature, humidity, and other climatic factors, sunlight affects fungi and their production of mycotoxins (Miraglia et al., 2009).

Interest in *Fusarium* spp. began in the 1800s with the observed association between *Fusarium* spp. infected grain and animal toxicosis and continued with Wollenweber and Reinking's work on *Fusarium* spp. taxonomy in 1935 (Özeren, 2022). Inoculation studies are currently being conducted worldwide, including in Turkiye, on inbred lines and varieties to identify corn genotypes resistant to *Fusarium* spp. In this context, attempts are being made to determine the level of resistance by inoculating plant stems and ears in the field (Cengiz, 2016). The main *Fusarium* spp. toxins are fumonisin, trichothecene, and zearelenone (Sardjono et al., 1998; Adejumo et al., 2007). In addition to these toxins,

many other toxins, such as fusarochromanone, fusaproliferin, wortmannin, sambutoxin, moniliformin, fusaric acid, fusarin C, equisetin, and fusariosin, are also produced by *Fusarium* spp. (Özeren, 2022). The mycotoxins produced by *Fusarium* spp. are the most common and have been studied by researchers due to frequent contamination of foods and crops with these toxins Deoxynivalenol, nivalenol, zearalenone, T-2 toxin, and fumonisin B1 (Fang et al., 2019). The toxins produced by *Fusarium* spp. are naturally occurring secondary metabolites (secondary metabolites (mnd p threat to global grain production, leading to food and animal feed contamination (Ferrigo et al., 2016). *Fusarium* spp. affects the plant economically by infecting the plant with various diseases that cause indirect losses, such as limiting seed germination, or infection with stem rot, etc., which affect crops directly. The effect of *Fusarium* spp. on plants varies depending on many factors, such as temperature, humidity, and environmental conditions, the toxins produced by *Fusarium* spp. are naturally produced secondary metabolites, they pose a threat to global grain production, leading to food and animal feed contamination.

1.6.2. Major Mycotoxins

1.6.2.1. Fumonisins

In 1988, researchers described the mycotoxin fumonisins (Bennett and Clich, 2003). Fumonisins as mycotoxins produced mainly by some species of *Fusarium* spp., such as *F. verticillioides* as well as by *F. proliferatum*, *F. napiforme*, and *F. nygamai* (Chehri et al., 2010). *Fusarium* spp. are classified into four groups: (A, B, C, and P), they represent more than 28 types of fumonisins (Alshannaq & Yu, 2017). Mycotoxins contain a backbone of 20 aliphatic carbon atoms, which is modified with methyl, hydroxyl, and amino moieties, and two esterified 1,2,3-propanetricarboxylic acid side chains, which are characteristic features (Kaltner et al., 2017). *Fusarium* spp. can cause brain diseases in horses and hepatitis in rats (Chehri et al., 2010). The World Health Organization (WHO) indicated that the concentration of this toxin is 2 micrograms/kg of body weight, the maximum permissible limit for *Fusarium* spp. toxins as a whole or individually (Kaltner et al., 2017). Fumonisins B1 (FB1) is one of the most common *Fusarium* spp. mycotoxins (Ug et al., 2021). Some studies have shown the presence of fumonisins in rice fields in several countries, including China, Argentina, Korea, and the United States, as well as in sorghum fields in Brazil and India, wheat fields in Spain were also surveyed for FB1

contamination and found to be present in 8 out of 17 wheat samples, at concentrations ranging from 0.2 to 8.8 mg/kg (average 2.9 mg/kg) (Shephard et al., 2005). Below is a brief overview of the toxins detected in this study.

1.6.2.2. Deoxynivalenol (DON)

Deoxynivalenol (DON) is one of the most important toxins contaminating grains such as corn, wheat, and barley. It is a fungal poison produced by *Fusarium* spp., forming the leucotoxin triad. It dramatically affects the health of humans and animals by stimulating appetite loss and increasing plasma levels of the satiety hormones cholecystokinin and peptide (Hui Jia et al., 2017). Morooka and his group were the first to discover and diagnose this toxin in Japan in 1972. It is a secondary metabolite of the fungus *F. graminearum*. Isolated from barley, it is called emetic poison (Vomitoxin), a name given to it by Vesonder in 1973 (Abdul Razzaq, 1989). DON belongs to the type B trichothecene group, it contains an epoxy group between carbon atoms 12 and 13. Also, it contains a trichothecene ring, one primary hydroxide group, two secondary hydroxide groups, and a carbonyl group on carbon atom 8 (Deijn et al., 1997). DON is a solid chemical substance that forms white crystals with a low molecular weight of 296.32 da, it can dissolve in water and polar solvents such as ethanol, ethyl acetate, methanol, and chloroform; it is also not affected by high temperatures (Eriksend et al., 1998). Many studies have shown that DON has high resistance and stability at high temperatures, such as those encountered during cooking extended storage periods (Ehling et al., 1997). Deoxynivalenol, Diacetoxyscrpenol, nivalenol, and toxin-2t are toxins of *Fusarium* spp. that cannot be detected without solutions to show, as they do not absorb ultraviolet radiation and therefore do not fluoresce (Abd al -Hamid, 2000). Other studies indicated that 12% of DON toxins could be reduced, and that it showed good stability at 100-120°C, while it was partially destroyed at170°C (Wolf et al., 1999).

The human body is sensitive to disease, and this sensitivity increases through its effect on growth regulators. Studies have shown that DON toxin affects these regulators, as well as its effect on protein synthesis, by inhibiting it by reducing the level of ribosomes. In addition, it inhibits the synthesis of DNA and RNA (Rotter, 1996). Intestinal poisoning with DON toxin, through oral ingestion has a significant impact on humans; the symptoms are nausea, dizziness, headache, vomiting, fever, and diarrhea. These

symptoms are very similar to *Bacillus cereus* poisoning. The percentage of DON toxin ranged between 1 and 40 micrograms/gram, among this high percentage, 7.818 victims were poisoned in China due to eating wheat and yellow corn contaminated with the toxin DON (Luo, 1988). This poison also clearly affected the absorption of nutrients, including sugars, lipids, and amino acids, the inhibition rate of food conversions ranged from 1 microgram/liter to 5 micrograms/liter, and its effect and inhibition rate were 50% and 76%, respectively. In addition, it has a significant effect on antibodies in the body, as it reduces them; thus, the body becomes more susceptible to viral and bacterial diseases (Maresca et al., 2002). In this study, a survey was conducted on wheat samples from the governorates of Iraq to detect this toxin.

1.6.2.3. Moniliformin MON

Moniliformin (3-hydroxycyclobut-3-ene-1,2-dione) (MON) is a mycotoxin produced by *Fusarium* spp., and approximately 40 species of *Fusarium* can produce it (Ivić et al., 2009; Radić et al., 2019). The discovery of MON dates back to 1973, from *Fusarium moniliforme* cultures, in a study by Cole et al. (1973). Dr. Alexis Nathaniel introduced the moniliformin form, which is the sodium or potassium salt of sucrose (hydrocyclobutanedione), derived from two acetate units via oxidation and hydration reactions (Jonsson, 2017; Schütt et al., 1998). In a study to determine the relationship between acidic environment and MON stability, it was observed that at pH 4, 7, and 10, MON was most stable at pH 4. The researchers reported that MON is stable in neutral or acidic conditions, as in bread, continued heating for two hours at 50°C caused losses in MON and made it stable under freeze-drying conditions. Water is a suitable solvent for MON and is used as an extraction solvent (Jestoi, 2008; Sch¨utt et al., 1998) reported that *F. chlamydosporum* produces moniliformin, the production of this toxin has been recorded from at least 24 species of *Fusarium* spp., and it has been reported that *F. oxysporum*, which produces this toxin (Rabie et al., 1982; Abbas et al., 1989; Sch¨utt et al., 1998). A study in Poland concluded that *F. culmorum* and *F. graminearum* may cause FHB disease in wheat, as well as *F. avenaceum.* Still, it is less capable than *F. culmorum* and *F. graminearum*, which caused a reduction in production and an increase in moniliformin concentrations (Goliński et al., 1997). The presence of this toxin is widespread in northern Europe resulting from the infection of wheat by several strains of *Fusarium* spp., including *F. proliferatum*, *F. nygamai*, *F. subglutinans*, *F. thapsinum*, *F.*

avenaceum, *F. tricinctum*, and *F. fujikuroi*. MON concentrations in wheat were low in Finland and Norway 0.81 and 0.95 mg/kg, respectively (Jonsson, 2017). This study investigated MON presence in wheat stores in Iraq.

1.7. Methods of Controlling and Reducing Fungi and Their Mycotoxins

After we know the reasons that help in the occurrence of mycotoxins, we must know the most important methods that help in avoiding the occurrence of mycotoxins, including lowering the crop storage temperature, reducing the moisture content, and storing in typical warehouses to avoid insect infestation, which are also among the factors that help in the occurrence of mycotoxins (Ismail, 2014). Preventing the occurrence of mycotoxins starts from the field through efficient harvesting operations, transporting grains, eating them, drying them, storing them, and the problems that accompany them and avoiding them, all of this creates a suitable environment for preventing mycotoxins and their occurrence, poor storage conditions, such as a temperature between 25 and 32 ºC, are considered an optimal temperature for the occurrence of mycotoxins. Likewise, the relative humidity, which ranges between 80-100%, is also one of the best humidity levels for this to occur, in addition to a very important factor, which is the moisture content of the crop, when it is between 16-30 be in its ideal conditions (Oadi, 2020).

Certain steps must be taken to prevent or reduce the incidence of mycotoxin contamination, segregation of grains (wheat, rice, corn, etc.), figs, beans, almonds, walnuts, and hazelnuts is important, as these crops are often susceptible to aflatoxin contamination. Examination is carried out for signs of mold, and any faded, moldy grains or those showing signs of fungal infection are discarded (Ogbonna et al., 2021). Mycotoxin contamination of crops increases with several factors, including temperature, humidity, moisture content, and the condition and integrity of the grains, therefore, it is essential to create an environment unfavorable to fungal growth and contaminants by planting resistant varieties, regulating harvest times, ensuring grain safety, and reducing grain moisture content, controlling grains and preventing insect infestation also contributes to fungal infection control, in addition to lowering storage temperatures (Semple et al., 1989; Matny, 2014). It is also important to purchase and store healthy and fresh grains or crops, and to store them in optimal storage conditions as much as possible to avoid insect infestation and damage resulting from storage, which is a suitable

environment for fungal growth and, consequently, the production of mycotoxins, diversifying food and nutritional sources also helps reduce the mycotoxins the human body may be exposed to, while providing a healthy diet to improve human nutrition, an important note is that grains and crops should not be stored for long periods (Ogbonna et al., 2021).

1.7.1. Physical Control

To understand how to manage and control fungi, we must understand the factors that can affect their growth and cause disruptions that can inhibit or eliminate them, these factors include: temperature, light, nutrients, pH, water activity, and aeration, most fungi grow between 10 and 35°C, although some thrive in extreme temperatures (Ali et al., 2017). Drying grains is an effective method for inhibiting fungal growth and thus preventing mycotoxins; providing a safer environment and reducing potential damage to the grain during harvest and before storage (Langseth et al., 1993). Airtight storage is an important method that has shown positive results in affecting the growth of microorganisms, this method depletes oxygen, transforming the environment into an unsuitable environment for fungal growth (Mohapatra et al., 2016).

The results of steam treatment of DON toxins at different temperatures, 110, 135, 160, and 185°C, with different steam speeds: 0.65, 1.3, 1.5 m/s, showed a significant effect on reducing DON toxin concentrations, the inhibition rate reached 52% when the steam temperature was 185°C and the toxin was exposed for 6 minutes (Pronyk et al., 2006). The effect of magnetized water on controlling *Fusarium* wilt disease in tomatoes, caused by the fungus *Fusarium oxysporum*, and on tomato production when using magnetized water (3000 Gauss) was studied. Inhibition of fungal growth by 100% (Hatem, 2020).

1.7.1.1. Ozone application

Many microorganisms have been treated with ozone; studies have proven it is a powerful oxidizing agent (Khader et al., 2001). The first person to discover it was Christian Friedrich Schönbein in 1839 (Zhu, 2018). The name ozone is named after the Greek word “Ozein”, which means “smell” (Catal and Ibanoglu, 2012). Grains were treated with ozone in the twentieth century and used as a sterilizing agent for organic matter on their surfaces (Campabadal et al., 2013). Ozone was used for several purposes, including

sterilizing drinking water in France in 1906, treating shellfish in France in 1936, and disinfecting swimming pool water in America in 1918, it was also used to disinfect salmonella from peeled eggs in Russia in 1977. In 1997.ozone was declared safe for food processing. It was deemed GRAS (generally recognized as safe) for bottled water in the USA (Sopher et al., 2002). Ozone is a molecule consisting of the union of three oxygen atoms (O3), this occurs by splitting the oxygen molecule into two atoms (free radicals), then, due to the increase in energy, it tends to combine with another oxygen atom to form O3 (trioxygen atoms), one of the most important features of ozone gas is its odorless density of 2.144 g/L (Campabadal, 2013).

Ozone penetration depends on many factors including ozone concentration and the period of exposure. (Raila et al., 2006). Studies have shown that one of the most important factors in slowing ozone penetration into grains is high humidity, which reduces the effect on microbial growth and the presence of insects and microorganisms (Steponavicienė et al., 2012). The type of wheat also played a role in ozone penetration; the penetration of water treated with ozone under the same conditions was easier in soft wheat than in hard wheat (Ibanoglu, 2002).

Increasing ozone concentration was associated with a significant decrease in treatment time, with insect mortality rates varying depending on their ozone resistance and sensitivity (Allen et al., 2003). Some studies confirmed that treatment occurs at temperatures between 20 and 40°C (Hansen et al., 2013). Other studies showed that fungal contamination is less resistant to ozone, with faster penetration associated with higher temperatures (Steponavicini et al., 2012). The duration of treatment, whether long or short, depends on several factors, such as the type of insect or microorganism, the ozone concentration, and others (Allen et al., 2003). Studies have shown that fungal contamination removal increased 2.2-fold when the grain moisture content was 15.2%. When it rose to 22%, removal tripled at a concentration of 700 ppm. The number of fungal spores decreased from 19.6% to 4.2% when the water activity of the barley decreased from 0.98 to 0.88 after 5 minutes of treating the barley with ozone (Allen et al., 2003; Mujumdar and Beke, 2003).

According to Dodd et al. (2011), the application of ozone at a concentration of 26 mg/cm³ for 120 minutes, following 2 and 6 hours of steeping, eliminated *Fusarium* spp. and the

mycotoxins it may produce, while preserving the barley. Ozone also affected *Fusarium* spp. growth and mycotoxin production, and its effects on DON were measured. Furthermore, it helped maintain barley quality. The effect of ozone treatment can vary depending on the type of fungus and its interactions with biological factors during the treatment procedure it is noted that 96% of fungal spores were eliminated when ozone was applied to fungi growing on barley at a rate of 0.16 mg/g of ozone (Isikber and Athanassiou, 2015). El-Desouky et al. (2012) demonstrated that ozone is an effective means of inhibiting AFB1 in wheat, as using ozone at a dose of 40 ppm resulted in an 83.21% inhibition of this toxin after 20 minutes of exposure water treated with ozone 1.5 and 11.5 mg ozone /l could reduce the total number of bacteria, yeasts and fungi by immersing the grains in water treated with ozone (Ibanoglu, 2002; Allen et al., 2003). Savi et al. (2014) showed that ozone gas, at a concentration of 60 mmol/mol for 120 minutes, reduced the growth of the fungus *F. graminearum* and caused the decomposition of DON, however, it did not cause any physical or chemical changes in the grain. The rate of DON degradation in *Fusarium graminearum* was correlated with the length of exposure to ozone and the increase in its concentration, this rate increased directly with increasing concentration and treatment period, the degradation rate reached 93.6% when ozone gas was used to treat 1 μg/ml of DON solution at a gas concentration of 10 mg/L (Li et al., 2015).

1.7.2. Biological Control

Researchers have developed numerous biological pesticide products to control root, fruit, and leaf diseases. Among the most important biological control agents (BCAs) are the bacteria *Bacillus, Bantoya, Streptomyces, Trichoderma, Clonostachys, Pseudomonas, Burkholderia*, and some yeast species (Lahlali et al., 2022). Due to the negative effects of chemical pesticides used to control fungi, some microorganisms have been developed as an alternative to these pesticides, which cause significant harm to humans and the environment. Examples include the bacteria *Bacillus subtilis, B. megaterium, Trichoderma viride, T. harzianum,* and *P. fluorescens* (Abdul Kader et al., 2021). To effectively manage diseases using biopesticides, environmental changes and other influencing factors must be identified as a viable and economically sound approach. These factors may affect the pathogen, microbial product, or plant, and include water, nutrition, seeds, light, field management, plant protection, machinery technology, air,

soil, population density, and others (Sondram et al., 2023). From another perspective, biological methods raise concerns about potential harm from nutrient uptake and the release of microbial metabolites (Afsah-Hajri et al., 2020).

It is essential to understand how organisms interact through direct and indirect contact and to identify biological control mechanisms. Interaction types are classified as symbiotic, primary cooperative, commensal, neutral, competitive, antagonistic, parasitic, and predative (Pall and Gardner, 2006). One method of biological control of toxic fungi is to introduce and treat the soil with non-toxic fungal species, such as *Aspergillus flavus and A. parasiticus,* which have significantly reduced aflatoxin contamination. Non-toxic strains of *Fusarium verticillioides* have also been successful in reducing or eliminating fungi capable of producing fumonisin (Conti et al., 2020).

1.7.3. Chemical Control

Chemical control (using pesticides) is the most widely used method worldwide, despite the damage it causes to the environment and non-target organisms, because it is easy to apply. It provides clear, quick results and can be applied across various environments (Panth et al., 2020). Chemicals occupied a distinguished and important place in pest control programs in the methods used to manage and control pests. The beginning was with lime sulfur in the middle of the nineteenth century. Many fungicides with therapeutic properties later mainstays until recently (Knight et al. 1997; Morton and Staub, 2008). Organic and inorganic salts are widely used because they are generally low-toxic to mammals. They can also be used as acidity regulators, food preservatives, and antimicrobials (Olivier et al., 1998).

Studies have shown that many salts can inhibit fungal growth. Types such as sodium sulfide, ammonium carbonate, and sodium chloride have been used. Their effectiveness has been proven against the fungus *A. flavus* growing on corn for 28 days at concentrations of 1, 2, 3, 4, and 5%. Ammonium carbonate at a concentration of 2% was the best concentration used (Thanaboripat et al., 2010).

On the other hand, calcium carbide was used at concentrations of 0.1 and 0.125% g/L, as it reduced *A. flavus* biomass and spore concentrations, and affected AFB1 toxin production (Abdel Aziz, 2015). Oxidizing agents played a major role in inhibiting

trichothecene toxins; Sodium hypochlorite (NaOCl) at 0.25% for 4 hours demonstrated good results in inhibiting biological activity (Rai et al., 2012).

Using sodium chloride at a concentration of 120 mg/g significantly inhibited the production of. *A. flavus* by 100% with a reduction in 1AFB production after it was incubated for 7 and 12 days, no effect of sodium chloride salt appeared when it was used at a concentration of 40 and 80 mg/g after infection for 14 days, while this concentration had an effect on AFB1 production and decreased by 41% and 54% (Thanaboripat et al., 1992).

Türkkan (2013), reported that 26 different salts, including ammonium carbonate, ammonium bicarbonate, and sodium metabisulfite, were applied to the fungus *Fusarium oxysporum f.* sp. *cepae*. Each of these salts completely inhibited fungal growth, with no significant differences in inhibition rates.

1.7.3.1. Effect of sea salt on fungi

Salt is a chemical compound used in human food, food processing, and preservation. According to the World Health Organization (WHO), a person's daily salt intake should be around 5 grams (less than 2 grams of sodium) (Chudy et al., 2025). Common table salt (sodium chloride) is known for enhancing the flavor of food. It has a crystalline structure and is extracted from salt mines or seawater (Shen et al., 2022). Salt has been used for a long time to preserve food, especially meat and fish. Saline solution has been used and proven to be more effective than dry salt.

Research has shown that salt can inhibit microbes at a concentration of 3-5%, and at high concentrations of 20-15% in preserving meat and fish, the effectiveness of saline solution lies in intracellular tonicity, equivalent to the force generated by a saline solution with a concentration of 0.85 - 0.9%. These saline solutions for bacterial dilutions are prepared at this concentration so that no change occurs inside the cell, and intracellular osmosis of microbial cells (Al-Muslih, 1990; Wade et al., 2000).

Abbas Al-Hamiri and Hussein (2020) showed the effect of common salt from local markets on the growth of *A. flavus* in PDA culture medium. He recorded an inhibition rates of 3.17% and 3.52% at concentrations of 100/gm3 and 2.5, respectively, with no

effect at 1%. Meanwhile, concentrations of 100/gm3, 2.5, and 1 ml of sea salt on a micro scale did not achieve reasonable inhibition rates, with 0, 5.8, and 12.58%, respectively.

Sodium chloride was applied to assess its potential to inhibit *A. flavus* growth, and it was found to have no effect at concentrations of 40 and 80 mg/g after 14 days of incubation. Still, the production rate of AFB1 toxins decreased to 41% and 54%. Applying sodium chloride at a concentration of 120 mg/g helped inhibit the fungus by 100% (Thanaboripat et al., 1992).

When applying a concentration of 10% sodium chloride to chicken feed, the growth of *A. flavus* was inhibited by 100% (Aboul-Nasr, 2014). Trichothecene toxins were removed by oxidation with NaOCl. Chemically, it is a potent oxidizing agent (Rai et al., 2012).

Sodium chloride, and sodium bisulfide were applied at concentrations of 1, 2, 3, 4, and 5%, and all of these salts helped reduce and prevent the growth of *A. flavus* on maize (Thanaboripat et al., 2010).

Wade et al. (2000) reported that sodium chloride solution affects some *Fusarium* spp. genus that cause plant diseases. When the solution was used at a rate of 0.25 - 0.5 g sodium chloride/liter on cyclamen plants grown in soil contaminated with *F. oxysporum*, this led to a reduction in the mortality rate and a reduction in the effect and severity of the disease. This study evaluated and studied the effectiveness of micro- and nano-sized sea salt on fungal growth and mycotoxin production. To the best of our knowledge, no research has examined the effect of sea salt in nano status on *Fusarium* spp. producing MON toxins.

1.7.4. Plant Extracts

Plants and their parts, such as leaves, bark, seeds, and flowers, have been traditionally used in many parts of the world, in addition to the products derived from these parts, such as oils and ashes, they have been used to control insects and microbes for a long time. Plant derivatives have been used as insecticides and fumigants, and are characterized by their biodegradability (Dubey et al., 2008).

Some studies have indicated that vegetable oil has played a role in preventing fungi growth and damage to stored grains through insect infestation. This type of application

has been applied in India, where the oil acts as a barrier that prevents the growth of fungi by reducing and limiting the oxygen reaching it and acting as a barrier to prevent moisture leakage, one of the features of this application is its effectiveness in storing grains and low cost (Mohapatra et al., 2016).

Flavonoids, isoflavonoids, terpenoids and their derivatives, they are natural plant derivatives, studies have proven their effect on fungi and the possibility of using them as an alternative to chemical substances. They have been used against fungi in stored grains; two fruit peels were used separately: lemon and pomegranate, lemon peels inhibited aflatoxin production by 100% when the rice was stored for three months at 18% humidity and 25°C. Pomegranate peels had a similar effect when the storage period was extended to 4 months (Naseer et al., 2014).

Many studies have confirmed the ability of plant essential oils to prevent fungal growth. However, their use in grain stores requires permits from regulatory bodies, and most experiments remain limited to laboratory settings (Mohapatra et al., 2016).

Proved that the ethanolic and aqueous extract of cress, rue and fenugreek plants inhibited the growth of the fungus *F. veticilloides* in varying proportions. It was found that the powder of the flower buds of carnation at a concentration of 1000 - 2000 mg/liter had a high inhibitory activity against 13 types of *Aspergillus* spp. by the food poisoning method (Kareem et al., 2009).

The antifungal activity of eugenol in a model system against the fusaria (*F. oxysporum* and *F. avenaceum*) was investigated, the radial growth of *A. terreus* and *F. avenaceum* was inhibited at 140 mg/liter, and the growth of *F. oxysporum* was completely inhibited at 150 mg/liter (Campaniello et al., 2010).

Plants produce various chemical compounds that differ in composition, quantity, distribution, and degree of accumulation within the plant, as well as in their metabolic processes and biological functions. Each compound has multiple and unique properties and functions (Siddiqi, 2021). The following are examples of plant chemical compounds: Tannins are water-soluble plant compounds, specifically natural polyphenols, used in various fields, including lipid oxidation, regulation of oxidative enzymes, antioxidant activity, and metal chelation. They also possess anti-inflammatory and antimicrobial

properties in the human body, making them highly valuable in numerous applications within the food and medical sectors (Singh & Kumar, 2020).

Saponins are active compounds with diverse biological functions, including emulsifying foaming agents and non-ionic surface tension reduction. They are used in the food industry as food additives (Krigel et al., 2017). Alkaloids are naturally occurring nitrogenous compounds found in most plants, characterized by their complex structure and wide distribution (Gutierrez-Grigalva et al., 2020). Flavonoids are naturally occurring phenolic compounds produced by plants; they are phenolic compounds found in fruits, vegetables, grains, and other plant parts such as roots, stems, and flowers. They can affect vital cellular enzymes and act as antioxidants and anti-inflammatories (Panche et al., 2016). Flavonoids are insect attractants and play an important role in protecting plants from ultraviolet radiation. Studies have also shown them to have antiviral and antifungal properties (Kaurinovic and Fastag, 2019). Resins are fat-soluble compounds found in herbaceous plants. They contain both volatile and non-volatile components and are characterized by their viscosity. They also play an important role in preventing bacterial infection (Bernhoft, 2010). Trees direct stored resin to the site of infection through special channels to combat pathogens that invade the plant or mechanical damage (Slinski et al., 2015). Terpenoids are chemical compounds found in plants and nature. They are a major component of essential oils and are used in therapeutic applications due to their antibacterial activity (Cox-Georgian et al., 2019). Glycosides are plant compounds that are secondary metabolites linked to monosaccharides, oligosaccharides, or uronic acid in various forms (Bernhoft, 2010). Cyanogenic glycosides are important toxic glycosides that produce hydrogen cyanide, a fungicidal compound. It has been shown to affect the fungal hyphae of the rice fungus *Magnaporthe grisea* (Dey, 2016).

1.7.4.1. Dodonaea viscosa plant

Dodonaea viscosa is believed to have originated in Australia, but it is found throughout the tropics and subtropics. The plant is distributed across Africa (Sudan, Ethiopia, Somalia), Asia (Iraq, Malaysia, India), South America (Brazil, Bahamas, Bermuda, Cuba), and North America (Mexico, United States). *D. viscosa* is a plant belonging to Kingdom: *Plantae*, Subkingdom: *Viridiplantae*, Infrakingdom: *Streptophyta*, Superdivision: *Embryophyta*, Division: *Tracheophyta*, Subdivision: *Spermatophytina*,

Class: *Magnoliopsida*, Superorder: *Rosanae*, Order: *Sapindales*, Family: *Sapindaceae*, Genus: *Dodonaea*, Species: *D. viscosa* (Al-Snafi, 2017).

D. viscosa is a medicinal plant belonging to the Sapindaceae family, commonly known as sticky hopbush. It contains chemical compounds of great importance in medicine, known as secondary metabolites. *D. viscosa* contains numerous alkaloids, glycosides, saponins, tannins, flavonoids, volatile oils, and some beneficial acids (Al-Aubaidi, 2016). *D. viscosa* is characterized by being a tall tree that can reach up to 5 meters, and sometimes it may be smaller. Its leaves are alternate, simple, spirally arranged, with a thick petiole that can reach 0.2 cm in length. The leaf has a pointed tip and a drooping base, and it has with about 16 pairs of secondary veins. The flower stalk reaches 0.5 cm in length, and the inflorescence can reach 7 cm (Maresca et al., 2002; Manjulatha, 2012).

1.7.5. Nanotechnology

Nanotechnology can be defined as the process of producing materials with one or more dimensions on a scale of 100 nanometers or less, consisting of separate functional parts either internally or on the surface, or forming aggregates or agglomerations with a size greater than 100 nanometers. (Peters et al., 2014). Nanoparticles can be classified into organic and inorganic nanoparticles (Ealia & Saravanakumar, 2017). Richard Feunemann, the physicist who pioneered nanotechnology in 1959, and whose 1982 invention marked the beginning of the nanoscale world, was followed by further developments, including the invention of another microscope, the atomic force microscope. These microscopes were further developed until a high-energy electron microscope was introduced in 2002. This development enabled the indirect observation of atoms and molecules (Azamal Husen & Siddiqi, 2014).

Nanotechnology relies on producing and manufacturing molecules with specific, planned specifications by rearranging of atoms (Neal, 2008; Sassolas et al., 2012). This principle is the basis of nanotechnology, as reducing the size of a molecule is directly proportional to the reaction rate (Guzman et al., 2009).

Nanoparticles achieve their function through multiple forms of contact with the bacterial cell, using various methods, such as hydrophobic interactions, van der Waals forces, electrostatic attraction, and receptor-ligand interactions, they then target the metabolic

pathway, which has a direct relationship and significant impact on the cell membrane, they then target ribosomes, lysosomes, DNA, and enzymes, which represent essential cell components, this disrupts cell permeability, inhibits enzymes, disrupts electrolyte balance, and disrupts proteins, most antibiotics and other therapeutics that can affect microbial cells involve contact with the outer cell wall and then affect it in various ways, however, nanoparticles differ in that they can penetrate the bacterial cell and inhibit its function through three mechanisms: inducing oxidative stress, releasing metal ions, and non-oxidative mechanisms (Wang et al., 2017).

One of the mechanisms by which nanoparticles work is to disrupt and damage mitochondrial DNA and the mitochondrial membrane, producing reactive oxygen species (ROS), which damage mitochondrial proteins and lipids, triggering inflammation and apoptosis, they interact with the sulfhydryl group, disrupting the mitochondrial transport chain and metabolic enzymes, disrupting the plasma membrane and DNA replication, they may also affect the cellular membrane and disrupt its structure, nanoparticles are characterized by their ability to transport the drug or substance to a specific location (Dutt et al., 2023).

1.7.5.1. Chitosan and nanotechnology

Chitin is a biopolymer that serves as the primary raw material for chitosan production. It is abundant in nature, second only to cellulose, and is found in eukaryotic organisms such as insects, fungi, and crustaceans (Eliyah & Hamblin, 2016). Its history dates back to 1859 with the work of Charles Roget, and it was named chitosan by Hoppe-Seyler in 1894. It has been used in diverse fields, including food, agriculture, medicine, pharmaceuticals, and packaging (Morin-Crini et al., 2019).

The properties enjoyed by chitosan, such as biological decomposition and insect, gave it the characteristic of use in agricultural applications without fear of damage to the consumer and not damage the environment. Its use in fertilizers, sheets and seeds paint, Chitosan is characterized by the presence of amino groups that give the ability to melt in mitigating acids (pH <6) and through this property it can be used to purify and treat sewage water by forming complexes with mineral ions, for soluble chitosan under mild conditions, depending on the pH (Ibrahim & El-Zairy, 2015). The US Food and Drug Administration approved chitosan as a safe food additive, and it was also approved in

Japan in the nineties of the last century, as it is considered a biologically active substance (Morin-Crini et al., 2019). Chitosan showed the ability to be used as an antimicrobial against *Escherichia coli,* and studies have shown that crustacean chitosan has a greater antibacterial ability than insect chitosan during the same incubation period of 49 hours and at the same pH 5.0 (Büyükyörük, 2021). Chitosan inhibits plant pathogens, including fungi, by halting the growth of suppressor fungi or killing them with fungicides, chitosan acts as a stimulant, activating and enhancing plant defense responses against pathogens, thereby increasing plant defense reactions against pathogens, thus accelerating the response and halting the pathogen's invasion, it can be considered an inducer of resistance (Benhamou et al., 1994).

Chitosan is used as a nanocarrier to combine pesticides or chemical substances with Chitosan via ionic or covalent bonds, or to encapsulate these substances within chitosan arrays. Due to its properties, chitosan provides homogeneous, stable packaging (Kashyap et al., 2015). In addition to its work as a nanocarrier for agricultural chemicals, nanoscale chitosan can act as an enzyme promoter and an effective antifungal, antiviral, and antibacterial agent (Figure 1) (Maluin & Hussein, 2020). The formation of chitosan nanoparticles is achieved through various strategies, including autogenesis, sedimentation, emulsion cross-linking, consolidation of emulsion droplets, reverse micelles, and sieving (Kashyap et al., 2015).

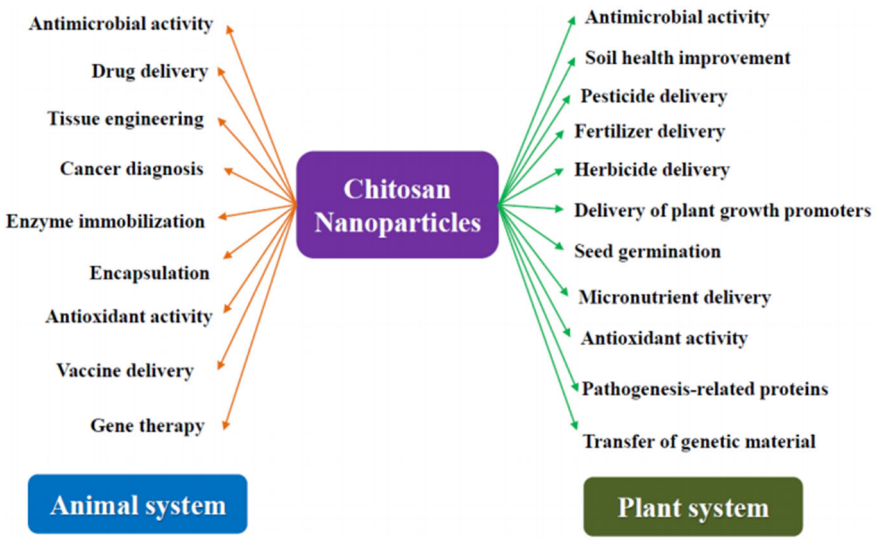


Figure 1. Chitosan nanoparticles and their applications in various fields (Chandrasekaran et al., 2020)

The high surface area of chitosan nanostructures that contact the surfaces of pathogens increases the mechanism's efficiency due to chitosan's small size; it thus enhances the absorption and penetration of chitosan into plant tissues and pathogens (Maluin & Hussein, 2020). There are many areas where chitosan nanoparticles (chitosan NPs) can be used, as they can encapsulate drugs or active molecules and act as nanocarriers that deliver treatments to specific locations with control (Yanat & Sheron, 2021). Chitosan nanoparticles have a positive surface charge and are highly biocompatible, which adds to their ability to adhere to mucosal membranes (Mohammed et al., 2017). Chitosan encapsulates plant actives, enabling controlled release and thereby enhancing their effectiveness. This also reduces waste due to their high bioavailability, furthermore, their nanoscale size facilitates greater cell penetration, protecting both the cell and DNA from the toxic effects of pesticides (Maluin & Hussein, 2020). One of the nano chitosan mechanisms of action is the electrostatic interaction between it as a carrier of positive charge and the cell membranes with negative charge. This interaction results in a change in the permeability of the membranes by causing a change in the cell surface, and thus a disruption in the flow of materials inside the cell and a disruption in the osmotic balance, all these problems and changes may lead to cell death (Shaghati & Jassim, 2023). In this study, the effect of the ethanolic plant extract of *D. viscosa* extract was evaluated, and its effect was assessed after it was converted to the nano-state by linking it to nano-chitosan, the effect of ozone and sea salt in its normal and nano-states was also studied. The effect of all these treatments on the production of mycotoxins DON and MON was tested through *Fusarium* strains isolated from stored wheat in different regions of Iraq.

CHAPTER 2

MATERIAL AND METHODS

2.1. Material

2.1.1. Equipment and Tools Used in the Study

The devices that are used in this study are as shown in the following table:

Table 1. Instruments and equipment used in the study

No.	Apparatus	Manufacturer	Country of origin
1	Autoclave	LAB Tech	South Korea
2	Centrifuge	Labortechnik	Germany
3	Incubator	Memmert	Germany
4	Distillation device	G.F.L.	Germany
5	Magnetic stirrer	Schott	Germany
6	Light microscope with a digital camera	Olympus	Japan
7	Atomic Force Microscopy (AFM)	Nanosurf company	Switzerland
8	High Performance Liquid Chromatography (HPLC)	Syknm, S401	Germany
9	Analytical balance	Denver	USA
10	Microwave oven	Memmert	Germany
11	Laminar Flow Hood Cabinet	Lab Tech	Korea
12	Water bath	DAIHAN scientific co.ltd	Korea
13	Refrigerator	Concord	Lebanon
14	Primers	Bioneer	Korea
15	AccuPower® PCR PreMix	Bioneer	Korea
16	UV-Vis spectrometer	Shimadzu (UV-1800)	Japan
17	PCR and accessories	Bioneer	Korea
18	Fourier Transform Infrared (FT-IR)	8400S	Japan
19	X-ray diffraction (XRD)	phillips xpert	Holland
20	GC-MS system QP2010 model	Shimadzu	Japan
21	Field-Emission Scanning Electron Microscopy	Tescan Mira3 SEM	French
22	Planetary bal mill. ISP04	Korea Process Technology Co., Ltd.	Korea
23	Granite ball mill	Retsch RS 200	Germany

In this study, disposable petri dishes, cover slides, universal tubes, erlenmeyer flask, eppendorf tube, loop, micropipettes and tips, cork borer, dextrose potato medium (PDA), ethanol, chitosan, sodium hypochlorate, distilled water, sodium chloride were used for laboratory studies.

2.2. Methods

2.2.1. Wheat Sampling and Isolation of *Fusarium* spp. Strains from Seeds

During the period from April to May 2021, wheat silos in the eighteen governorates (Baghdad, Al-Anbar, Erbil, Basra, Babil, Dhiqar, Duhok, Diyala, Karbala, Ta'mim, Nineveh, Najaf, Saladin, Muthanna, Maysan, Qadisiyah, Wasit, Sulaymaiyah) representing the southern central and northern regions of Iraq were visited for wheat sampling (Figure 2). These regions were characterized by different environmental conditions in terms of temperature, humidity, rainfall and soil type. Samples were collected from the warehouses and Silos of the General Company for Grain Trade affiliated with the Iraqi Ministry of Trade according to the International Standards Organization (ISO) 136,901.2 (Armitage, 2003). The collected samples were treated as a composite (bulk) sample, where all subsamples from each batch were combined, homogenized, and subsequently reduced to a 3 kg laboratory sample using a rotary divider. All samples were placed in labeled plastic bags and stored at 4 ℃ until analysis. Each wheat samples were surface-sterilized using 1% sodium hypochlorite (NaOCl) for 3 min, rinsed twice with sterile distilled water, and then air-dried on sterile filter paper. Subsequently, ten grains per plate were cultured on PDA media, supplemented with chloramphenicol (50 mg/L). The plates were incubated at 25 ± 2 ℃ for 5 days, after fungal colonies which emerging were subcultured on fresh for purification and identification (Pitt & Hocking, 2009). Pure cultures of the *Fusarium* spp. strains were kept in a refrigerator at 4°C on PDA slant media as stock cultures, and subcultures were performed every six weeks from these stock cultures (Ramires et al., 2018).

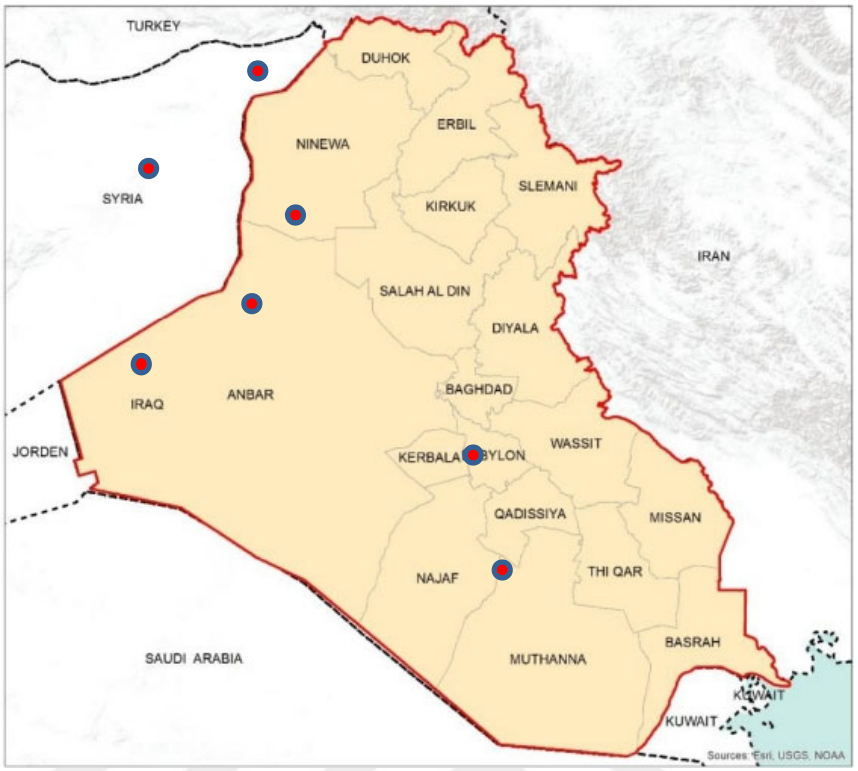


Figure 2. Iraq Administrative map (Zada, 2018)

2.2.2. Morphological identification of the *Fusarium* spp. strains

Purified strains were identified at the genus level based on macroscopic colony characteristics (color, morphology, growth pattern) and microscopic examination with a digital microscope.

Microscopic slides were prepared with lactophenol cotton blue stain (Olympus, Tokyo, Japan), and fungal mrphological identification was performed according to established taxonomic keys and standard mycological procedures (Alsohaili & Bani-Hasan, 2018).

2.2.3. Molecular identification of *Fusarium* spp. strains

The *Fusarium* spp. strains were genetically identified by Polymerase Chain Reaction (PCR) technique using the appropriate primers, ITS1 (5′ TCCTCCGCTTATTGATATGC 3′) and ITS4 (5′ TCCGTAGGTGAACCTGCGG 3′). DNAs of the strains were isolated using the Presto Mini gDNA Yeast kit (GBYB100, Geneaid Biotech, New Taipei City, Taiwan) and PCR was performed in a total volume of 20 µL containing 1 µL of each primer pairs, 6.5 µL AccuPower® PCR PreMix, 5 µL of extracted DNA, and 6.5 µL nuclease free water (White et al.,1990). Amplification was

performed in a thermocycler (Bio-Rad, Pleasanton, CA, USA) under the following conditions: initial denaturation at 95 ºC for 5 min, followed by 35 cycles of denaturation at 95 ◦C for 30 s, annealing at 55 ◦C for 30 s, and extension at 72 ºC for 1 min, with a final extension at 72 ºC for 5 min. Prior to sequencing, PCR amplicons were separated by electrophoresis in a 1X TAE Buffer using agarose gel (1% w/v) stained with ethidium bromide at 0.1 µg/mL. The size of the PCR products was estimated by using a 100 bp size marker (Bioneer, Daejeon, Korea) (Zhang et al., 2012).

2.2.4. Sequencing and data analysis

Commercially prepared PCR amplicons of each strain were sequenced in both forward and reverse directions by an automated DNA sequencer (ABI3730XL) according to the instruction manuals of Macrogen Company (Daejeon, Republic of Korea). The DNA sequences were edited, and aligned, and consensus sequences were generated using the BioEdit Sequence Alignment Editor Software version 7.1 (DNASTAR, Madison, WI, USA). Each of the consensus sequences of the *Fusarium* spp. strains was subjected to the Basic Local Alignment Search Tool (BLAST, version 2.15.0+) program and compared with those strains available at the National Center for Biotechnology Information (NCBI) and deposited in GenBank. For phylogenetic analysis, the accession numbers of these strains are listed and MEGAX software (Version 10.1) was used to construct a phylogenetic tree using the neighbor-joining method (Kumar et al., 2018). The FASTA sequences of the three *Fusarium* spp. isolates identified in this study were deposited in GenBank (supported by Macrogen, Seoul, Republic of Korea).

2.2.5 Pathogenicity test of *Fusarium* spp. strains

For the pathogenicity of *Fusarium* spp. strains, the plates method was used. A disk with a diameter of 0.5 cm was taken from the pure fungal colony growing on PDA medium and inoculated plates were incubated for 3 days at 25±2 °C (Christensen et al., 1988). The wheat grains were surface-sterilized using a 1% sodium hypochlorite solution, and 10 seeds were planted at the edges of the growing colonies in the petri dish, with three replicates. All petri dishes were incubated at 25 ± 2°C until all seeds germinated. The test was conducted twice.

2.2.6. Preparation of ethanolic Extract for *Dodonaea viscosa* (DVE)

D. viscosa leaves were collected from the gardens of Baghdad University, dried and ground into powder. To prepare the *D. viscosa* extract (DVE), one liter of ethyl alcohol (96%) was added to 300 g of *D. viscosa* leaves powder in a glass jar and stirred for three days at room temperature (20-25 °C), the mixture was filtered with a Buchner funnel and then filtered with a glass funnel to remove impurities. A rotary evaporator was used to remove the solvent and dry the solution at 40–60. After three hours, a viscous liquid was obtained and placed in tightly sealed containers in the freezer at −20 °C until use. After solvent evaporation, a viscous crude extract was obtained (48.6 g from 300 g of dry leaf powder), corresponding to an extraction yield of 16.2% (w/w), (Figure 3), (Harborne, 1973; Butler et al., 2013).

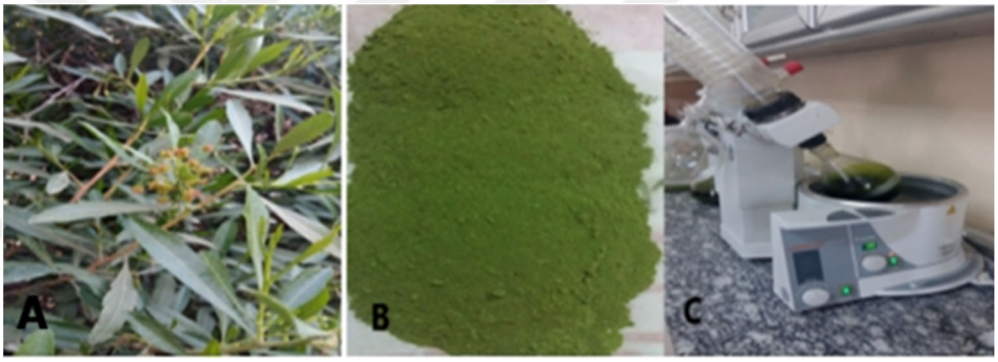


Figure 3. A) *D. viscosa* tree and leaves, B) Grinding the leaves into powder, C: Extraction of ethanolic extract for *D. viscosa* (DVE) process

2.2.7. Identification of the Major Components of DVE Using GC-MS System

A GC-MS system QP2010 (Shimadzu, Kyoto, Japan) was used to identify of components of DVE. Helium was used as a carrier gas, and a micro-syringe was used to inject eight µL of DVE into the GC-MS system. The column temperature program started at 40 °C, the injector temperature was 280 °C while the detector was at 200 °C and, the split ratio was 1:30. The data was processed using software to match and identify the organic compounds in the extracts. The results were evaluated by comparing the retention indices and fragmentation patterns of the mass spectra with those stored in the computer library. The compounds were identified by comparing their spectra with those in the NIST08.LIB mass spectra libraries (Hameed et al., 2015).

2.2.8. Biosynthesis of Chitosan Nanoparticles Loaded DVE

Chitosan (AC00671K, Avonchem Ltd., Macclesfield, UK) was purchased from a commercial supplier. It was dissolved in acetic acid (200 mg/100 mL acetic acid) and mixed with *D. viscosa* extract (1 g DVE/100 mL DW) in equal amounts, and the reaction was carried out using a reflux distillation apparatus. The product was separated using syringe filters, washed three times with pure methanol, and hot distilled water to remove polar and irrelevant compounds, and finally dried in an electric oven at 50 °C (Abd El-Ghaffar and Hashem, 2010). The ionic gelation method was used to produce chitosan nanoparticles loaded with DVE. Acetic acid was used as a solvent at 1%, and 5 mg/mL of the product (chitosan NPs loaded with DVE) was dissolved in the acetic acid solvent. Tripolyphosphate (TPP) was used at a 1:2.5 (w/w) ratio and stirring was continued while adjusting the pH to 7. This reaction was carried out at 25 °C and continued for 6h (Shaghati and Jassim, 2023).

2.2.9. Measurement and Characterization of Nanoparticles

2.2.9.1. UV-Visible spectroscopy

UV-Vis spectrophotometry is a well-established, simple, and cost-effective technique for examining the concentration, and agglomeration of nanoparticles. This technique measures light transmitted through a sample, including both scattering and absorption. Nanoparticles exhibit distinctive optical properties influenced by factors such as size, shape, concentration, agglomeration, and the refractive index near their surface. (Quevedo et al., 2021). The differentiation between the extract and the nanomaterial arises from size-related or quantum effects, such as an increased specific surface area per unit volume, as well as distinct reactivity, optical, thermal, electrical, and magnetic properties (Rauscher et al., 2017). A dual-beam UV-Vis spectrophotometer (Shimadzu UV-1800/ Kyoto, Japan) was used, and all spectra were recorded in a 1 cm quartz cell at room temperature. Distilled deionized water was used as a control, absorbance was calculated using 200-800 nm. Concentrated samples were diluted 1:10 (Agarwal et al., 2018).

2.2.9.2. Fourier-Transform infrared spectroscopy (FT-IR)

The difference in vibrational energy of the functional groups of the compounds corresponds to transition energies in the middle infrared region (4000-400 cm^{-1}) using a

FT-IR spectrometer (Shimadzu 8400S/Japan), and the functional groups were identified, and the absorption peak is observed appears within this region (Mohamed et al., 2017).

2.2.9.3. Atomic Force Microscopy (AFM)

Atomic Force Microscopy (AFM) allows the acquisition of a very accurate, near-atomic image to measure sample topography and provide a clear picture of the sample surface, including roughness and other features. This examination was conducted chitosan nanoparticles loaded with DVE to study the properties of the sample surface and ensure that it reached the nano-size. The same examination was conducted on salt samples that had been ground in special mills to ensure they reached a nano-size suitable for application to the diagnosed *Fusarium* spp. strains (Du et al., 2008).

2.2.9.4. Field-Emission Scanning Electron Microscopy (FE-SEM)

Using scanning electron microscopy (SEM), a beam of electrons is directed at the atoms to reveal the surface topography of the sample, providing a high-resolution image of the sample's shape. A Scanning Electron Microscope (SEM, TESCAN-MIRA3 Czech Republic) was used to investigate the morphology of chitosan NPs-loaded DVE at different magnifications (100 kX, 50 kX, and 30 kX) (Shaghati, 2022).

2.2.9.5. X-ray Diffraction (XRD)

XRD analyses was performed by using XRD Philips XPert PA (Holland), the resulting interference is for a monochromatic beam of rays. International Center for Diffraction Data (ICDD) is an accredited body for searching the X-ray diffraction database, through which the phase of crystalline samples is determined, and includes a wide spectrum of samples. This measurement's range of deviation angles (2θ) was taken between 10 and 80 degrees using monochromatic light (1.5104 nm) from a CuKα source.

2.2.9.6. Energy-dispersive X-ray spectroscopy

EDS is one of the methods used in materials science is based on energy-dispersive X-ray spectroscopy, in which an interaction occurs between the surface of the material and X-rays. It is a physical phenomenon that produces a series of peaks in the electromagnetic spectrum, which gives a picture of the atomic structure of chemical elements. This emitted

energy is recorded and measured through an energy-dispersive spectrometer (Table 2) (Scimeca et al., 2018).

Table 2. Analysis conditions of energy-dispersive X-ray spectroscopy

Condition	used measurement
Accelerating Voltage (kV)	15.0
Beam Current (nA)	1.200
Magnification	63000
Live Time (s)	15
Preset Time (s)	15
Nb Channels	1024
Ev / Channel	10
Offset (keV)	0
Width (keV)	10

2.2.10. *In Vitro* Efficacy of DVE and Chitosan NPs Loaded with DVE in Inhibiting the Growth of *Fusarium* spp.

The DVE was added at three concentrations (0.5, 1, and 1.5%) to each 100 mL of PDA after autoclave, and, after the medium solidified, all plates were inoculated with each freshly grown *Fusarium* spp. strains (1 cm piece in size taken with a cork hole) and placed in the center of the plate. The control group dishes inoculated with *Fusarium* spp. strains (without added DVE/nanoparticles). The experiment was conducted with three replicates for each concentration and incubated at 25 °C for seven days in an incubator. The same previous steps were carried out to examine the effect of the DVE-loaded chitosan NPs with the concentration of 0.75% being used representing half the highest concentration of the *D. viscosa* ethanolic extract (DVE) (Nwankiti & Gwa, 2018). The inhibition rate was calculated using the following formula (Korsten & De Jager, 1995).

$$Inhibition\ percentage\ (\%) = \left((R - R1)/R\right) \times 100 \quad (1)$$

Where,

R = growth diameter rate in control dishes (distance measured in mm)

R1 = growth diameter rate in treatment dishes

2.2.11. Ozone Gas Application and Its Effects on *Fusarium* spp. Strains on PDA

PDA culture medium was poured into Petri dishes, and the dishes were inoculated with *Fusarium* spp. strains at a rate of 1 cm² per Petri dish, with three replicates per group. Ozone gas was generated from a corona discharge ozone generator (5000 mg/h, Anhui Morhon Technology, China). *Fusarium* spp. strains were treated with ozone gas at flow rates of 2 and 4 liters per minute for 30 and 60 minutesand the control group remained untreated. All petri dishes were incubated at 25 ± 2°C for seven days (Figure 4). Three plates were used for each and the percentage of fungal growth inhibition were calculated according to the equation mentioned above in paragraph 2.2.10.



Figure 4. The ozone gas treatment of *Fusarium* spp. strains

2.2.12. Efficiency of Sea Salt and Nano Sea Salt in inhibiting *Fusarium* spp. strains

Sea salt samples were sent to the laboratories of the Materials Department at the Ministry of Science and Technology in Iraq for grinding and converting it to a nanoscale size using a mill (Retsch RS 200) and a granite ball mill (Planetary Bal Mill.isp 04). The *Fusarium* spp. strains were treated with the following concentrations 1, 2, 2.5, and 3% of sea salt - nano sea salt and a control group was left untreated. A 1 cm diameter colony disc was inoculated into the center of the plate using a cork punch from the edges of a fungal colony grown for seven days on PDA culture medium. The plates were then incubated at 25 ± 2 °C for seven days (Cooley et al., 1996). The growth rate and percentage inhibition were calculated using the equation described in Section 2.2.10.

2.2.13. Testing the DON and MON Mycotoxins production from *Fusarium* spp. strains after treatments

For mycotoxin induction, 150 g of wheat was moistened with 100 mL of distilled water to serve as the culture substrate. The glass incubation bottles were sterilized in an autoclave at 121 ºC and 1.5 kg/cm2 pressure for 20 min, after which they were inoculated with *Fusarium* spp. previously grown on PDA. The inoculated wheat was thoroughly mixed and incubated at 25 ± 2 ºC for 21 days. The DVE, its nano-chitosan-loaded formulation, sea salt, nano sea salt and ozone gas were applied only during the active toxin production phase at different concentrations. The reduction in DON and MON levels as a direct result of the treatments interference with active mycotoxin biosynthesis was quantified using high-performance liquid chromatography (HPLC). A HPLC system (Syknm S4011, Stuttgart, Germany) was used to measure DON and MON concentrations, following previously reported protocols with minor modifications (Shotwell et al., 1966; Lai et al., 2015). For the extraction of DON and MON, 20 g of sample was mixed with 100 mL of distilled water in Nalgene bottles and shaken for 1 h using a reciprocating shaker. The toxins mixture was then centrifuged at 3200× g for 5 min and filtered through Whatman No. 1 folded filter paper. A 2 mL aliquot of the filtrate was diluted to 10 mL with distilled water and clarified using a microsyringe and a 0.45 µm membrane filter. For HPLC confirmation, another 2 mL aliquot was diluted to 10 mL with water and loaded onto an Oasis HLB cartridge preconditioned with 5 mL of methanol followed by 5 mL of water. The cartridge was washed with 2 mL of water, dried under vacuum for 15 min, and eluted with 4 mL of methanol. The eluate was evaporated to dryness under a gentle nitrogen stream and reconstituted in 200 µL of methanol/0.1% aqueous acetic acid + 1 mM ammonium acetate (20:80, v/v). HPLC separation was performed using a Zorbax SB-C18 column (25 cm × 4.6 mm i.d.) with a mobile phase consisting of water and acetonitrile (30:70, v/v) at a flow rate of 1.2 mL/min (Gonçalves et al., 2020). Calibration curves were constructed using certified DON and MON standards over the range of 1–5 µg/L; both curves showed linearity ($R^2 > 0.999$). The retention times were 3.9 and 6 min for DON and MON, respectively. LOD and LOQ values were 0.062 and 0.189 µg/L for MON while they were 0.137 and 0.415 µg/L for DON, respectively. The following equation was used to calculate the mycotoxin inhibition ratio:

$$\text{Inhibition ratio (\%)} = ((B0 - B1)/B0) \times 100 \quad (2)$$

B0, B1 values represent the DON and MON mycotoxin concentration produced before treatment (control group), and after treatment, respectively (Yazid et al., 2023).

2.2.14. Statistical Analysis

Laboratory experiments were conducted using three replicates for each treatment. Statistical analysis was applied to all results and data obtained from the above-mentioned tests. The Statistical Packages of Social Sciences-SPSS (2019) program was usedto detect the effect of difference factors in study parameters. Least significantdifference-LSD was used to significant compare between means in this study.

CHAPTER 3

RESULTS

3.1. Wheat Sampling

3.1.1. Wheat Sampling for *Fusarium* spp. Strains

A total of 51 stored wheat samples were collected from eighteen governorates in Iraq (Table 3). Seven strains of *Fusarium* were isolated from seven governorates: *Fusarium pseudograminearum* 2 (Duhok), *Fusarium pseudograminearum* 3 (Maysan), *Fusarium oxysporum* 4 (Anbar), *Fusarium oxysporum* 5 (Nineveh), *Fusarium pseudograminearum* 6 (Tamim), *Fusarium pseudograminearum* 7 (Salah ad-Din), and *Fusarium chlamydosporum* 8 (Basra).

Table 3. Wheat sampling from different Governorates of Iraq

NO.	Governorates	Number of wheat samples
1	Baghdad	4
2	Al-Anbar	3
3	Erbil	2
4	Babil	2
5	Basra	2
6	Dhi Qar	3
7	Duhok	3
8	Diyala	3
9	Karbala	3
10	Ta'mim (Kirkuk)	3
11	Muthanna	3
12	Maysan	2
13	Nineveh	4
14	Najaf	3
15	Qadisiyah	2
16	Saladin	2
17	Sulaymaniyah	3
18	Wasit	4
	Total	51

3.1.2. Morphological identificatication of *Fusarium* spp. strains

After isolation seven strains from wheat samples, were morphologically identified and found to be these strains belonged to three *Fusarium* spp.: *Fusarium oxysporum*, *F. pseudograminearum*, and *F. chlamydosporum*. On PDA medium, the colonies exhibited soft, pale, cottony mycelial growth. Strains 4 and 5 were identified as *F. oxysporum*, showing colony colors ranging from white to pale purple. Strains 2, 3, 6, and 7 were classified as *F. pseudograminearum*, with colonies displaying white to cream pigmentation. Strain 8 was identified as *F. chlamydosporum*, characterized by a light pink to dark red colony color (Figure 5), (Figure 6).

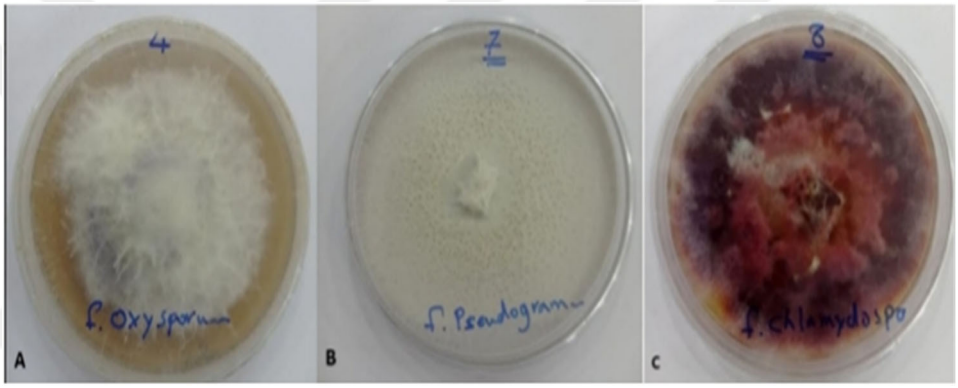


Figure 5. Morphological characteristics of three *Fusarium* spp. on PDA. a: *Fusarium oxysporum* strain 4, b: *Fusarium pseudograminearum* strain 7 and c: *Fusarium chlamydosporum* strain 8

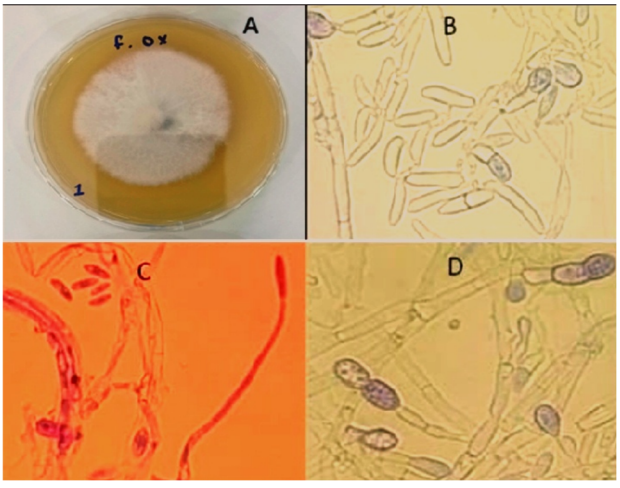


Figure 6. The microscopic examination of *Fusarium* strains distinguished by their morphological characteristics; A) *Fusarium oxysporum* growing on a PDA, B) macroconidia of *Fusarium*, C) Conidiophores of *Fusarium oxysporum*, and D) Spore-forming stimuli in *Fusarium* species

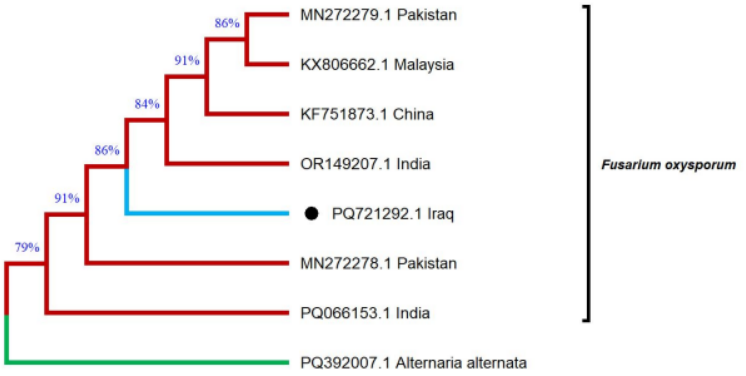
3.1.3. Molecular identificatication of *Fusarium* spp. strains

The genetic identity of all strains was confirmed by (PCR) analysis, as presented in Table 4. Three *Fusarium* spp. strains representing the species previously identified morphologically were further confirmed at the molecular level and deposited in the GenBank database. Their corresponding accession numbers are: *F. oxysporum* strain 4 PQ721292.1, *F. pseudograminearum* strain 2, PQ721291.1, and *F. chlamydosporum* strain 8 PQ721294.1, respectively.

Table 4. *Fusarium* spp. strains gen bank accession numbers

Identity of the strains	Location	GenBank acc. No
Fusarium pseudograminearum strain 2	Iraq	PQ721291.1
Fusarium pseudograminearum strain 3	Iraq	MT465500.1
Fusarium oxysporum strain 4	Iraq	PQ721292.1
Fusarium oxysporum strain 5	Pakistan	MN272279.1
Fusarium pseudograminearum strain 6	Iraq	MT465500.1
Fusarium pseudograminearum strain 7	China	MZ312460.1
Fusarium chlamydosporum strain 8	Iraq	PQ721294.1

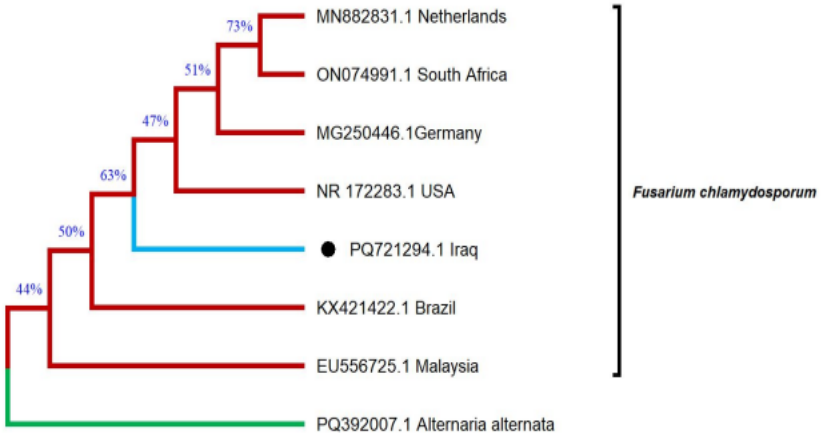
The phylogenetic clustering of these isolates with reference strains from different geographical regions validates their taxonomic identity and demonstrates their genetic relatedness at a global scale (Figure 7). This molecular confirmation not only supports the accuracy of strain identification but also contributes to the enrichment of publicly available *Fusarium* spp. *genomic* data from Iraq. After purification *Fusarium* spp. strains were stored on PDA slant media in a refrigerator at 4°C.



(a)



(b)



(c)

Figure 7. A phylogenetic tree was constructed for three isolates belonging to three *Fusarium* spp. strains from wheat stored in Iraq. a) *F. oxysporum* (PQ721292.1 Iraq), b) *F. pseudograminearum* (PQ721291.1 Iraq), c) *F. chlamydosporum* (PQ721294.1 Iraq)

3.1.3. Pathogenicity test of *Fusarium* spp. Strains

The results showed that all tested *Fusarium* spp. strains caused a significant decrease in the germination percentage of wheat seeds (Figure 8) which ranged from 16.66% to 6.66%, compared to the control treatment, which had a germination percentage of 100% to 96.99%, as shown in Table 5. The highest inhibition percentage was observed for strain 3, where the germination percentage decreased from 100% to 6.66%, while strain 4 showed the lowest inhibition percentage, with a decrease from 100% to 16.66%. Inhibition rates for the other strains ranged between these two values. The test was performed with three replicates for each strain.

Table 5. Pathogenicity test for *Fusarium* strains shows the effect of the fungus on seed germination on PDA in *vitro*

***Fusarium* strains**	**Germination rate (%) control group**	**Germination rate (%) with *Fusarium* strains**	**L.S.D.**
F. pseudograminearum strain 2	96.66 ±3.68 ^{Aa}	10.00 ±0.62 ^{ABb}	5.69 NS
F. pseudograminearum strain 3	100 ±0.00 ^{Aa}	6.66 ±0.47 ^{Bb}	9.72 *
F. oxysporum strain 4	100 ±0.00 ^{Aa}	16.66 ±1.04 ^{Ab}	10.08 *
F. oxysporum strain 5	96.66 ±3.68 ^{Aa}	13.33 ±0.84 ^{ABb}	9.66 *
F. pseudograminearum strain 6	100 ±0.00 ^{Aa}	10.00 ±0.62 ^{ABb}	10.00 *
F. pseudograminearum strain 7	100 ±0.00 ^{Aa}	13.33 ±0.84 ^{ABb}	9.85 *
F. chlamydosporum strain 8	96.66 ±3.68 ^{Aa}	13.33 ±0.84 ^{ABb}	9.66 *
L.S.D.	4.98 NS	7.083 *	---

Means having different big letters in same column and small letters in same row differed significantly. * (P≤0.05), NS: Non-Significant

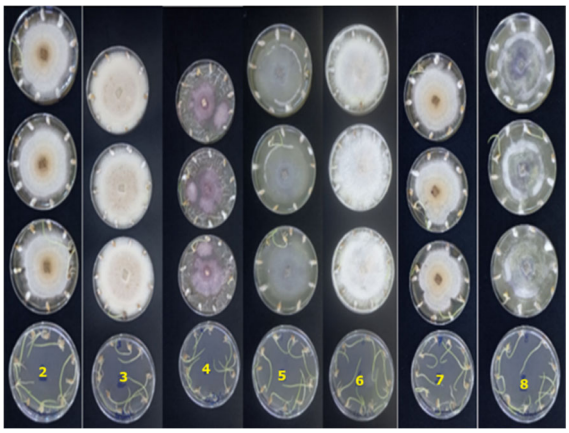


Figure 8. Pathogenicity test for *Fusarium* spp. strains on PDA; *F. pseudograminearum* strain 2, *F. pseudograminearum* strain 3, *F. oxysporum* strain 4, *F. oxysporum* strain 5, *F. pseudograminearum* strain 6, *F. pseudograminearum* strain 7 and *F. chlamydosporum* strain 8. The plates numbered in yellow at the bottom represent the control group, and the others are the replicates

3.1.4. Testing the Effect of DVE on the Growth of *Fusarium* spp. Strains

The inhibitory effect of DVE on the tested *Fusarium* spp. strains increased progressively with rising extract concentration (Figure 9), (Table 6). At an extract concentration of 0.5%, the highest growth inhibition was observed in *F. oxysporum* strain 5 (63.37%), whereas the lowest was recorded in *F. pseudograminearum* strain 6 (15.16%). Increasing the extract concentration to 1.0% further enhanced the inhibitory effect, with *F. oxysporum* strain 5 again showing the strongest response (67.13%), while *F. pseudograminearum* strain 6 remained the least affected (20.64%). The maximum inhibition levels were recorded at 1.5% DVE, reaching 68.94% in *F. oxysporum* strain 5, compared to only 22.58% inhibition in *F. pseudograminearum* strain 6.

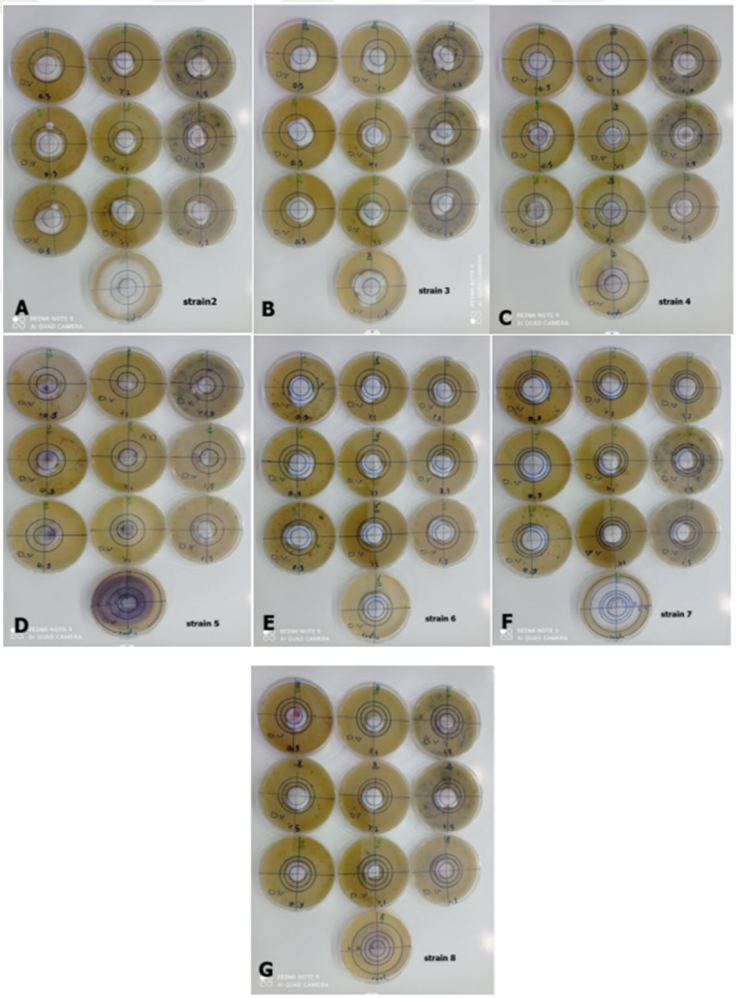


Figure 9. The effect of the ethanolic extract of *D. viscosa* leaves (DVE) in inhibiting the growth of *Fusarium* spp. strains, (a): *F. pseudograminearum* strain 2, (b): *F. pseudograminearum* strain 3, (c): *F. oxysporum* strain 4, (d): *F. oxysporum* strain 5, (e): *F. pseudograminearum* strain 6, (f): *F. pseudograminearum* strain 7, and (g): *F. chlamydosporum* strain 8

Analysis of variance confirmed that the effect of DVE was statistically significant across all strains and concentrations. Post hoc LSD analysis further revealed that the inhibition at 1.5% was significantly higher than at 0.5% for all strains, while the differences between adjacent concentrations (0.5% vs. 1.0% and 1.0% vs. 1.5%) were comparatively less pronounced.

Table 6. Mean inhibition percentage (%) of *Fusarium* spp. strains treated with different concentrations of *D. viscosa* extract (DVE)

***Fusarium* spp. Strains**	**Inhibition Ratio (%) After 0.5% DVE Treatment**	**Inhibition Ratio (%) After 1% DVE Treatment**	**Inhibition Ratio (%) After 1.5% DVE Treatment**	**L.S.D.**
F. pseudograminearum strain 2	61.11 ±3.51 $^{A\,b}$	66.25 ±3.75 $^{A\,ab}$	68.00 ±3.83 $^{A\,a}$	6.092 *
F. pseudograminearum strain 3	34.25 ±2.07 $^{C\,a}$	36.75 ±2.41 $^{C\,a}$	39.25 ±2.55 $^{C\,a}$	5.188 ^{NS}
F. oxysporum strain 4	35.85 ±2.37 $^{C\,b}$	39.02 ±2.76 $^{C\,ab}$	42.43 ±2.17 $^{C\,a}$	5.863 *
F. oxysporum strain 5	63.37 ±3.81 $^{A\,b}$	67.13 ±4.02 $^{A\,ab}$	68.94 ±4.60 $^{A\,a}$	5.337 *
F. pseudograminearum strain 6	15.16 ±0.83 $^{D\,b}$	20.64 ±2.17 $^{D\,ab}$	22.58 ±1.36 $^{D\,a}$	5.074 *
F. pseudograminearum strain 7	58.23 ±2.94 $^{A\,b}$	63.62 ±3.70 $^{A\,ab}$	64.76 ±2.98 $^{A\,a}$	5.859 *
F. chlamydosporum strain8	45.00 ±2.67 $^{B\,b}$	51.75 ±2.81 $^{B\,a}$	55.00 ±2.62 $^{B\,a}$	6.045 *
L.S.D.	7.537 *	7.911 *	6.805*	---

Means having different big letters in same column and small letters in same row differed significantly. * (P≤0.05), NS: Non-Significant

3.1.5. Identification of the components of DVE by using a GC-MS system

A total of 27 compounds were detected in the DVE based on gas chromatography–mass spectrometry (GC–MS) analysis (Table 7). The major chemical classes identified were glycosides, saponins, and alkaloids, the most abundant compound was 4-Cyclohexyl-1-(furan- 2-ylmethyl)-4H,5H,7H-pyrazolo [3,4-b]pyridin-6-one, followed by 4′ ,5,7-trihydroxy-3,6- dimethoxyflavone, 6-methoxy-2-[2-(imidazol-1-yl)ethoxy]-8-nitroquinoline, and 3-heptanol (TMS derivative), *Dodonaea viscosa* is a member of the Sapindaceae family and has been reported to contain antimicrobial, antitoxic, and cytotoxic bioactive compounds (Al-Snafi, 2017). It also contains catechol, a phenolic compound known for its inhibitory effects against certain fungi and bacteria, including *Fusarium oxysporum* and *Penicillium italicum* (Kocaçalışkan et al., 2006). In addition, neophytadiene, a terpenoid constituent of the leaf extract, has been documented as a

strong antioxidant and an active antimicrobial agent against fungal and microbial infections (Pratama et al., 2019).

Omosa et al. (2014) further reported the isolation of flavonoids such as 5-hydroxy- 3,4′ ,7-trimethoxyflavone, santin, and pinocembrin, as well as diterpenoids including dodonic acid and hautriwaic acid from the leaf surface exudates of D. *angustifolia*, these phytochemical classes exhibit strong chemical similarity to the major constituents identified in the present study, therefore, the current findings strongly confirm that *D. viscosa* possesses a phytochemical profile predominantly characterized by flavonoids and diterpenoids (Figure 10).

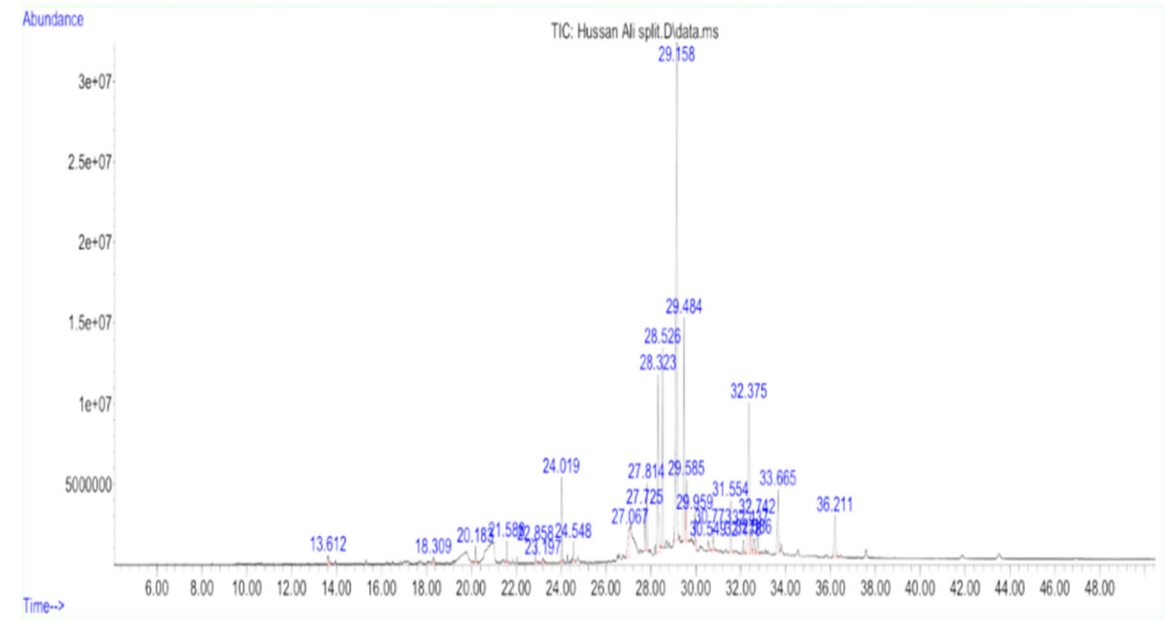


Figure 10. Gas chromatography-mass spectrometry (GC-MS) chromatogram of the ethanolic *D. viscosa* extract

Table 7. Identified components of ethanolic leaf extract of *D. viscosa* using GC-MS system

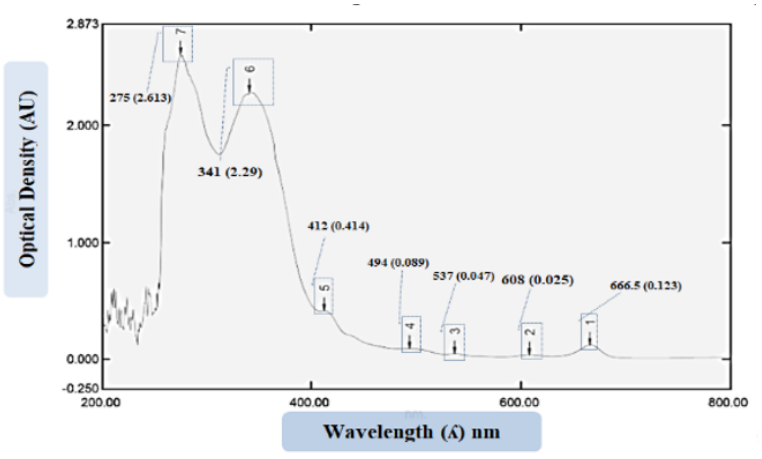
Peak	RT	Area%	Name
1	13.612	0.6533	Catechol
2	18.309	0.437	Methyl 4-O-methyl-.beta.-D-xylopyranoside
3	20.183	0.537	Benzene, 1,2-dimethoxy-4-(1-propenyl)-
4	21.588	0.5637	Neophytadiene
5	22.858	0.6602	n-Hexadecanoic acid
6	23.197	0.3448	2H-2,4a-Ethanonaphthalene, 1,3,4,5,6,7-hexahydro-2,5,5-trimethyl-
7	24.019	2.509	Diallylphenylvinylsilane
8	24.548	0.7617	9,12,15-Octadecatrienoic acid, (Z,Z,Z)-
9	27.067	3.2703	Phosphinic acid, diphenyl-, methyl ester
10	27.725	1.5871	4H-1-Benzopyran-4-one, 2,3-dihydro-5,7-dihydroxy-2-phenyl-, (S)-
11	27.814	3.0364	Alizarin, 1,2-O-(phenylboranediyl)-
12	28.323	9.2764	3-Heptanol, TMS derivative
13	28.526	6.6795	(3aR,9aS)-2,2,3a-Trimethyl-3,3a,4,5-tetrahydroindeno[7a,1-b]furan-7(2H)-one
14	29.158	32.2167	4-Cyclohexyl-1-(furan-2-ylmethyl)-4H,5H,7H-pyrazolo[3,4-b]pyridin-6-one
15	29.484	9.379	6-Methoxy-2-[2-[imidazol-1-yl]ethoxy]-8-nitroquinoline
16	29.585	2.919	Cyclohexanol, 1-ethynyl-
17	29.959	0.9615	16-Heptadecyn-4-one, 1,2-dihydroxy-
18	30.549	0.4411	Eicosane
19	30.773	1.169	trans-1-Methyl-7-methylenebicyclo(4.4.0)decan-3-one
20	31.554	1.9718	2-(4-Hydroxyphenyl)-3,6,7-trimethoxy-5-hydroxy-4H-1-benzopyran-4-one (penduletin)
21	32.118	0.5439	Eicosane
22	32.375	9.8093	4',5,7-Trihydroxy-3,6-dimethoxyflavone
23	32.437	1.1655	Vitamin E
24	32.586	0.9355	Naphthalene, 6-(1-ethylpropyl)-1,2,3,4-tetrahydro-
25	32.742	1.6076	3,4'-Di-O-methyleupalitin
26	33.665	3.8315	2-(4-Hydroxyphenyl)-3,6,7-trimethoxy-5-hydroxy-4H-1-benzopyran-4-one (penduletin)
27	36.211	2.7323	D: A-Friedooleanane

3.1.7. Conformational and morphological analysis of chitosan NPs loaded with DVE

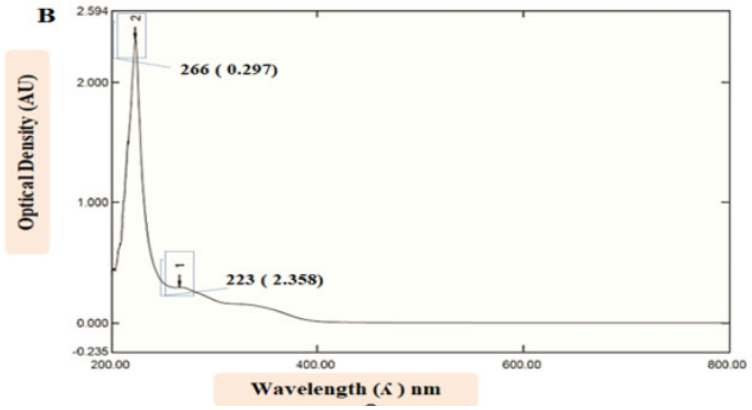
3.1.7.1. UV-Visible Spectroscopy

Ultraviolet (UV–Vis) spectrophotometer was used as an initial confirmatory technique to verify the biosynthesis of chitosan NPs loaded with DVE. The UV–Vis spectrum of the DVE (Figure 11.A) exhibited two characteristic absorption bands at 266 nm (OD ≈ 2.358) and 233 nm (OD ≈ 0.297), which are typical for aromatic phenolic and flavonoid compounds, in contrast, the spectrum of the DVE-loaded chitosan nanoparticles (Figure 11 B) revealed a distinct bathochromic (red) shift in the main peak toward 275 nm (OD ≈ 2.613), accompanied by a secondary absorption band at 341 nm, indicating strong

intermolecular interactions between DVE phytochemicals and the protonated amino groups of chitosan. This wavelength shift, along with the notable increase in absorbance intensity, confirms the successful encapsulation and molecular stabilization of DVE within chitosan. Furthermore, the broad secondary absorbance region spanning 400–700 nm in the nanoparticle spectrum suggests enhanced light scattering due to nanoscale colloidal behavior and surface roughness, a feature typical of plant-derived biopolymeric nanocarriers. The absence of additional degradation peaks suggests that no photolytic breakdown occurred during nanoparticle synthesis.



(a)



(b)

Figure 11. UV–Visible spectrophotometer test: a) DVE, b) Chitosan NPs loaded with DVE

3.1.7.2. Fourier transform infrared spectroscopy (FT-IR)

The spectrum of the DVE (Figure 12A) exhibits distinct peaks characteristic of various biomolecules, including phenol and alcohol (3610-3640). These observations are consistent with the expected composition of DVE and chitosan molecules. The spectrum

of the biosynthesized nanoencapsulated particles (Figure 12B) demonstrates a high degree of similarity to the DVE spectrum, suggesting the successful attachment of biomolecules from the extract to the surface of the nanoparticles. These biomolecules could include phenol, alkaloid, Terpenoid, flavonoids, and water molecules. Additionally, residual O-H groups originating from the synthesis process might contribute to the observed peaks. A detailed breakdown of the identified functional groups and their corresponding wavenumbers is provided in (Table 8). A key observation is the difference in intensity between the amide I peak (1699.29) cm^{-1} in the chitosan NPs loaded with DVE spectrum and the corresponding peak (1639.94) cm^{-1} in the DVE/Chitosan NPs spectrum. The higher intensity in the nanoparticle's spectrum suggests a higher concentration of amides associated with the nanoparticles. This finding could be attributed to the attachment of many biomolecules during the synthesis process, which may act as stabilizing agents. In other hand the absent of some peaks in chitosan NPs loaded with DVE (1150-1300, 1685- 1710, 2850- 3000) were refer into the attachment sit between DVE and chitosan molecules to biosynthesis encapsulated nanoparticles was agree the result of Sathiyabama et al., (2024). When the C-H stretch was seen at 2927 cm^{-1}, it provided structural information on chitosan.

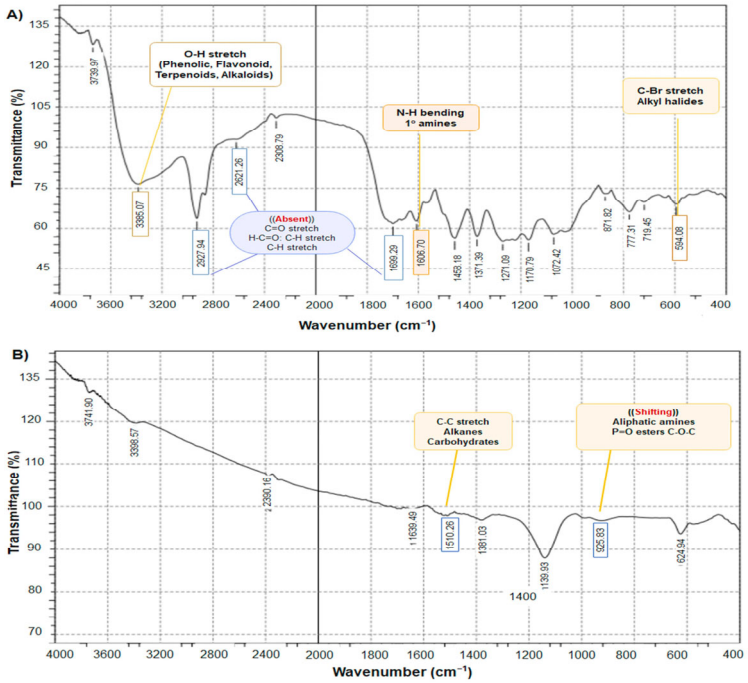


Figure 12. FTIR spectra, A) DVE, B) chitosan NPs loaded with DVE

By comparing the DVE/chitosan NPs loaded with DVE, it was noticed that the absence of many peaks due to the cross-linking of TPP may be attributed to the fact that the large molecules were fragmented into smaller units. The interaction between chitosan and TPP was responsible for the increase in the total surface area, as shown in Figure 11 B, indicating that the repositioned chemical groups facilitated the efficient loading of the extract into the chitosan/TPP matrix and the formation of nanoencapsulation of the extract. As additional supporting evidence, the shifted peaks are consistent with the formation of a new complex. Modifications to the functional groups of bioactive molecules suggest a relationship with the synthesis of DVE/chitosan NPs (Almukhtar and Karam, 2020).

Table 8. Results the FTIR analysis of DVE, chitosan NPs loaded with DVE

DVE Functional groups cm^{-1}	**Description**	**Chitosan NPs loaded with DVE Functional groups cm^{-1}**
594.08 C-Br stretch	Alkyl halides	624.94 Higher intensity compared to the DVEt suggest higher concentration alkyl halides compound (saponin, coumarin, terpenoids groups)
(665-910) 719.45, 777.31, 871.82 N-H wag	1',2' amines	925.83 Shifting to three peaks and reducing to one peak on the other hand, higher intensity compared to the Dodoneae extract suggests higher concentrations of amine compounds (alkaloids, proteins, phenolics, Terpenoids).
1020- 1250 1072.42, 1170.79 C-N stretch	Aliphatic amines P=O esters C-O-C	1139.93 shifting the two peaks likely due to C-O stretching in alcohols, esters, and ethers, possibly from encapsulated biomolecules (phenolic, flavonic, terpenoids, alkaloid and saponin) compounds with TPP brig connection to chitosan compound
1150-1300 1271.09 C-H wag (-CH2X)	Alkyl halides	Absent this peak may be sit of attachment with chitosan molecules possibly from encapsulated biomolecules
1371.39 C-H rock P=O, C-F, C-O,C -OH	Alkanes	1381.03 Likely due to C-OH stretching in alcohols, esters, and ethers, possibly from encapsulated biomolecules (phenolic, flavonic, terpenoids, alkoloids) compounds and with higher intensity than extract because biosynthesis nanoparticles with higher surface structure with lower the size of particles
1400-1500 1458.18 C-C stretch (in –ring)	Alkanes	1510.26 may be refer to the chitosan molecule and carbohydrate of DVE
1580- 1650 1606.7 N-H bend	1' amines	1639.94 higher intensity compared to the DVE suggest higher concentration compound (saponin, alkoloids, phenol) groups
1685-1710 1699.29 C=O stretch	A, β- Unsaturated ketone	Absent Sit of reaction and attachment between chitosan and active compound of DVE to biosynthesis nanoencapsulation particles

2308.79 C-N stretch	Nitriles	2380.16 higher intensity compared to the DVE suggest higher concentration compound (saponin, alkoloids, phenol) groups
2695-2830	Aldehydes	Absent
2621.26 H-C=O: C-H stretch		Sit of reaction and attachment between chitosan molecule and active compound of DVE to biosynthesis nanoencapsulation particles
2850- 3000	Alkanes	Absent
2927.94 C-H stretch		Sit of reaction and attachment between chitosan molecule and active compound of DVE to biosynthesis nanoencapsulation particles
3200- 3500	Alcohols, phenols	3398.57 Likely due to O-H stretching and H-bonded in alcohols, phenol, possibly from encapsulated biomolecules (phenolic, flavonic, terpenoids, alkoloids) compounds
3385.07 O-H stretch, H-bonded		
3610-3640	Alcohols, phenols	3741.90 Likely due to O-H stretching and H-bonded in alcohols, phenol, possibly from encapsulated biomolecules (phenolic, flavonic, terpenoids, alkoloids) compounds and chitosan molecules
3739.97 O-H stretch		

3.1.7.3. Atomic Force Spectroscopy (AFM)

The AFM analysis of the biosynthesized chitosan NPs loaded with DVE is presented in Figure 13. A total of 158 individual nanoparticles were characterized, with a particle density of 9.92×10^6 particles/mm^2, the particles exhibited a high degree of morphological heterogeneity, showing predominantly elongated and plate-like structures with occasional sharp edges and clustered aggregates. According to the statistical output, the mean particle diameter was 105.7 nm, which is consistent with the expected nanoscale range. The surface topography displayed a relatively rough and uneven texture, as confirmed by the 3D scan, which enhances the available surface area for potential interactions with bioactive molecules such as plant-derived compounds. The mean Z-height of the particles was 205.4 nm, indicating pronounced vertical protrusions rather than a flat morphology. The observed nanoparticle aggregation could partially be attributed to sample handling and drying effects during AFM preparation, which is a common observation in chitosan-based nanostructures. These findings are in agreement with Shaghati & Jassim (2023), who reported similar AFM features for clove-extract-loaded chitosan nanoparticles, including non-spherical particles and moderate aggregation due to intermolecular interactions between chitosan and the phytochemical constituents.

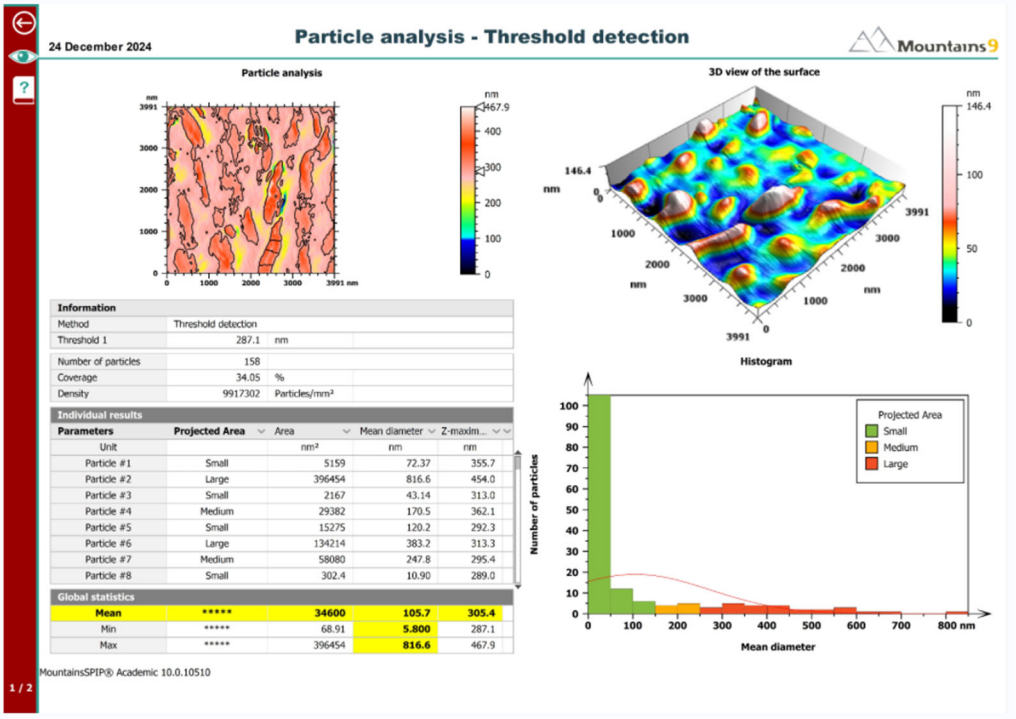


Figure 13. AFM surface morphology and particle size distribution of chitosan NPs loaded with DVE

3.1.7.4. Field Emission Scanning Electron Microscopy (FESEM)

FESEM was used to investigate the morphology of nanoparticles prepared from *Dodonaea viscosa* plant extract-loaded chitosan at different magnifications (100 kX, 50 kX, and 30 kX). Figure 14A shows that spherical nanoparticles with diameters of approximately 57–86 nm indicate successful ionic gelation with TPP.This morphological feature is commonly observed in chitosan-based nanoparticle systems and corresponds to the early-stage of nanoparticle aggregation following fabrication (Figure 14B). In the 30kX image (Figure 14C), the surface appears more complex and interlaced, with high-density regions composed of tightly packed nanoparticles are interspersed with low-density areas exhibiting pore- or void-like structures. These structural differences may be attributed to the non-homogeneous dispersion of the plant extract within the chitosan matrix or rapid solvent evaporation, which can lead to surface shrinkage. The majority of the nanoparticles exhibited a spherical morphology with a relatively uniform size distribution ranging between 38 and 79 nm.

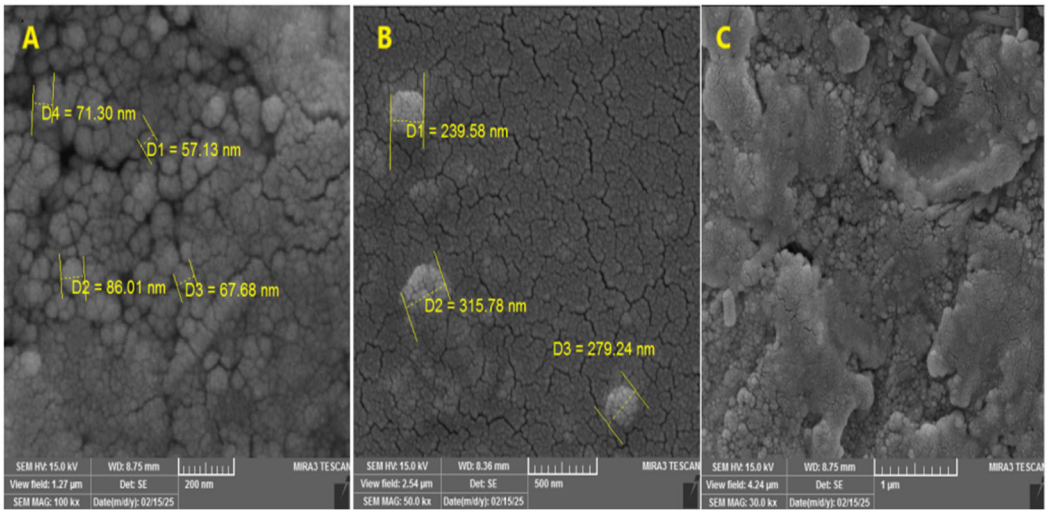


Figure 14. SEM micrographs of chitosan NPs loaded with DVE: (A) primary nanoparticles (100,000×), B) secondary agglomerates after drying (50,000×), and C) irregular surface morphology with apparent porosity (30,000×)

3.1.7.5. Energy-dispersive X-ray spectroscopy (EDX)

To cross-check the elemental constituents of the nanoparticles synthesized from chitosan and *D. viscosa* plant extract using sodium tripolyphosphate (TPP), the energy dispersive X-ray spectroscopy (EDX) technique was utilized. EDX is also an excellent analytical tool, often coupled with scanning electron microscopy, that helps obtain qualitative and semi-quantitative information about elements of the sample by measuring the energies of X-rays emitted when bombarding a high-energy electron beam on the sample (Hodoroaba, 2019).

The EDX analysis and the weight gain analysis showed that the nanoparticles of chitosan and plant extract were successfully prepared. This confirms the presence of some significant chemical elements introduced into the nanoparticles due to the ionic gelation reaction. It also indicates some contaminants, most likely originating from the raw materials source or the preparation environment (Figure 15).

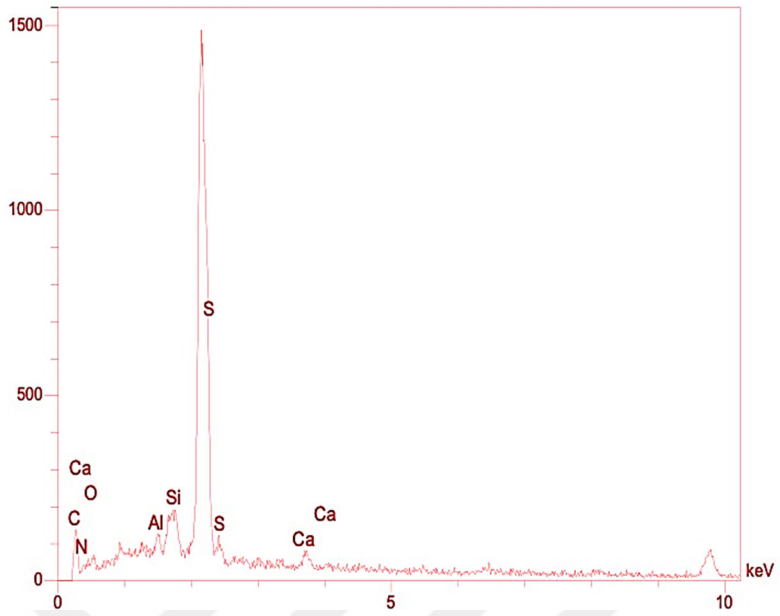


Figure 15. EDX analysis of chitosan NPs loaded with DVE

3.1.7.6. X-ray Diffraction (XRD)

X-ray diffraction (XRD) is performed to investigate the crystalline structure of the materials. It is a widely used technique for studying changes in the internal structure and conformation induced by chemical modification or loading with active molecules. This technique is based on scanning X-rays through atomic planes in the material, producing a unique diffraction pattern that identifies crystal type, degree of crystallinity, crystal dimensions, and crystal modifications (Seeck & Murphy, 2015).

The Figure 16 shows the XRD spectrum of the sample where two important peaks can be observed at the diffraction angles, 2θ = 14.985 and 22.604. The emergence of these peaks indicates a different fraction of intermolecular crystalline order than that observed in raw chitosan, which shows a specific peak at ≈20.5. The shift in the peak and the significant change in diffraction intensity was attributed to the chemical interaction between chitosan and the active compounds in the plant extract of *D. viscosa*. These compounds are phenolic or terpenoid and can form hydrogen or covalent bonds with the amine group in chitosan. The interaction allows for rearrangement of the polymer chains, and a change in the crystal lattice results in increased crystallinity, as shown in the peak at 22.6. These are more significant than 40% high peak widths (FWHM) (0.678 and 0.838) with the small crystallite size (9–12 nm), indicating that nanoparticles with intermediate crystallinity are created.

These findings demonstrate that incorporating plant extracts into chitosan can sometimes facilitate crystallization by molecular organization during the reaction. It also verifies that the variations in the diffraction pattern are directly caused by the interaction of chitosan with the natural extract, through both physical and chemical bonds. Kahdestani et al. (2021) have shown that changes in the molecular arrangement in the crystal lattice can account for differences in the patterns, and the pattern of teicoplanin-loaded chitosan nanoparticles shows decreased peaks at 2θ 22 and 25, indicating a decrease in intensity. As stated by Shaghati (2022), the peaks in the XRD pattern of the chitosan were found at 2θ = 20.53 at an intensity of about 1200 counts, while the extract-loaded sample was found at 2θ = 22.8596 at 736.55 counts. The changes in intensity were ascribed to a change in the sample's crystalline structure upon interaction with the extract, which increased crystallinity.

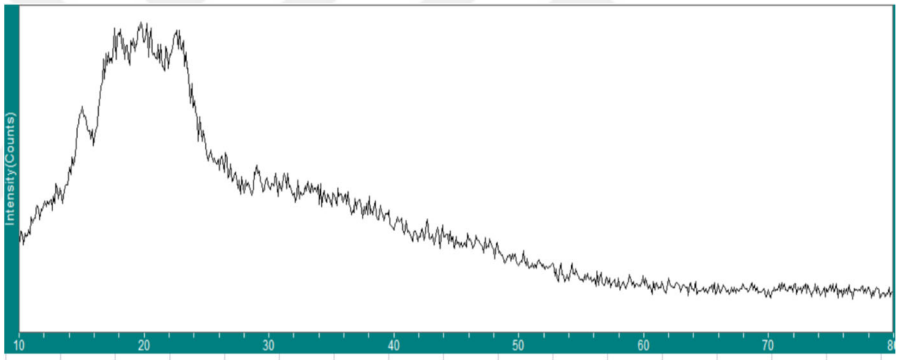


Figure 16. XRD spectrums of chitosan NPs loaded with DVE

3.1.8. Effect of chitosan NPs loaded with DVE on *Fusarium* spp. strains

The antifungal activity of chitosan NPs loaded with DVE was evaluated at 0.75%, which corresponds to the average concentration used for the ethanolic extract in the standard formulation, the nanoparticles exhibited an apparent inhibitory effect against all *Fusarium* spp. strains tested. The highest inhibition rate (70.58%) was recorded against *F. pseudograminearum* strain 7, whereas the lowest inhibition rate (61.17%) was observed in *F. chlamydosporum* strain 8. Statistical analysis confirmed that the treatment exerted a significant inhibitory effect (LSD = 6.429 *), with *F. pseudograminearum* strain 7 being the most susceptible strain (Table 9), (Figure 17).

Table 9. Inhibition percentage (%) of *Fusarium* spp. strains treated with the chitosan NPs loaded with DVE

***Fusarium* spp. Strains**	**Inhibition Ratio (%) After Chitosan NPs Loaded with DVE**
F. pseudograminearum strain 2	64.70 ±3.15 ^{ABC}
F. pseudograminearum strain 3	67.05 ±3.73 ^{ABC}
F. oxysporum strain 4	65.88 ±3.08 ^{ABC}
F. oxysporum strain 5	63.52 ±2.79 ^{BC}
F. pseudograminearum strain 6	68.23 ±3.41 ^{AB}
F. pseudograminearum strain 7	70.58 ±4.05 ^{A}
F. chlamydosporum strain 8	61.17 ±3.26 ^{C}
L.S.D. value	6.429 *

Means having different big letters in same column differed significantly. * (P≤0.05),

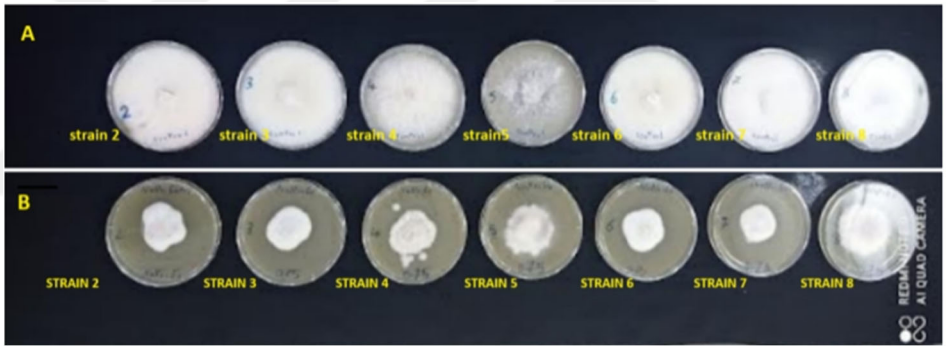
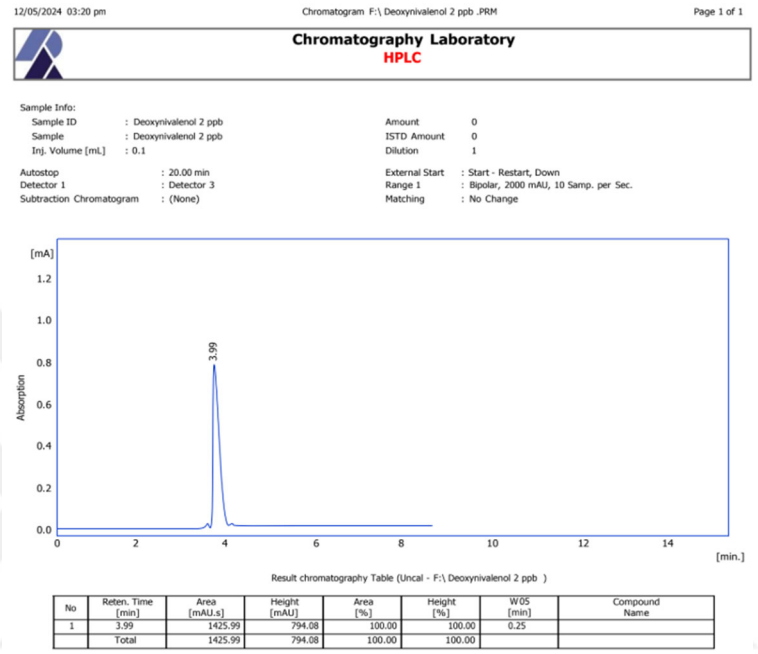


Figure 17. The efficiency of the DVE loaded chitosan NPs on *Fusarium* spp. strains on PDA, (A) control group for seven strains (B) strains growth after DVE-loaded chitosan NPs. (*Fusarium pseudograminearum* strain 2, *Fusarium pseudograminearum* strain 3, *Fusarium oxysporum* strain 4, *Fusarium oxysporum* strain 5, *Fusarium pseudograminearum* strain 6, *Fusarium pseudograminearum* strain 7 and *Fusarium chlamydosporum* strain 8)

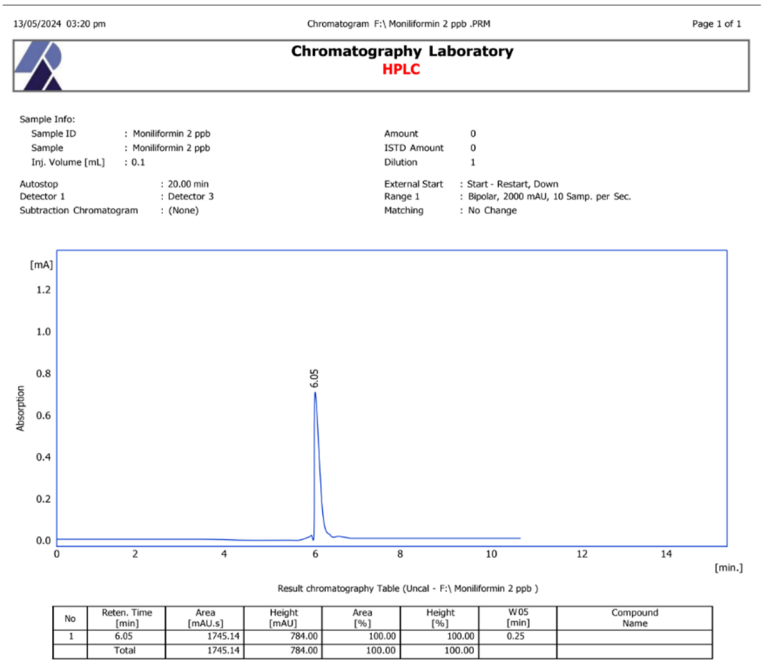
3.1.9. Effect of DVE and Chitosan NPs Loaded with DVE on the Production of DON and MON Mycotoxins

The samples were analyzed using an HPLC system, and the corresponding standard chromatograms are provided in Figure 18. Statistical analysis revealed clear significant differences between the three treatments (control, DVE, and chitosan NPs loaded with DVE) (Table 10-11). The average DON concentration decreased after DVE treatment, and the highest inhibition rate was observed in *F. pseudograminearum* strain 6 (60.23%), while the lowest was observed in strain 2 (58.35%). When the strains were treated with

chitosan NPs loaded with DVE, DON concentrations were further reduced, resulting in a marked increase in the inhibition rate. Under this treatment, the highest inhibition was recorded for *F. pseudograminearum* strain 2 (73.75%), whereas the lowest was observed in *F. pseudograminearum* strain 6 (68.87%).



(a)



(b)

Figure 18. Deoxynivalenol and Moniliformin standard chromatogram by HPLC analysis, a) DON standard, b) MON standard

It should also be noted that within the same treatment group, the differences between strains were not statistically significant (NS), consistent with the L.S.D. values. *F. oxysporum* strain 4, *F. oxysporum* strain 5 and *F. chlamydosporum* strain 8 which are known MON-producing strains were treated with DVE and NPs loaded with DVE. Statistical analysis confirmed significant differences in MON inhibition among the control, DVE, and NPs loaded with DVE treatments. When free DVE was applied, the highest inhibition rate was observed in *F. oxysporum* strain 4 (53.67%), while the lowest was recorded in *F. oxysporum* strain 5 (48.25%). Upon using NPs loaded with DVE, the inhibition rate, increased in all strains, reaching the highest level in *F. chlamydosporum* strain 8 (73.62%), followed by *F.oxysporum* strain 4 (72.09%) and *F. oxysporum* strain 5 (68.18%). Within each treatment group (control, DVE, and NPs loaded with DVE), there were no statistically significant differences (NS) between MON concentrations of the three *Fusarium* spp. strains. However, numerically, the lowest MON concentration after NPs loaded with DVE treatment was observed in *F. oxysporum* strain 4 (12.44 µg/L), while the highest was recorded in *F. oxysporum* strain 5 (13.25 µg/L).

Table 10. Deoxynivalenol (µg/L) concentrations of *Fusarium* spp. strains after treatment with the DVE and chitosan NPs loaded with DVE and inhibition ratios

***Fusarium* spp. Strains**	**DON (µg/L) Before Treatment**	**DON (µg/L) After DVE Treatment 3%**	**DON (µg/L) After Chitosan NPs Loaded with DVE 0.75%**	**Inhibition Ratio % After DVE Treatment**	**Inhibition Ratio % After Chitosan NPs Loaded with DVE**
F. pseudograminearum strain 2	43.82 ±2.17 A a	18.25 ±1.05 A b	11.50 ± 0.74 A c	58.35 A	73.75 A
F. pseudograminearum strain 3	47.24 ±3.26 Aa	19.11 ±1.48 A b	12.65 ± 0.91 Ac	59.67 A	73.22 A
F. pseudograminearum strain 6	43.86 ±2.37 A a	17.44 ±0.97 A b	13.65 ± 0.96 A b	60.23 A	68.87 B
F. pseudograminearum strain 7	47.23 ±3.61 A a	18.95 ±1.29 A b	12.65 ± 0.88 A c	59.87 A	73.21 A
L.S.D. value	3.551 NS	1.802 NS	2.076 NS	5.911 NS	3.967 *

Means having different big letters in same column and small letters in same row differed significantly. * (P≤0.05), NS: Non-Significant

HPLC analysis further confirmed the presence of MON toxin, produced by *F. oxysporum* strains 4 and 5, and *F. chlamydosporum* strain 8. To the best of our knowledge, this is the first report to demonstrate MON production by *Fusarium* spp. isolated from wheat samples stored in Iraq. Research on MON remains limited, and further studies are needed to clarify its toxicological impact, behavior under storage and processing conditions, and the efficacy of control strategies (Radic et al., 2019). Multiple factors, including microbial interactions within the matrix, agricultural practices, and environmental conditions such as temperature and humidity, influence mycotoxin biosynthesis by *Fusarium* spp. For instance, DON production has been shown to be maximized at approximately 28 ºC. Therefore, discrepancies observed among different studies are likely attributable to variations in fungal strains, substrate composition, and experimental conditions (Mahmoud et al., 2023). The chromatograms related to treatments are given in Figure S1, S2 and S3.

Table 11. Moniliformin (µg/L) concentrations of *Fusarium* spp. strains after treatment with the DVE and chitosan NPs loaded with DVE and inhibition ratios

***Fusarium* spp. strains**	**MON (µg/L) Before Treatment**	**MON (µg/L) After DVE Treatment 1.5%**	**MON (µg/L) After Chitosan NPs Loaded with DVE 0.75%**	**Inhibition Ratio % after DVE Treatment**	**Inhibition Ratio % After Chitosan NPs Loaded with DVE**
F. oxysporum strain 4	44.58 ±2.79 $^{A\,a}$	20.65 ±1.63 $^{A\,b}$	12.44 ±0.74 $^{A\,c}$	53.67 ^{A}	72.09 ^{AB}
F. oxysporum strain 5	41.65 ±2.05 $^{A\,a}$	21.55 ±1.48 $^{A\,b}$	13.25 ±0.93 $^{A\,c}$	48.25 ^{B}	68.18 ^{B}
F. chlamydosporum strain 8	42.65 ±3.18 ^{Aa}	19.80 ±1.04 $^{A\,b}$	11.25 ± 0.62 $^{A\,c}$	53.57 ^{A}	73.62 ^{A}
L.S.D. value	3.094 ^{NS}	2.067 ^{NS}	2.178 ^{NS}	3.962 *	4.208 *

Means having different big letters in same column and small letters in same row differed significantly. * (P≤0.05), NS: Non-Significant

3.1.10. Evaluation of the effect of ozone gas on the growth of *Fusarium* spp. strains

The results of applying ozone gas at different flow rates and exposure periods also showed that it inhibited the growth of fungal strains; there were clear, significant differences in the statistical analysis. Exposing the strains to ozone gas at a flow rate of 2 liters/minute for 30 minutes recorded an inhibition rate of 29.41% for *F. pseudograminearum* strain 2.

When the exposure time to the gas was increased to 60 minutes, the inhibition rate for strain 2 increased to 51.76%. Ozone application at a rate of 4 liters/minute for 60 minutes achieved the highest effect on the growth of fungal strains, as the highest inhibition rate was 74.11% on *F. oxysporum* strain 5. By comparing the results of the inhibition rates, we observe an increase in the rate of growth inhibition of *Fusarium* strains with increasing exposure time and gas flow rate. This confirms the effectiveness of ozone gas for decreasing the growth of *Fusarium* strains (Table 12-13), (Figure 19).

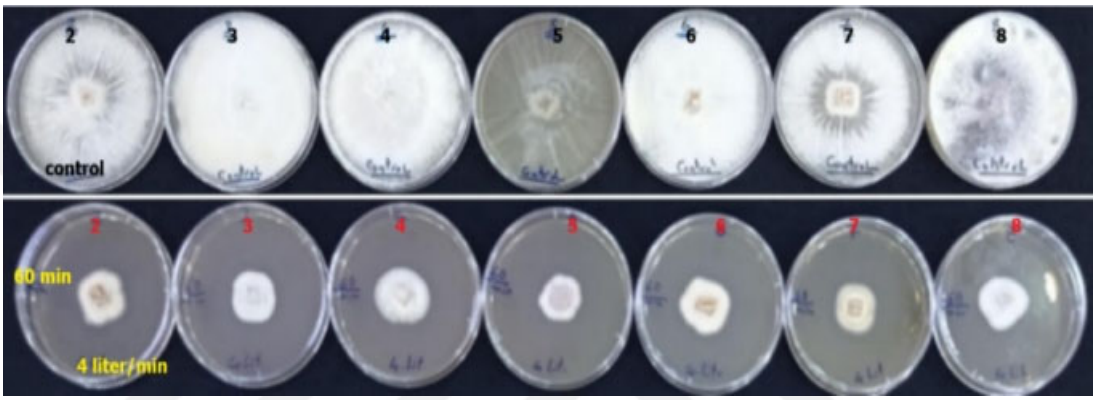


Figure 19. Ozone gas treatment on *Fusarium* spp. strains (4 liters/minute for 60 minutes) on seven *Fusarium* spp. strains (*F. pseudograminearum* strain 2, *F. pseudograminearum* strain 3, *F. oxysporum* strain 4, *F. oxysporum* strain 5, *F. pseudograminearum* strain 6, *F. pseudograminearum* strain 7, *F. chlamydosporum* strain 8)

Table 12. The effect of ozone gas on the growth of *Fusarium* spp. strains on PDA at different concentrations and different exposure periods

***Fusairum* spp. Strains**	**Control group**	**O3 2 L/min 30 min**	**O3 2 L/min 60min**	**O3 4 L/min 30 min**	**O3 4 L/min 60 min**	**L.S.D.**
F. pseudograminearum strain 2	8.5 ±0.20 Aa	6.0 ±0.52 Ab	4.1 ±0.26 Abc	5.2 ±0.36 Ab	2.6 ±0.16 Ac	2.39 *
F. pseudograminearum strain 3	8.5 ±0.20 Aa	6.6 ±0.46 Aab	4.4 ±0.31 Abc	5.0 ±0.32 Ab	2.5 ±0.09 Ac	2.44 *
F. oxysporum strain 4	8.5 ±0.20 Aa	6.2 ±0.49 Aab	4.9 ±0.37 Abc	5.4 ±0.45 Abc	2.9 ±0.14 Ac	2.71 *
F. oxysporum strain 5	8.5 ±0.20 Aa	6.1 ±0.38 Ab	4.8 ±0.43 Ab	4.2 ±0.32 Abc	2.2 ±0.12 Ac	2.08 *
F. pseudograminearum strain 6	8.5 ±0.20 Aa	6.2 ±0.41 Aab	4.9 ±0.38 Abc	4.7 ±0.46 Abc	2.7 ±0.18 Ac	2.56 *
F. pseudograminearum strain 7	8.5 ±0.20 Aa	6.1 ±0.38 Aab	5.1 ±0.36 Ab	4.5 ±0.42 Abc	2.4 ±0.12 Ac	2.63 *
F. chlamydosporum strain 8	8.5 ±0.20 Aa	6.4 ±0.58 Aab	5.2 ±0.42 Abc	5.1 ±0.44 Abc	2.7 ±0.18 Ac	2.70 *
L.S.D.	0.00 NS	1.07 NS	1.33 NS	1.74 NS	1.02 NS	---

Means having different big letters in same column and small letters in same row differed significantly. * (P≤0.05), NS: Non-Significant.

Table 13. The inhibition ratio (%) values of ozone gas on the growth of *Fusarium* spp. strains at different concentrations and different exposure periods

***Fusarium* Strains**	**Control**	**O3 2 L/min 30 min**	**O3 2 L/min 60min**	**O3 4 L/min 30 min**	**O3 4 L/min 60 min**	**L.S.D.**
F. pseudograminearum strain 2	0 ±0 ^{Ae}	29.41 ± 2.16 ^{Ad}	51.76 ±3.05 ^{Ab}	38.82 ± 2.16 ^{Cc}	69.41 ±3.52 ^{ABa}	8.31 *
F. pseudograminearum strain 3	0 ±0 ^{Ad}	22.35 ± 1.56 ^{Ac}	48.23 ±2.78 ^{ABb}	41.17 ± 2.54 ^{BCb}	70.58 ±3.66 ^{ABa}	9.02 *
F. oxysporum strain 4	0 ±0 ^{Ad}	27.05 ± 1.84 ^{Ac}	42.35 ±2.41 ^{BCb}	36.47 ± 1.93 ^{Cb}	65.88 ±3.02 ^{Ba}	8.66 *
F. oxysporum strain 5	0 ±0 ^{Ad}	28.23 ± 1.90 ^{Ac}	43.52 ±2.50 ^{BCb}	50.58 ± 3.26 ^{Ab}	74.11 ±3.67 ^{Aa}	8.37 *
F. pseudograminearum strain 6	0 ±0 ^{Ad}	27.05 ± 1.37 ^{Ac}	42.35 ±2.09 ^{BCb}	44.70 ± 2.61 ^{ABb}	68.23 ±3.89 ^{ABa}	9.42 *
F. pseudograminearum strain 7	0 ±0 ^{Ad}	28.23 ± 2.04 ^{Acc}	40.00 ±2.15 ^{Cbb}	47.05 ± 2.27 ^{ABbb}	71.76 ±3.05 ^{ABa}	8.56 *
F. chlamydosporum strain 8	0 ±0 ^{Ad}	24.70 ± 1.27 ^{Ac}	38.82 ±1.93 ^{Cb}	40.00 ± 2.15 ^{BCb}	68.23 ±2.97 ^{ABa}	8.71 *
L.S.D.	0.00 ^{NS}	5.02 ^{NS}	7.58 *	7.83 *	6.97 *	---

Means having with the different big letters in same column and small letters in same row differed significantly. * (P≤0.05), NS: Non-Significant.

3.1.11. The Effect of Ozone Gas on Mycotoxins Production

The concentration 4 liters/minute for 60 minutes was choosen on seven *Fusarium* spp. strains to check effectiveness of ozone gas in reducing mycotoxins production. This treatment was applied to the *Fusarium* spp. strains growing on wheat, and the concentrations of mycotoxins were measured after treatment by comparing them with the control group. The results of this study showed that the inhibition rate of DON production was highest on *F. pseudograminearum* strain 7, where DON production rate decreased from 47.23 (µg/L) to 21.80 (µg/L), and the inhibition rate was 53.84%. The effect was evident on all strains in terms of reducing DON concentrations before and after the ozone application and the apparent inhibition for all strains, which ranged between 48.56% and 52.20%. The statistical analysis showed no significant differences in the treatment effect

across the four *Fusarium* spp. strains: *F. pseudograminearum* strain 2, *F. pseudograminearum* strain 3, *F. pseudograminearum* strain 6, and *F. pseudograminearum* strain 7 (Table 14).

Table 14. Deoxynivalenol (DON) concentrations (µg/L) and inhibition ratio (%) of *Fusarium* spp. strains before and after ozone treatment

***Fusarium* spp. strains**	**DON (µg/L) before ozone treatment**	**DON (µg/L) after ozone treatment 4 L/min for 60 min**	**Inhibition ratio %**
F. pseudograminearum strain 2	43.82 ±2.17	21.5 ±1.06	50.93 ±2.47
F. pseudograminearum strain 3	47.24 ±3.52	22.58 ±1.87	52.20 ±2.68
F. pseudograminearum strain 6	43.86 ±2.97	22.56 ±1.58	48.56 ±2.07
F. pseudograminearum strain 7	47.23 ±3.76	21.80 ±2.05	53.84 ±3.01
L.S.D.	4.902 ^{NS}	2.669 ^{NS}	5.982 ^{NS}

NS: Non-Significant

Treating *Fusarium* spp. strains with ozone gas had a role in reducing the production of MON toxins, and there were significant differences in the results of the statistical analysis, as the highest inhibition rate for MON toxins was 44.54% for *F. chlamydosporum* strain 8. Ozone gas treatment showed a clear effect on all strains, with varying levels of inhibition in toxin production (Table 15). The chromatograms related to treatments are given in Figure S4.

Table 15. Moniliformin (MON) concentrations (µg/L) and inhibition ratio (%) of *Fusarium* spp. strains before and after ozone treatment

***Fusarium* spp. strains**	**MON (µg/L) before ozone treatment**	**MON(µg/L) after ozone treatment 4 L/min for 60 min**	**Inhibition ratio %**
F. oxysporum strain 4	44.58 ±2.91	25.14 ±1.70	43.60 ±2.66 ^{A}
F. oxysporum strain 5	41.65 ±2.37	26.11 ±1.83	37.30 ±1.96 ^{B}
F. chlamydosporum strain 8	42.65 ±3.05	23.65 ±2.17	44.54 ±2.19 ^{A}
L.S.D.	4.615 ^{NS}	3.855 ^{NS}	5.417 *

Means having with the different big letters in same column and differed significantly. * (P≤0.05),NS: Non-Significant

3.1.12. The Efficiency of normal and nano sea salt on inhibiting *Fusarium* spp. Strains

The results showed that natural salt at a concentration of 1% had an inhibitory effect on the growth of some *Fusarium* spp. strains. An effect was observed at a 1% concentration (the lowest concentration used) of normal sea salt on *F. pseudograminearum* strain 6, reaching 22.5%. At a 3% concentration (the highest concentration), the effect of the salt was even greater, reaching the highest inhibition rate of 50.0% for *F. pseudograminearum* strain 6 and the lowest inhibition rate of 15.2% for *F. pseudograminearum* strain 2. The inhibition rates for the remaining five *Fusarium* spp. strains ranged from 17.6% to 47.0% (Figure 20), (Table 16).

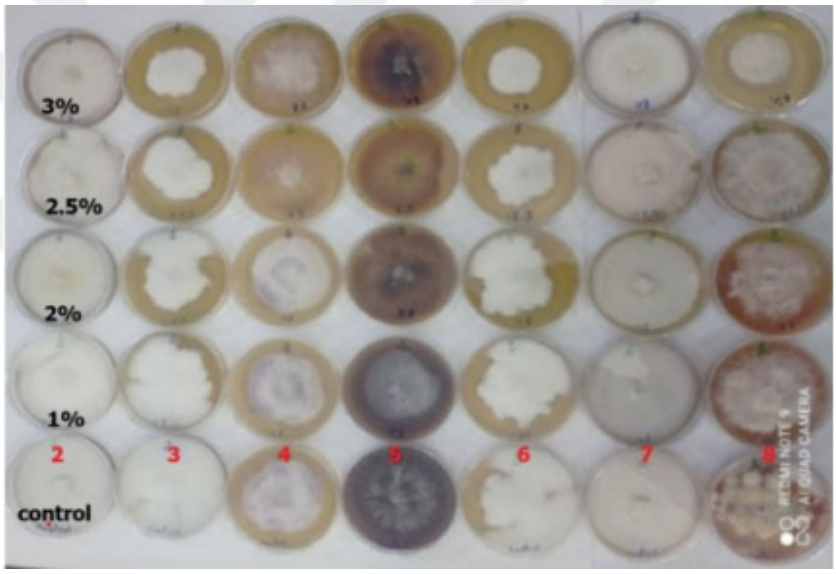


Figure 20. Effect of four concentrations (1, 2, 2.5 and 3 %) of normal sea salt on seven *Fusarium* spp. strains on PDA *in vitro*, the plates numbered in red color at the bottom of the figure represent the control group. The plates in the rows above represent the application of sea salt at four different concentrations, as recorded on plates (1, 2, 2.5 and 3 %) on *Fusarium* strains: (*Fusarium pseudograminearum* strain 2, *Fusarium pseudograminearum* strain 3, *Fusarium oxysporum* strain 4, *Fusarium oxysporum* strain 5, *Fusarium pseudograminearum* strain 6, *Fusarium pseudograminearum* strain 7 and *Fusarium chlamydosporum* strain 8)

As shown in Figure 21, after preparing the sea salt to nanoscale by grinding it with special mills, the produced quantity was sent to the laboratory to confirm that it had reached the nanoscale state using an AFM, the results were as follows: average grain size (47.11 nm). This is consistent with the European Commission's definition of nanomaterials as a natural or manufactured material or by product containing particles, in an undefined,

aggregated or agglomerated state, such that 50% or more of its particles are of one or more dimensions (Peters et al., 2014).

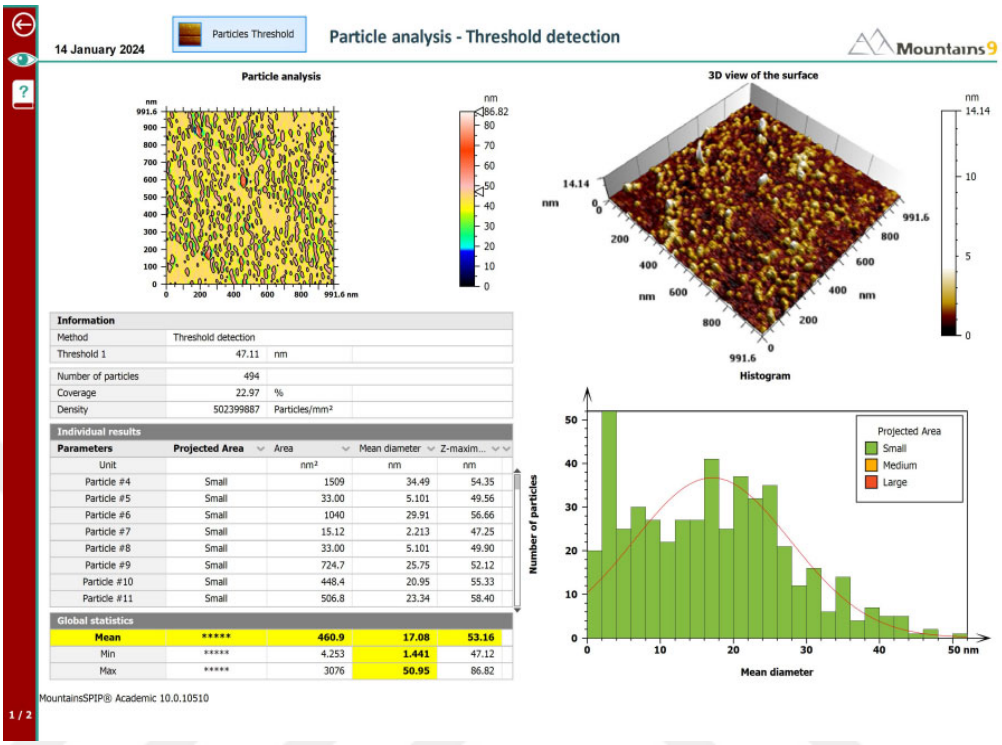


Figure 21. AFM surface morphology and particle size distribution of nano sea salt

The results showed that nano-sea salt was superior to normal sea salt in its effect on the growth of *Fusarium* spp. strains. There were clear, significant differences in the results, with the highest inhibition rate recorded with nano-salt at 3%, reaching 71.7% for *F. chlamydosporum* strain 8, while the lowest inhibition rate was recorded for *F. pseudograminearum* strain 6, reaching 50.0%. It can be observed that nano-salt was superior to natural sea salt in inhibiting the growth of *Fusarium* spp. strains. It inhibited all *Fusarium* spp. strains at all concentrations used, from 1% to 3% (Figure 22), (Table 16).

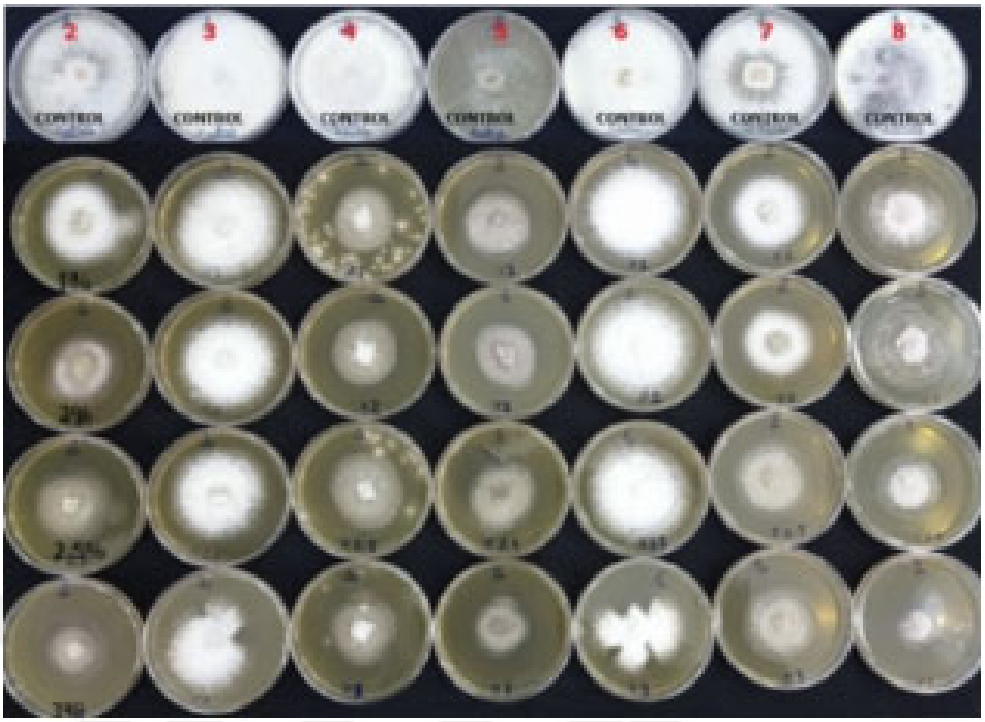


Figure 22. Effect of four concentrations (1, 2, 2.5 and 3 %) of nano sea salt on seven *Fusarium* spp. strains on PDA *in vitro*, the plates numbered in red color at the top row of the figure represent the control group. The plates in the rows under represent the application of nano sea salt at four different concentrations, as recorded on plates (1, 2, 2.5 and 3 %) on *Fusarium* strains: *Fusarium pseudograminearum* strain 2, *Fusarium pseudograminearum* strain 3, *Fusarium oxysporum* strain 4, *Fusarium oxysporum* strain 5, *Fusarium pseudograminearum* strain 6, *Fusarium pseudograminearum* strain 7 and *Fusarium chlamydosporum* strain 8

Table 16. The effect of normal and nano sea salt at different concentrations on the growth of seven *Fusarium* spp. strains

***Fusarium* strains**	**1% normal**	**1%Nano**	**2% normal**	**2%Nano**	**2.5% normal**	**2.5%Nano**	**3% normal**	**3%Nano**	**L.S.D.**
F. pseudograminearum strain 2	0 ±0 ^{Ce}	35 ±2.4 ^{DEc}	5.8 ±0.46 ^{B}	48.2 ±2.3 ^{ABCb}	8.8 ±0.6 ^{Cd}	50.5 ±2.4 ^{BCab}	15.2 ±0.7 ^{Cd}	57.6 ±3.1 ^{BCa}	8.027 *
F. pseudograminearum strain 3	14.1 ±0.8 ^{Be}	29 ±1.8 ^{EFd}	27.0 ±1.4 ^{Ad}	41.7 ±1.6 ^{CDbc}	38.8 ±2.5 ^{Ac}	45.8 ±2.1 ^{CDabc}	47.0 ±2.4 ^{Aab}	52.9 ±2.8 ^{BCa}	8.55 *
F. oxysporum strain 4	4.5 ±0.5 ^{d}	48.2 ±2.7 ^{ABb}	11.7 ±0.72 ^{Bcd}	52.9 ±2.8 ^{ABab}	20.1 ±0.9 ^{Bc}	57.64 ±2.8 ^{ABa}	26.4 ±1.3 ^{B}	58.8 ±2.5 ^{BCa}	9.41 *
F. oxysporum strain 5	0 ±0 ^{Cd}	51 ±2.9 ^{Ab}	5.8 ±0.76 ^{Bd}	54.1 ±2.5 ^{Ab}	15.2 ±0.6 ^{BCc}	57.0 ±3.1 ^{ABab}	24.7 ±1.2 ^{B}	65.8 ±3.5 ^{ABa}	8.37 *
F. pseudograminearum strain 6	22.5 ±1.5 ^{Af}	25.8 ±1.6 ^{Fef}	31.2 ±1.8 ^{Ade}	34.10 ±1.3 ^{Dcd}	43.0 ±2.6 ^{Aab}	41.1 ±1.9 ^{Dbc}	50.0 ±2.5 ^{Aa}	50.0 ±2.2 ^{Ca}	7.97 *
F. pseudograminearum strain 7	2.5 ±0.08 ^{Cd}	41 ±2.2 ^{BCDc}	8.8 ±0.6 ^{Bd}	44.7 ±2.0 ^{Bbc}	11.7 ±0.8 ^{C}	50.5 ±2.4 ^{Bab}	17.6 ±0.9 ^{C}	57.6 ±2.5 ^{BCa}	8.25 *
F. chlamydosporum strain 8	0 ±0 ^{Cf}	40 ±1.7 ^{CDd}	5.8 ±0.6 ^{Bef}	48.2 ±3.1 ^{ABCc}	8.8 ±0.6 ^{Ce}	58.8 ±3.0 ^{Ab}	47.0 ±2.3 ^{Ac}	71.7 ±3.5 ^{Aa}	8.16 *
L.S.D.	6.47 *	8.05 *	6.97 *	7.55 *	7.03 *	8.16 *	7.22 *	8.41 *	---

Means having with the different big letters in same column and small letters in same row differed significantly. * ($p \leq 0.05$), NS: Non-Significant

3.1.13. The Effect of Nano Sea Salt on the Production of Mycotoxins

Treating *Fusarium* spp. strains with 3% nano-sea salt achieved the highest inhibition rate for the growth of *F. pseudograminearum* strains capable of producing the DON mycotoxin and reducing its production. The highest inhibition rate of toxin production reached 83.38% for *F. pseudograminearum* strain 3 (Table 17). The same concentration of nano-sea salt was applied to *Fusarium* strains (*F. oxysporum* 4, *F. oxysporum* 5, and *F. chlamydosporum* 8) to determine the salt's ability to reduce the production of MON mycotoxin, the highest inhibition rate reached 87.69% for *F. chlamydosporum* 8, the inhibition rates for MON toxin production in the remaining strains ranged from 81.42% to 83.08% as shown in Table 18. The chromatograms related to treatments are given in Figure S5.

Table 17. Deoxynivalenol (DON) concentrations (µg/L) and inhibition ratio (%) of *Fusarium* spp. strains before and after nano sea salt treatment NS: Non-Significant.

***Fusarium* spp. strains**	**DON (µg/L) before sea salt treatment 3%**	**DON (µg/L) after nano sea salt treatment 3%**	**Inhibition ratio %**
F. pseudograminearum strain 2	43.82 ±2.72	8.22 ±0.68	81.42 ±3.62
F. pseudograminearum strain 3	47.24 ±3.66	7.85 ±0.71	83.38 ±3.07
F. pseudograminearum strain 6	43.86 ±2.78	7.99 ±0.74	81.78 ±.28
F. pseudograminearum strain 7	47.23 ±3.65	7.99 ±0.62	83.08 ±3.51
L.S.D.	4.519 ^{NS}	2.066 ^{NS}	3.429 ^{NS}

Table 18. Moniliformin (MON) concentrations (µg/L) and inhibition ratio (%) of *Fusarium* spp. strains before and after nano sea salt treatment

***Fusarium* spp. strains**	**MON (µg/L) before nano sea salt treatment**	**MON(µg/L) after nano sea salt treatment**	**Inhibition ratio (%)**
F. oxysporum strain 4	44.58 ±3.57	7.15 ±0.69 ^{A}	83.96 ±3.58 ^{AB}
F. oxysporum strain 5	41.65 ±2.83	8.08 ±0.71 ^{A}	80.60 ±2.94 ^{B}
chlamydosporum strain 8	42.65 ±3.08	5.25 ±.36 ^{B}	87.69 ±3.17 ^{A}
L.S.D.	3.75 ^{NS}	2.781 *	5.812 *

Means having with the different big letters in same column differed significantly.* (P≤0.05), NS: Non-Significant.

3.1.14. Evaluation of the Best Four Treatments Applied to *Fusarium* spp. Strains

After evaluating the ability of the above treatments to inhibit the growth of *Fusarium* spp. strains, the same treatments were used to assess whether these strains produced mycotoxins after growth. Significant differences were observed in concentrations of toxins after the HPLC device measured them. A comparison was made of the toxin inhibition percentages across the four treatments. After using the best concentrations from all previous treatments. The results of the inhibition rates of the treatment of DVE and DVE loaded on chitosan nanoparticles at a concentration of 0.75 for each of them and using nano sea salt at a concentration of 3% and using ozone gas at a flow rate of 4 liters/minute per hour, and the inhibition rate of these treatments for the production of mycotoxins was 81.42%, 83.38%, 81.78% and 83.08% for DON toxins. *F. pseudograminearum* strain 3 recorded the highest rate of inhibition of toxin production 83.38% , which represent the values of the inhibition rate for the salt treatment at a rate of 3% for strains 2, 3, 6 and 7. Where nano sea salt treatment had the greatest effect in inhibiting the production of DON toxins,this is followed by applications of chitosan NPs Loaded with DVE, DVE and ozone treatment, respectively (Table 19), (Figure 23).

Table 19. Difference in inhibition values (%) of DON production between four different treatments estimated by HPLC

***Fusarium* spp. strains**	**DVE 1.5%**	**Chitosan NPs Loaded with DVE 0.75%**	**Nano sea salt 3%**	**O3 4 L/min. for 60 min**	**L.S.D.**
F. pseudograminearum strain 2	58.35 ±2.57 Ac	73.75 ±3.65 Ab	81.42 ±4.21 Aa	50.92 ±2.14 Ad	7.82 *
F. pseudograminearum strain 3	59.67 ±3.02 Ac	73.22 ±3.92 Ab	83.38 ±3.27 Aa	52.20 ±2.45 Ac	7.66 *
F. pseudograminearum strain 6	60.23 ±3.18 Ac	68.87 ±3.55 Ab	81.78 ± 3.87 Aa	48.56 ±2.08 Ad	8.02 *
*F. pseudograminear*um strain 7	59.87 ±2.77 Ac	73.21 ±3.08 Ab	83.08 ±3.91 Aa	53.84 ±2.35 Ac	7.36 *
L.S.D.	4.28 NS	5.98 NS	3.76 NS	5.02 NS	---

Means having with the different big letters in same column and small letters in same row differed significantly. * ($p \leq 0.05$), NS: Non-Significant.

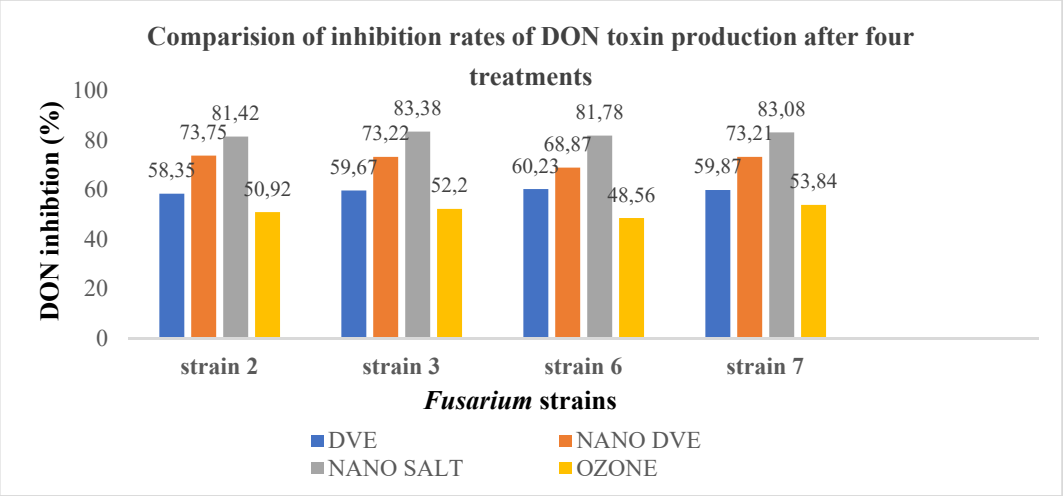


Figure 23. Comparison of inhibition rates of DON toxin production after the four treatments

As for the inhibition rates of the MON toxins as a result of applying the above treatments, the highest inhibition rate and the most effective treatment were the nano sea salt treatment as well, and the rates were 87.69% for *F. chlamydosporum* strain 8, 83.96%, 80.60%, for *F. oxysporum* strain 4 and *F. oxysporum* strain 5. This is followed by applications of chitosan NPs loaded with DVE, DVE, and ozone treatment, respectively (Table 20), (Figure 24).

Table 20. Difference in percentage of inhibition of MON production between four treatments estimated by HPLC

***Fusarium* spp. strains**	**DVE 1.5%**	**Chitosan NPs Loaded with DVE 0.75%**	**Nano sea salt 3%**	**O3 4 L/min for 60 min.**	**L.S.D.**
F. oxysporum strain 4	53.67 ± 2.34 ^{Ac}	72.09 ±3.62 ^{Ab}	83.96 ± 4.02 ^{Aa}	43.60 ±2.15 ^{Ad}	9.61 *
F. oxysporum strain 5	48.25 ± 1.92 ^{Ac}	68.18 ±3.55 ^{Ab}	80.60 ± 3.57 ^{Aa}	37.31 ±1.96 ^{Ac}	9.55 *
F. chlamydosporum strain 8	53.57 ± 2.46 ^{Ac}	73.62 ±3.71 ^{Ab}	87.69 ± 3.87 ^{Aa}	44.54 ±2.45 ^{Ac}	10.04 *
L.S.D.	5.85 ^{NS}	5.79 ^{NS}	7.12 ^{NS}	7.42 ^{NS}	---

Means having with the different big letters in same column and small letters in same row differed significantly. * ($p \leq 0.05$), NS: Non-Significant

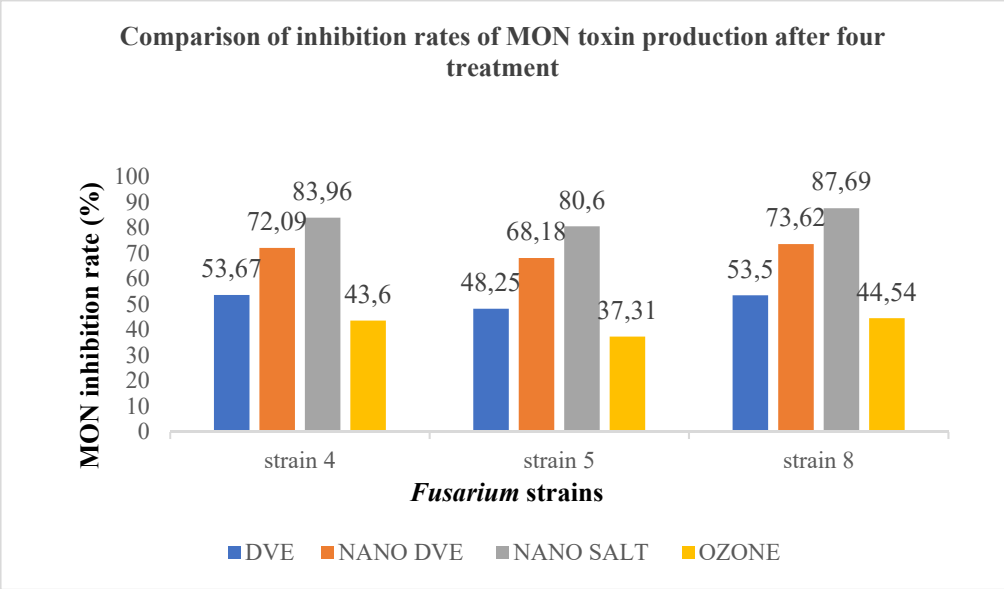


Figure 24. Comparison of inhibition rates of MON toxin production after the four treatments

CHAPTER 4

DISCUSSION, CONCLUSION, FUTURE STUDIES

4.1. Discussion

Wheat is regarded as one of the world's most extensively cultivated crops and a fundamental food source for humans. Increasing wheat production globally and in Iraq, particularly in recent years, to satisfy population needs requires effective solutions to the problems associated with its production, both in the field and during storage. A suitable environment must be available for grain storage to preserve the grains for as long as possible without spoilage. It starts with receiving the grains and continues through storage. Although mice, grain-storage insects, and other pests pose serious risks to grains, fungi and the mycotoxins they secrete are no less hazardous, since they may cause disease or even death at certain concentrations. *Fusarium* spp. and their associated mycotoxins, especially deoxynivalenol (DON) and moniliformin (MON), are among the major fungal threats to grains. Numerous chemical and other fumigation methods have been applied to minimize the risks associated with these fungi and their toxins. However, due to the adverse effects of such methods on the environment and worker safety, as well as their potential to leave residues on grains, this study was undertaken to explore alternative strategies that are environmentally friendly, cost-effective, and readily available. This chapter presents the results of the study, focusing on the effects of these methods on mycotoxin levels and on the fungi's capacity for toxin production.

4.1.1. Identification of *Fusarium* spp. strains isolated from local wheat samples

The results of the present study are in agreement with the findings of Al-Dairi and Al-Waily (2023). During the 2020/2021 agricultural season, those authors analyzed 27 wheat samples randomly collected from Basra, Maysan, and Dhi Qar governorates and

successfully isolated and identified *Fusarium pseudograminearum* strains. Similarly, the isolation and identification of *F. pseudograminearum* in the current study are consistent with previous reports from Basra Governorate, where several *Fusarium* species, including *F. pseudograminearum*, were identified. These observations also correspond with earlier studies conducted on wheat and barley in Iraq (Hameed et al., 2012). In the same study, *Fusarium chlamydosporum* was isolated from wheat in Iraq and reported for the first time; its presence was confirmed again in the present study, representing the second report of this species in Iraqi wheat. Some *Fusarium* species, particularly *Fusarium pseudograminearum* and *Fusarium chlamydosporum*, are important causal agents of major wheat diseases, including Fusarium crown rot (FCR), Fusarium head blight (FHB), and Fusarium root rot (FRR) in wheat fields in Iraq (Minati & Mohammed-Ameen, 2019).

4.1.2. The Pathogenicity Test of *Fusarium* spp. strains

The results of the present study are consistent with those reported by Argyris et al. (2003), who demonstrated that *Fusarium graminearum* Schwabe adversely affects seeds, leading to unacceptable germination. The findings are also in agreement with Hassani (2019), who reported that *F. graminearum*, the causal agent of Fusarium head blight (FHB), negatively influences seed quality and reduces the germination rate, as reflected by a lower germination index. In addition, fungi belonging to the genera *Aspergillus*, *Fusarium*, *Penicillium*, and *Rhizoctonia* significantly impair seed quality and reduce seed viability through mycotoxin production. These observations further support the results obtained in the present study.

4.1.3. Effect of DVE on the growth of *Fusarium* spp. strains

Many factors, compounds, and reasons help inhibit fungal growth. GC–MS analysis of the ethanolic extract revealed the presence of 27 compounds, with glycosides, saponins, and alkaloids identified as the major constituents. Glycosides, which are soluble in water and alcohol, are known to inhibit fungi by disrupting oxidative phosphorylation, thereby reducing energy production and suppressing fungal growth (Al Mosowi et al., 2010).

GC–MS analysis showed that the major compound in the extract was 4-Cyclohexyl-1-(furan-2-ylmethyl)-4H,5H,7H-pyrazolo[3,4-b]pyridin-6-one, followed by 4′,5,7-Trihydroxy-3,6-dimethoxyflavone, 6-Methoxy-2-[2-(imidazol-1-yl)ethoxy]-8-

nitroquinoline, and 3-Heptanol, TMS derivative. The presence of 4′,5,7-Trihydroxy-3,6-dimethoxyflavone is particularly noteworthy, as this phenolic compound is recognized for both its antioxidant capacity and its enzyme-inhibitory effects (Durmaz, 2021). Furthermore, N-hexadecanoic acid (palmitic acid; $C_{16}H_{32}O_2$), another compound identified in the extract, has been reported to exhibit antibacterial and antifungal activity, including against *Candida albicans* (Saranya & Divyabharathi, 2019). The compounds identified above were the most abundant, while the other constituents detected in the extract are presented in Figure 9 and Table 7, *D. viscosa* belongs to the *Saponaceae* family, and previous studies have reported that it contains compounds with antimicrobial, antitoxic, and cytotoxic properties (Al-Snafi, 2017). It also contains Catechol; a chemical compound found in plants. The effect of catechol on some fungi and bacteria, such as *Fusarium oxysporum* and *Penicillium italicum* has been studied. (Kocaçalışkan et al., 2006). In addition, neophytadine is an antioxidant and a strong, active compound against fungi, infections, and microbes. It is one of the terpenoid compounds in the plant leaf extracts (Pratama et al., 2019).

The ethanolic extract of *D. viscosa* contains phenolic compounds that may inhibit membrane permeability and inhibit enzymes such as ATPase and phospholipase A2 (El-Mohamedy & Abdalla, 2014). *D. viscosa* extract contains many compounds, such as polyphenols, that have an inhibitory effect on microorganisms. A previous study showed that phenolic rings inhibit bacterial growth by binding to proteins and membranes, forming complexes that prevent growth. This supports the rationale for inhibiting *Fusarium* spp. growth (Pérez-Narváez et al., 2023). An important observation reported in previous studies is that fungi differ in their sensitivity to plant extracts, and the extent of this sensitivity depends on the age of the fungal culture. Older fungal cultures tend to be less sensitive to plant extracts than younger ones (Muthomi et al., 2017).

These findings are consistent with earlier reports demonstrating the strong antifungal activity of *D. viscosa* ethanolic extract (DVE) against pathogenic fungi, including *Aspergillus niger* and *A. flavus*. Variations in strain sensitivity may be related to differences in the phytochemical composition of the extract, which largely depends on the extraction solvent. Previous studies have likewise shown that ethanolic extracts of *D. viscosa* exhibit variable inhibitory effects among different fungal species (Al-Snafi, 2017).

The application of plant extracts to fruits has also been shown to reduce spoilage and decomposition. In a practical experiment involving the treatment of fruits with extracts of moringa, basil, and *D. viscosa*, the highest rate of decomposition after 18 days was observed in untreated fruits (control group), whereas treated fruits showed lower spoilage rates due to the presence of inhibitory compounds such as tannins, alkoloids, and flavonoids. These bioactive compounds enable plant extracts to inhibit both fungi and bacteria. In particular, *D. viscosa* extract may disrupt and damage the fungal cell wall, thereby interfering with essential processes such as hyphal formation, budding, and cell division. The extract contains several biologically active constituents, including alkaloids, saponins, tannins, flavonoids, volatile oils, and phenolic compounds, all of which contribute to its significant antimicrobial effects (Elkeleny & Mohamed, 2023).

The antifungal effect of plant extracts has been well documented. For example, *Moringa oleifera* extract has been reported to be effective against *Fusarium oxysporum* by inhibiting spore germination. This activity is mainly attributed to the biologically active constituents present in the extract, such as alkaloids, flavonoids, saponins, and tannins, which exhibit strong antifungal properties and show promising potential for future applications. (El-Mohamedy & Abdalla, 2014). The statistical analysis revealed that the inhibition rate varied among different *Fusarium* spp. strains, even when the extract was applied at the same concentration. This variation may be attributed to differences in cell permeability to chemical agents and to the differential effectiveness of the extracted compounds against the tested strains, in agreement with the findings of Al-Sallami and Jaleel (2015).

4.1.4. Effect of DVE-loaded chitosan NPs on *Fusarium* spp. strains

After phytochemicals in plant extracts were shown to reduce fungal growth and mycotoxin production, subsequent studies highlighted the potential of combining these extracts with nanotechnology to enhance their effectiveness through the encapsulation of these bioactive compounds. This encapsulation increased the surface area compared to the free form and helped preserve the bioactive substances and compounds, protecting them from thermal and photodegradation (Makhuvele et al., 2020). After converting the ethanolic extract to the nanoparticles using chitosan and obtaining DVE-loaded chitosan NPs, its activity was evaluated by applying it to *Fusarium* spp. strains isolated in this

study. The results showed clear significant differences in the growth inhibition of the *Fusarium* spp. strains and in the inhibition percentages. Some analyses were conducted to ensure that the extract reached the nanoscale before applying it to the strains. The activity of the extract loaded with chitosan nanoparticles was then evaluated. Next part is a discussion of the results of analyses conducted on the DVE-loaded chitosan NPs and an explanation of the factors that contributed to the inhibition of *Fusarium* spp. strains.

4.1.4.1. UV-Vis spectroscopy

The observed spectral changes strongly support the formation of chitosan NPs loaded with DVE and are consistent with previous findings for plant-extract-based biopolymeric nanocarriers (El-Naggar et al., 2023; Duraisamy et al., 2022). They reported that the UV–Vis spectrum of chitosan nanoparticles ranged between 200 and 322 nm due to the presence of the CO group. By comparing the DVE/chitosan nanoparticles with DVE, it was noticed that the absence of many peaks due to the cross-linking of TPP may be attributed to the fact that the large molecules were fragmented into smaller units. Overall, the observed spectral changes strongly affirm the formation of chitosan NPs loaded with DVE and are consistent with previous findings for plant-extract-based biopolymeric nanocarriers.

The interaction between chitosan and TPP was responsible for the increase in total surface area, indicating that the repositioned chemical groups facilitated the efficient loading of the extract into the chitosan/TPP matrix and the formation of nanoencapsulation of the extract. As additional supporting evidence, the shifted peaks are consistent with the formation of a new complex. The modifications in the functional groups of the bioactive molecules suggest a relationship with the synthesis of DVE/chitosan NPs (Agarwal et al., 2018; Almukhtar & Karam, 2020).

4.1.4.2. Fourier transform infrared spectroscopy (FTIR)

The higher intensity in the spectrum of nanoparticle suggests a higher concentration of amides associated with the nanoparticles. This finding could be attributed to the attachment of many biomolecules during the synthesis process, which may act as stabilizing agents. On the other hand, the absence of some peaks in chitosan NPs loaded with DVE (1150–1300, 1685–1710, 2850–3000 cm^{-1}) indicated the attachment between

DVE and chitosan molecules, and our results agreed with those of the previous study by Sathiyabama et al. (2024). When the C-H stretch was seen at 2927 cm^{-1}, it provided structural information on chitosan.

4.1.4.3. Atomic Force Microscopy

The outcomes of the AFM examination of biosynthesized DVE-loaded chitosan NPs are shown in Figure 13. Although there is considerable form diversity in the picture, the average nanoparticle size was 105.7 nm. The particles have a rough, protrusive surface texture. Compared to smoother surfaces with smaller contact areas, rough surfaces may allow biological processes, including plant active chemicals, to interact more extensively. On average, particles were 105.7 nm tall, while surface protrusions were about 75.62 nm tall. In addition to their elongated shape and parallel plates, nanoparticle aggregates include several sharp edges. The findings colloborated those of Shaghati & Jassim (2023) who used AFM examination to study clove extract loaded with chitosan NPs, their 3D image showed a uniform population of particles with regular surfaces. The AFM image revealed an intelligent interaction between chitosan nanoparticles loaded with *D. viscosa* extract, leading to the formation of distinct aggregates. Conversely, research by Fauzi et al. (2020), suggests that the thin film's surface morphology is fairly smooth and homogeneous, confirming that Fe_2O_3 interacts with chitosan. Meanwhile, research by Daniyal et al. (2018), shows that chitosan can improve the thin film's surface; the nanostructured maghemite in the chitosan thin film was intentionally made rougher to improve its performance as a sensing element.

4.1.4.4. Field-emission scanning electron microscope (FESEM)

To study the morphology of nanoparticles prepared from chitosan loaded with *D. viscosa* extract, a field-emission scanning electron microscope (FESEM) was used to verify the successful synthesis of the nanoparticles. They provided primary particles that were homogeneous, small, and highly porous.

Secondary agglomerates were observed in the second image taken at 50kX magnification, where they form during the drying process because, by evaporation of water, the electrostatic repulsive forces that pull the particles apart are reduced, which allows the

particles to touch each other by weak van der Waals force or hydrogen bonds according to Shrestha et al. (2020).

4.1.4.5. Energy-dispersive X-ray spectroscopy (EDX)

The EDX spectrum of the nanoparticles exhibited multiple peaks, indicating the presence of different elements. Similarly, the sulfur (S) signal shows a strong peak at about 2.3 keV, suggesting the potential presence of a sulfur-containing compound in the plant extract. The peaks noted, based on the organic nature of chitosan and the plant extract, correspond to carbon (C) at 0.39 keV, nitrogen (N) at 0.39 keV, and oxygen (O) at 0.52 keV. The identified peaks for hydroxyl (O-OH) and carboxyl functional groups confirmed the multifunctional composition of the nanomaterial.

Detected at the highest energy ranges, the peaks correspond to 1.48 keV (Al) and 1.745 keV (Si), likely due to impurities from the preparation utensils or to remnant materials from the plant (Alcaraz et al., 2025). Peaks of Ca were observed at 3.7 keV (Kα) and 4.0 keV (Kβ), indicating minimal presence, most likely from the chitosan residue or plant extract. The analytical data of sample corroborated this, reporting that carbon was present at the highest weight percentage (39.97%), followed by nitrogen (21.21%) and oxygen (19.44%) thus verifying the organic structure of the nanoparticles. Consequently, nitrogen is an excellent marker for chitosan because of the amino groups ($–NH_2$) attached to glucosamine units. Luthfiyana et al. (2022) reported that EDX nitrogen reflects the chitosan deacetylation level. Sulfur (8.09%) is most likely of plant origin, since plants of *D. viscosa* are known to contain sulfurous compounds or sulfate salts derived from the substrate. Previous study by Salman et al., (2023), it has already demonstrated the presence of sulfur signals in plant-based nanoparticles, similar to those observed in the present study.

Oxygen's high percentage is due to the density of hydroxyl and ether groups in chitosan and the oxidized compounds in the plant extract. This study aligns with the findings of Liu et al. (2024), who showed that up to 48% of the weight of chitosan nanoparticles was attributable to oxygen. Similarly, El-Najjar et al. (2023) observed robust oxygen, carbon, and nitrogen signals in comparable nanoparticles.

Calcium may come from non-removable chitosan impurities derived from crustacean shell patterns or natural nutritional components in *D. viscosa* leaves as reported by Hossain et al. (2018). The absence of any phosphorus (P) peak in the spectrum demonstrates that calcium was not complexed with TPP to form calcium phosphate and indicates an incipient origin. In contrast, Ahmed et al. (2024), confirmed TPP interaction with chitosan using EDX. Distinct peaks for sodium and phosphorus were detected, supporting the assertion that TPP in the sample used in the present study was not spectrally visible.

4.1.4.6. X-ray diffraction (XRD)

X-ray diffraction (XRD) analysis was performed to accurately describe the crystalline materials' crystalline type, dimensions, and structure. These findings demonstrate that incorporating plant extracts in to chitosan can sometimes facilitate crystallization through molecular organization mediated by the reaction. It also verifies that the variations in the diffraction pattern are directly caused by the interaction between chitosan and the natural extract, through both physical and chemical bonds. It has been shown that changes in the molecular arrangement in the crystal lattice can account for differences in the patterns, and the pattern of teicoplanin-loaded chitosan nanoparticles shows decreased peaks at 2θ 22 and 25 (Kahdestani et al., 2021), indicating a decrease in intensity. As stated by Shaghati (2022), the peaks in the XRD pattern of the chitosan were found at 2θ = 20.53 at an intensity of about 1200 counts, while the extract-loaded sample (DVE-loaded chitosan NPs) was found at 2θ = 22.8596 at 736.55 counts. This displacement of the maximum and the changes in intensity were ascribed to a change in crystalline structure of the samples upon interaction with the extract, which increased crystallinity.

To enhance the efficacy of the active ingredients in the *D. viscosa* plant extract by converting it to the nanoscale, chitosan was chosen because it is a natural, readily available substance that does not harm the environment or humans. The inhibition rate of the growth of *Fusarium* spp. strains increased when using the nano-extract compared to the natural extract. The active chemical components in the nanoparticles become more active when encapsulated, reducing their toxicity and making them less volatile and more environmentally friendly. Nano-chitosan facilitates the effective absorption of the

compound through the cell membrane, thereby increasing the availability of active substances within the nanoparticles (Kashyap et al., 2015).

Researchers propose three mechanisms for fungal inhibition. The first is that chitosan facilitates interaction and binding to phospholipids in the fungal membrane because it carries a negative charge, and because it carries a negative charge, and because chitosan carries a positive charge, which certainly helps in cell death by leaking its components and increasing the permeability of the fungal cell membrane. The second mechanism is the binding of chitosan to essential nutrients necessary for the normal growth of fungi, serving as a chelating agent. The third mechanism is to penetrate the fungal cell wall, which helps bind to its DNA, preventing or inhibiting the production of essential enzymes, proteins and mRNA synthesis (Ing et al., 2012).

Nanotechnology is considered one of the most important applications proposed and is poised to play a promising role in sustainable agriculture and food security. The inhibition of fungal growth that appears in the previous results is consistent with what was mentioned (Al-Hamiri & Hussein, 2020), as the small size of the compounds in the nano state gives them the ability to absorb the contents of cells in addition to penetrating cell membranes, and this is an important physical property that helped increase the effectiveness of the compounds or materials.

4.1.5. Effect of The Treatments on the Growth and Mycotoxin Production of *Fusarium* spp. Strains

F. pseudograminearum may indicate the presence of mycotoxins produced by this fungus, such as DON toxin, and evidence of its high concentration in plant tissues. It may be without disease symptoms (Xu et al., 2024). The results obtained in this study were consistent with those of a study conducted on samples from 17 wheat fields in Basra Governorate. DON toxins were confirmed in six fields, with concentrations ranging from 8 µg/kg to 1060 µg/kg (Minati and Mohammed-Ameen, 2019). HPLC results showed the presence of MON toxin produced by *F. oxysporum* strains 4, 5, and *F. chlamydosporum* strain 8. This study is considered the first work to investigate the presence of MON produced by *Fusarium* spp. strains growing on wheat samples stored in Iraq. MON is a toxin associated with some *Fusarium* spp. has a significant effect on humans, livestock, and can be a cause of cell death in humans and mice. It has also been detected in wheat

fields in many countries. MON has been associated with the fungus *F. oxysporum* in wheat fields (Ivić et al., 2009). There are about 40 species of *Fusarium* spp. responsible for the production of MON, and its presence has been confirmed in wheat and other grains. It should be noted that research on this toxin is limited, further studies are needed to characterize its toxicity, behavior, and the effects of treatments (Radić et al., 2019). Mycotoxin production may be affected by factors such as the presence of other microorganisms in the same environment, the type of agricultural practices in the field, and climate. Studies have shown that DON production by *Fusarium spp. are* greater at 28°C. The differences in results between studies depend on several factors, including isolates, substrates, and test conditions (Mahmoud et al., 2023).

4.1.5.1. Effect of ethanolic DVE and DVE-loaded Chitosan NPs on Production of Mycotoxin by Fusarium spp.

The results of applying the ethanolic extract to the isolated strains in this study showed growth inhibition in all strains, thereby reducing mycotoxin production. The inhibition rate of mycotoxin production increased with the application of DVE-loaded Chitosan NPs. The application of the ethanolic extract and DVE-loaded Chitosan NPs inhibited fungal growth and reduced mycotoxin production, as demonstrated in the results obtained above through testing using the HPLC device. This finding is consistent with the results reported by Al-Warshan et al. (2023), who showed that the application of plant extracts—neem, ginger, and eucalyptus—at concentrations of 12, 24, and 48 mg/mL exerted an inhibitory effect on the growth of *A. flavus* and reduced AFB1 production by 100%.

The researchers explained the effect of the plant extracts through their impact on the fungal cell and cell membrane, which disrupts ion exchange, as well as through binding to cell wall proteins and enzymes. This effect may be direct or indirect due to the active compounds present in the plant extracts. All of these factors have an effect that inhibits or prevents the production of mycotoxins. Plant extracts stimulate detoxification pathways and biotransformation and alter the equilibrium state in the cellular compartment, including osmotic and redox balances. A study has shown the effects of biologically active compounds on the growth of fungi, such as *A. favus*, *A. oryzae*, *A. niger*, *Alternaria alternata*, *F. moniliforme*, *F. graminearum*, *Penicillium citrinum*, and *P. viridicatum*, and their associated mycotoxins (Makhuvele et al., 2020).

Explained the ability of nanoparticles to penetrate cell membranes due to their small size, the difference in their physical properties and their ability to absorb cell contents (Kim et al., 2005). The rate of fungal inhibition increased with increasing nanoparticle concentration. This may be attributed to the interaction of nanoparticles with DNA affecting its ability to reproduce and its loss, as well as the ribosome subunit and the disruption of proteins.

In a study conducted by Hamad et al. (2023), they reported that the effects of polyphenols and flavonoids present in plant extracts can be attributed to four different aspects: (a) they play a significant role in biological activity through their ability to absorb lipids and their antioxidant properties; (b) they can alter and modify the fungal membrane, leading to the inhibition of mycotoxin production; (c) they also have a significant effect on gene expression and inhibition of the gene responsible for mycotoxin production; and (d) they also have an effect that inhibits enzymatic activity. It was confirmed that the phenolic compounds present in plant extracts are an important and vital pathway for influencing fungal growth and inhibiting mycotoxin production. Plant extracts also possess biologically active molecules that have a potent and detrimental effect on mycotoxins.

A. alternata is a phytopathogenic fungus responsible for leaf spot disease in tomato and potato. Methanolic extract of *D. viscosa*, at concentrations ranging from 100 to 2000 µg/mL, has demonstrated significant inhibitory activity against *A. alternata*. It has also been reported to inhibit the radial growth of *A. solani* (56.96%), *Macrophomina phaseolina* (52.06%), and *Rhizoctonia solani* (51.54%). These findings are consistent with the results of the present study and further confirm the antifungal potential of *D. viscosa* extract against these fungi (Behiry et al., 2022).

In another study, an aqueous extract of *D. viscosa* at 2 mg/mL showed inhibitory activity against *F. verticillioides*, a known producer of fumonisin B1. Similarly, the methanolic extract of *D. viscosa* exhibited antifungal activity against *F. verticillioides*, with an inhibition rate of 36.1 ± 0.21% at the same concentration (Thippeswamy et al., 2013). These findings are consistent with the results of the present study, indicating that *D. viscosa* extract can suppress the growth of *Fusarium* spp. strains and reduce mycotoxin production.

4.1.5.2. Effect of Ozone Gas on the Growth of Fusarium spp. Strains and Its Mycotoxins Production

After applying ozone gas to *Fusarium* spp. at different gas flow rates and exposure periods, the results showed significant differences between the control group and the ozone-exposed groups. The growth of *Fusarium* spp. strains was clearly inhibited, and the inhibition rate increased with increasing ozone gas flow rate and exposure time. Applying ozone at a rate of 4 liters/minute for 60 minutes had the greatest effect on fungal strain growth. It could be stated that ozone gas can inhibit the growth of microorganisms due to its rapid decomposition properties (Dong et al., 2015). Therefore, it has been widely used in several fields, including food sterilization. Ozone affects microorganisms and causes their death by affecting the cell membrane and oxidizing cell components such as amino acids, proteins, and polyunsaturated fatty acids (Xu, 1999). The oxidative effect of ozone gas is attributed to its ability to oxidize cell wall components, which contain numerous disulfide bonds as well as approximately 80% carbohydrates, 10% proteins, and glycoproteins. This mechanism helps explain the fungicidal effect of ozone on fungal cells (Karaca & Velioglu, 2007).

Nur et al. (2015) reported that ozone reduced and inhibited fungal spore counts. Applying ozone at a dose of 0.16 ozone/(g barley)·min to fungi reduced fungal spore counts by up to 96%, and this effect increased with increasing wheat moisture (Allen et al., 2003). The results of a study conducted by Wu et al. (2006) showed that storing wheat grains in sealed jars after ozone treatment had an inhibitory effect on fungal spores. The study also concluded that yeast and mold contents were reduced by washing wheat with ozonated water.

The effectiveness of ozone depends on several factors in its impact on mold, one of which is temperature (Isikber & Athanassiou, 2015). This may be because high temperatures stimulate the growth of organisms in stored wheat, particularly mold, in tightly sealed storage, this inhibits mold growth by depleting oxygen (Rajandrin, 2003). To understand how to deal with fungi growing on grains, the effect of ozone on the grains themselves must be studied to avoid any potential damage, even though ozone gas is one of the alternatives that has been approved as environmentally friendly, as mentioned above, the effect of ozone on grains also depends on several factors, including the flow rate,

exposure duration, and moisture level. It is emphasized that exposure duration is more important than gas flow rate, and that temperature and grain characteristics also play a role in increasing the effectiveness of ozone on grains, the gas's effect on grains begins at the grain's outer layer, and ozone then diffuses through it (Tiwari et al., 2010).

Mycotoxin analysis showed that ozone gas affected mycotoxin production for all strains, with significant differences, this is consistent with what was reported by Al-Dasouqi et al. (2012), who reported that applying ozone gas to infected wheat grains had a significant effect in reducing AFB1 toxins by 83.21% when the grains were exposed to ozone at a concentration of 40 parts per million for 20 minutes.

These results are consistent with what Wu et al. (2006) reported, which showed that ozone inhibited 39% of *A. flavus* spores after 5 minutes of exposureThis finding is consistent with the report of Afsah-Hejri et al. (2020), who described ozone as a strong oxidizing agent. Their study demonstrated that ozone can inhibit fungal growth by disrupting the cell wall, attacking polyunsaturated fatty acids, and oxidizing sulfhydryl groups, thereby suppressing fungal activities such as germination and toxin production. The exact mechanism by which ozone affects mycotoxins is still unclear. Still, some explanations for this effect include altering the structure of mycotoxins through ozone's interaction with functional groups within the mycotoxin molecule. These effects also vary depending on the moisture content of products, temperature, ozone concentration, and exposure time. This may explain and be consistent with the reduced mycotoxin production by *Fusarium* spp. strains in this study.

In a different study, DON toxins were reduced in ozone-treated wheat (55 g O3 h^{-1} for 6 hours) by 29%, the gas effectively disinfected grains, maintaining chemical and rheological parameters after it was applied to semolina, pasta and durum wheat. This is one of the most important advantages of ozone gas, as it is generally recognized as safe (GRAS). This supports the findings of the present study and confirms that ozone is a promising alternative for grain fumigation and for controlling fungi and other pathogens, including bacteria (Piemontese et al., 2018). Wang et al. (2016) reported that wheat samples exposed to ozone at a concentration of 75 mg/L for 30, 60, and 90 min showed deoxynivalenol detoxification rates of 26.40%, 39.16%, and 53.48%, respectively. These

findings indicate that exposure duration plays a significant role in enhancing the effectiveness of ozone treatment against mycotoxins.

4.1.5.3. Effect of The Sea Salt on The Normal and Nano-Particle Scale on Fusarium spp. Strains and Their Mycotoxins Production

Converting sea salt to the nano-state and applying it to *Fusarium* spp. strains increased the effect of sea salt. There was a clear significant difference and increase in the inhibition rates. The obtained results are consistent with those reported by Waheed et al. (2019), who confirmed that sodium chloride affects fungal growth and reduces the number of viable fungal colonies. They also noted that this effect depends on both the salt concentration and the age of the fungal culture. Asghari et al., (2008) obtained 100% inhibition of *Aspergillus niger* fungi when they used sodium chloride at a concentration of 40%. The results of the present study are consistent with those reported by Thanapuripat et al. (2010), who showed that sodium chloride applied at a microscopic scale completely inhibited the growth of *A. flavus* at a concentration of 10%. The enhanced effectiveness of salt in its nanoscale form, compared with its conventional form, may be attributed to the small particle size, which facilitates penetration through cell membranes and confers unique physicochemical properties. This may explain the higher inhibition rates observed in the present study when the salt was applied in its nanoscale form (Al-Hamiri & Hussein, 2020).

The antimicrobial mechanism of nanomaterials involves their penetration into microbial cells, followed by interactions with intracellular components such as DNA and proteins, leading to structural damage and the generation of reactive oxygen species (ROS). In addition, nanoparticles (NPs) may inhibit cells by accumulating on the cell surface, where adsorption occurs through functional groups. The binding of negatively charged proteins to NPs can further disrupt protein integrity, ultimately resulting in cell death (Sharmin et al., 2021). In another study, several salts, including calcium chloride, ammonium chloride, and manganese chloride, were evaluated for their inhibitory effects against Fusarium crown and root rot. Among them, sodium chloride was found to be more effective in controlling the fungi responsible for these diseases, namely *F. oxysporum* f. sp. *asparagi* and *F. proliferatum*. However, sodium chloride at concentrations of 0.25 and 0.50 g/L did not inhibit *F. oxysporum* f. sp. *cyclaminis*. These findings support the results

of the present study, in which no inhibitory effect was observed at a concentration of 1% against *F. pseudograminearum* strain 2, *F. oxysporum* strain 5, and *F. chlamydosporum* strain 8, all of which showed an inhibition rate of zero. This indicates that fungal species and genera differ in their sensitivity to salts, including sodium chloride (Türkkan, 2013). The mechanism of nanomaterials' effect on cells involves their interaction with the cell membrane, which stimulates programmed cell death and inhibits mitochondrial function in microorganisms (Kaundal et al., 2017). Nanoparticles affect the membrane's morphology and permeability, disrupting its function and allowing nanoparticles to enter the bacterial cell, increasing the likelihood of interaction with bacterial nucleic acids and leading to cell death (Morones, 2005).

Nanomaterials have been shown to interact with various compounds while exhibiting distinctive properties, such as a high surface area-to-size ratio (Gontero et al., 2017). Their inhibitory effects on microorganisms have been demonstrated in previous studies, including that of Rico et al. (2011). Nanoparticles have been reported to interfere with the formation of proteins involved in ATP production in fungal cells, which may help explain the inhibition of *Fusarium* spp. growth observed in the present study (Yamanaka et al., 2005). Their effects are not limited to fungal mycelia, as nanoparticles have also been shown to damage fungal spores and contribute to their destruction (Kasprowicz et al., 2010). In addition, Wani et al. (2015) demonstrated the effectiveness of magnesium oxide nanoparticles in inhibiting plant pathogenic fungi, including *Fusarium* spp. Collectively, these studies help explain the increased inhibition rates observed with nano sea salt and highlight its potential as an effective antifungal agent.

The results of this study are consistent with those reported by Al-Hamiri & Hussein (2020), in which sea salt and common natural salt were applied to an isolate of the fungus *Aspergillus flavus Asf 04*. The salt concentration ratios for both types of salt were 1%, 2.5%, and 3%, the experiment was carried out and sea salt was applied to dishes containing a laboratory culture medium, and the inhibition ratios for the growth of the fungal isolate were achieved at 0, 5.8, and 12.58% for sea salt and 0, 3.17, and 3.52% for common salt, respectively. The application of nano sea salt at a rate of 2.5% resulted in achieving the highest inhibition rate of AFB1 toxin production, which was 84.86%, in which the toxin concentration decreased from 22.88 parts per billion in the control group to 3.44 ppb in stored rice grains. These results are consistent with the findings of Horky

et al. (2018), who reported that most mycotoxins are non-polar compounds and, unlike polar compounds, cannot be easily removed because of their poor solubility in water.

4.1.6. Evaluation of the Best Four Treatments Applied to *Fusarium* spp. Strains

The above findings indicate that nano sea salt was the most effective treatment, followed by the nanoformulated ethanolic extract of *D. viscosa* and ozone gas, respectively. The results in Tables 19-20 and Figures 23-24, show that nano-salt exhibited the highest inhibition rates of fungal growth on wheat grains, surpassing all other treatments. This may be attributed to the strong inhibitory effect of nano-salt on the growth of *Fusarium* spp. strains, together with the large surface area of the nanoparticles relative to their small size. These properties likely enhanced their adhesion to the outer surface of the grains, allowing them to cover *Fusarium* spores associated with the grain and interfere with spore components, thereby preventing germination. If some spores succeeded in germinating, nano-salt could inhibit the developing germ tube by absorbing its contents and interacting with the fungal cell membrane. The results obtained in the present study are consistent with those reported by Al-Jumaili (2014), who found that treating yellow corn grains with a sodium chloride solution reduced aflatoxin levels by 86%.

The effectiveness of *D. viscosa* extract in inhibiting fungal growth can also be attributed to its content of the aforementioned phytochemicals, which have a strong inhibitory effect on fungal growth (Güneşer et al., 2018). Furthermore, nanoparticles can modify certain bonds, affecting important chemical groups such as COH, COOH, and CH3, thereby reducing the toxicity of mycotoxins or rendering them non-toxic (Gontero et al., 2017). It is worth noting that most mycotoxins are nonpolar, and nonpolar compounds are not easily eliminated because they are not soluble in water like polar compounds. Nanomaterials can alter the properties of toxins under different physical and chemical conditions, making them polar and thus eliminating them (Horky et al., 2018).

4.2. Conclusions

1. *Dodonaea viscosa* is a good source of phytochemicals that can be an alternative to industrial chemicals.

2. *Dodonaea viscosa* phytochemicals are highly effective in inhibiting the growth of *Fusarium* spp. strains.

3. This study demonstrated the effectiveness of the ethanolic extract of *Dodonaea vicosa* in both natural and nano forms in inhibiting the production of DON and MON mycotoxins.

4. It was proven that sea salt played a role in reducing the growth of *Fusarium* spp. strains and their ability to produce the mycotoxins associated with them.

5. The use of salt in nanoscale form enhanced the ability of sea salt to inhibit strain growth and reduce toxin production.

6. Ozone treatment in this study confirmed that ozone gas, at appropriate concentrations, exhibits antifungal activity and may be considered a potential alternative to chemical fungicides because of its favorable properties.

7. This is the first study in which MON toxins in wheat in Iraq have been detected.

8. Three new strains of *Fusarium* spp. were recorded for the first time, representing three types of *Fusarium* spp. present in stored grains.

9. The use of nanotechnology in converting the ethanolic extract into nanoparticles by using chitosan had a significant impact in improving the properties of the extract and increasing its effectiveness.

4.3. Future Studies

1. Study the possibility of commercially manufacturing a fungicide from *D. viscosa* extract.

2. Study the possibility of the effect of the ethanolic extract of *D. viscosa* as an inhibitor for other fungi.

3. Emphasizing the use of the extract in the nano state because of its effect in raising the efficiency of the extract.

4. Expanding the scope of using sea salt and studying its effects on different crops.

5. Ozone gas is an effective, easy-to-use, environmentally friendly and inexpensive gas, so it is necessary to focus and increase research in its use as a fungicide, insecticide and others on a commercial scale.

REFERENCES

Abbas Al-Hamiri, K. A. K., Hussein, H. Z. 2020. Efficacy of normal and nanoscale table salt on inhibiting the growth of fungi *Aspergillus flavus* in the culture medium and reducing aflatoxin B1 on stored rice grains. **International Journal of Agricultural Statistical Sciences, 16**.

Abbas, H. K., Mirocha, C. J., Gunther, R. 1989. Mycotoxins produced by toxic *Fusarium* isolates obtained from agricultural and non-agricultural areas (Arctic) of Norway. **Mycopathologia, 105**, 143–151.

Abd Al-Hamid, A. A. M. 2000. Fair and fungi of the fungus. College of Agriculture, Mansoura University.

Abd El-Ghaffar, M. A., Hashem, M. S. 2010. Chitosan and its amino acids condensation adducts as reactive natural polymer supports for cellulase immobilization. **Carbohydrate Polymers, 81(3)**, 507–516.

Abdel Aziz, A. K. 2015. The use of calcium carbide in the reduction of C1AFB yellow corn grains. Master's thesis, College of Agriculture, University of Baghdad.

Abdel Razzaq, A. A. W. 1989. Fungal content and the presence of emetic toxin deoxynivalenol in local and imported wheat. Master's thesis, Department of Life Sciences, College of Science, University of Baghdad.

Abdel-Kader, M. M., El-Mougy, N. S., Khalil, M. S. A., El-Gamal, N. G. 2021. Biocontrol agents for controlling wheat root rot disease under greenhouse conditions. **Indian Journal of Agricultural Research, 55(2)**, 239–242.

Aboul-Nasr, M. B. 2014. Effect of sodium chloride on the growth and aflatoxin production of *Aspergillus flavus* isolated from poultry feedstuff samples.

Adejumo, T. O., Hettwer, U., Karlovsky, P. 2007. Occurrence of *Fusarium* species and trichothecenes in Nigerian maize. **International Journal of Food Microbiology, 116**, 350–357.

Afsah-Hejri, L., Hajeb, P., Ehsani, R. J. 2020. Application of ozone for degradation of mycotoxins in food: A review. **Comprehensive Reviews in Food Science and Food Safety, 19(4)**, 1777–1808.

Agarwal, M., Agarwal, M. K., Shrivastav, N., Pandey, S., Das, R., Gaur, P. 2018. Preparation of chitosan nanoparticles and their in-vitro characterization. **International Journal of Life-Sciences Scientific Research, 4(2)**, 1713–1720.

Ahmed, M. E., Mohamed, M. I., Ahmed, H. Y., Elaasser, M. M., Kandile, N. G. 2024. Fabrication and characterization of unique sustain modified chitosan nanoparticles for biomedical applications. **Scientific Reports, 14(1)**. https://doi.org/10.1038/s41598-024-64017-4

Ahmed, E. G. H. 2005. Effect of bran particle size on wheat flour dough and bread quality. Faculty of Agriculture, University of Khartoum.

Alcaraz, L., Sotillo, B., Fernández, P., López, F. A. 2025. Carbochlorination reduction process of Waelz ZnO: Characterization of resulting ZnO-based oxides. **Crystals, 15(4)**, 326. https://doi.org/10.3390/cryst15040326

Al-Dairi, S. S., Al-Waily, D. S. 2023. Isolation and diagnosis of some *Fusarium* species causing head blight in wheat in the southern region of Iraq. **IOP Conference Series: Earth and Environmental Science, 1262(9)**, 092011.

Ali, S. R., Fradi, A. J., Al-Aaraji, A. M. 2017. Effect of some physical factors on growth of five fungal species. **European Academic Research, 2(2)**, 1069–1078.

Al-Jumaili, S. A.-R. 2014. *Mycotoxins*. Dar Al-Kutub.

Alkadri, D. 2012. *Fusarium* species responsible for mycotoxin production in wheat crop: Involvement in food safety.

Al-Aubaidi, H. K. 2016. Increasing some medicinal flavonoid compounds of *Dodonaea viscosa* using $AgNO_3$ nanoparticles in vitro. **Iraqi Journal of Science**, 338–343.

Allen, B., Wu, J., Doan, H. 2003. Inactivation of fungi associated with barley grain by gaseous ozone. **Journal of Environmental Science and Health, Part B, 38(5)**, 617–630.

Almosowi, M. H., Al-Mofti, D. M. M., Al-Kiessy, D. M. D. 2010. Effect of *Dodonaea viscosa* on the activity of *Fusarium* spp. **University of Thi-Qar Journal, 5(6)**.

Almukhtar, J. G. J., Karam, F. F. 2020. Preparation, characterization, and application of chitosan nanoparticles as drug carrier. **Journal of Physics: Conference Series, 1664(1)**, 012071.

Al-Musleh, R. M. 1990. *Microorganisms in food* (2nd ed.). Higher Education Press.

Al-Sallami, I. A., Jaleel, R. M. 2015. Inhibitory effect of *Dodonaea viscosa* leaves extracts on radial growth and spore germination of some plant pathogenic fungi. **Euphrates Journal of Agricultural Science, 7(4)**.

Alshannaq, A., Yu, J. H. 2017. Occurrence, toxicity, and analysis of major mycotoxins in food. **International Journal of Environmental Research and Public Health, 14(6)**, 632.

Al-Sharmani, H. R., Al-Kalabi, H. H., Al-Abedy, A. N. 2019. Efficacy of rice husks compost and *Trichoderma harzianum* on *Rhizoctonia solani* and its effect on seed germination and seedling health. **IOP Conference Series: Earth and Environmental Science, 388(1)**, 012002.

Al-Snafi, A. E. 2017. A review on *Dodonaea viscosa*: A potential medicinal plant. **IOSR Journal of Pharmacy, 7(2)**, 10–21.

Alsohaili, S. A., Bani-Hasan, B. M. 2018. Morphological and molecular identification of fungi isolated from different environmental sources in the north-eastern desert of Jordan. **Jordan Journal of Biological Sciences, 11(3)**.

AlTaweel, K., Amarasinghe, C. C., Brûlé-Babel, A. L., Fernando, W. G. D. 2017. Gene expression analysis of host–pathogen interaction between wheat and *Fusarium graminearum*. **European Journal of Plant Pathology, 148(3)**, 617–629.

Al-Warshan, S. H., Hadi, S. T., Sultan, L. J. 2023. Efficiency of plant extracts on *Aspergillus* growth and aflatoxin B1 production in *Zea mays*. **Pakistan Journal of Botany, 55(4)**, 1545–1550.

Armitage, D. 2003. Grain sampling methods to achieve consumer confidence and food safety.

Asghari, H. R., Amerian, M. R., Gorbani, H. 2008. Soil salinity affects arbuscular mycorrhizal colonization of halophytes. **Pakistan Journal of Biological Sciences, 11(15)**, 1909–1915.

Askun, T. 2018. Introductory chapter: *Fusarium* pathogenicity, infections, diseases, mycotoxins and management. **Fusarium: Plant Diseases, Pathogen Diversity, Genetic Diversity, Resistance and Molecular Markers**.

Husen, A., Siddiqi, K. S. 2014. Plants and microbes assisted selenium nanoparticles: Characterization and application. **Journal of Nanobiotechnology**.

Beccari, G., Colasante, V., Tini, F., Senatore, M. T., Prodi, A., Sulyok, M., Covarelli, L. 2018. Causal agents of *Fusarium* head blight of durum wheat and their in vitro biosynthesis of secondary metabolites. **Food Microbiology, 70**, 17–27.

Behiry, S. I., Philip, B., Salem, M. Z., Amer, M. A., El-Samra, I. A., Abdelkhalek, A., Heflish, A. 2022. *Urtica dioica* and *Dodonaea viscosa* leaf extracts as eco-friendly bioagents against *Alternaria alternata*. **Scientific Reports, 12(1)**, 16468.

Benhamou, N., Lafontaine, P. J., Nicole, M. 1994. Seed treatment with chitosan induces systemic resistance to *Fusarium* crown and root rot in tomato plants. **Phytopathology, 84(12)**, 1432–1444.

Bennett, J. W., Klich, M. 2003. Mycotoxins. **Clinical Microbiology Reviews, 16(3)**, 497–516. https://doi.org/10.1128/CMR.16.3.497-516.2003

Bernhoft, A. 2010. A brief review on bioactive compounds in plants. **Bioactive Compounds in Plants—Benefits and Risks for Man and Animals, 50**, 11–17.

Beshah, F., Hunde, Y., Getachew, M., Bachheti, R. K., Husen, A., Bachheti, A. 2020. Ethnopharmacological, phytochemistry and other potential applications of *Dodonaea* genus: A comprehensive review. **Current Research in Biotechnology, 2**, 103–119.

Bevan, J. R., Firth, C., Neicho, M. 1997. Storage of organically produced crops.

Bolanos-Carriel, C. 2018. Epidemiology and management of fusarium head blight and foliar fungal diseases of wheat. University of Nebraska-Lincoln.

Bhatnagar, D., Cary, J. W., Ehrlich, K., Yu, J., Cleveland, T. E. 2006. Understanding the genetics of regulation of aflatoxin biosynthesis.

Bryła, M., Pierzgalski, A., Zapaśnik, A., Uwineza, P. A., Ksieniewicz-Woźniak, E., Modrzewska, M., Waśkiewicz, A. 2022. Recent research on *Fusarium* mycotoxins in maize—A review. **Foods, 11(21)**, 3465.

Burgess, L. W., Phan, H. T., Knight, T. E., Tesoriero, L. 2008. *Diagnostic manual for plant diseases in Vietnam*.

Butler, J. M., Johnson, J. E., Boone, W. R. 2013. The heat is on: Room temperature affects laboratory equipment—An observational study. **Journal of Assisted Reproduction and Genetics, 30(10)**, 1389–1393.

Büyükyörük, S. 2021. Chitosan for using food protection. IntechOpen.

Campabadal, C. A. 2013. Ozonation systems as a non-chemical alternative for stored grain protection.

Campabadal, C. A., Maier, D. E., Mason, L. J. 2013. Efficacy of fixed bed ozonation treatment to control insects in stored bulk grain. **Applied Engineering in Agriculture, 29(5)**, 693–704.

Cengiz, R. 2016. Türkiye'de kamu mısır araştırmaları. **Tarla Bitkileri Merkez Araştırma Enstitüsü Dergisi, 25(Özel Sayı-1)**, 304–310.

Chandrasekaran, M., Kim, K. D., Chun, S. C. 2020. Antibacterial activity of chitosan nanoparticles: A review. **Processes, 8(9)**, 1173.

Chehri, K., Jahromi, S. T., Reddy, K. R., Abbasi, S., Salleh, B. 2010. Occurrence of *Fusarium* spp. and fumonisins in stored wheat grains marketed in Iran. **Toxins, 2(12)**, 2816–2823.

Christensen, C. M., Kaufmann, H. H. 1965. Deterioration of stored grains by fungi. **Annual Review of Phytopathology, 3(1)**, 69–84.

Christensen, M. J., Falloon, R. E., Skipp, R. A. 1988. A Petri plate technique for testing pathogenicity of fungi to seedlings and inducing fungal sporulation. **Australasian Plant Pathology, 17(2)**, 45–47.

Chudy, S., Makowska, A., Kowalski, R. 2025. Sodium chloride in food. **Foods, 14(15)**, 2741.

Cochrane, V. W. 1958. *Physiology of fungi*. Wiley.

Cole, R. J., Kirksey, J. W., Cutler, H. G., Doupnik, B. L., Peckham, J. C. 1973. Toxin from *Fusarium moniliforme*: Effects on plants and animals. **Science, 179(4080)**, 1324–1326.

Conte, G., Fontanelli, M., Galli, F., Cotrozzi, L., Pagni, L., Pellegrini, E. 2020. Mycotoxins in feed and food and the role of ozone in their detoxification and degradation: An update. **Toxins, 12(8)**, 486.

Cooley, D. R., Mullins, R. F., Bradley, P. M., Wilce, R. T. 2011. Culture of the upper littoral zone marine alga *Pseudendoclonium submarinum* induces pathogenic interaction with the fungus *Cladosporium cladosporioides*. **Phycologia, 50(5)**, 541–547.

Cooper, R. 2015. Re-discovering ancient wheat varieties as functional foods. **Journal of Traditional and Complementary Medicine, 5(3)**, 138–143.

Cox-Georgian, D., Ramadoss, N., Dona, C., Basu, C. 2019. Therapeutic and medicinal uses of terpenes. In *Medicinal Plants: From Farm to Pharmacy* (pp. 333–359).

Cui, H., Wang, S., Yang, X., Zhang, W., Chen, M., Wu, Y., Li, S., Li, L., Cai, D., Guo, B., Ye, J. 2022. Predictive models for assessing the risk of *Fusarium pseudograminearum* mycotoxin contamination in post-harvest wheat with multi-

parameter integrated sensors. **Food Chemistry: X, 16**, 100472. https://doi.org/10.1016/j.fochx.2022.100472

Çatal, H., İbanoğlu, S. 2012. Structure, physico-chemical and microbiological properties of ozone-oxidized wheat, corn and potato. **Journal of Food Science and Engineering, 2(4)**.

Daniyal, W. M. E. M. M., Fen, Y. W., Abdullah, J., Saleviter, S., Omar, N. A. S. 2018. Preparation and characterization of hexadecyltrimethylammonium bromide modified nanocrystalline cellulose/graphene oxide composite thin film and its potential in sensing copper ion using surface plasmon resonance technique. **Optik, 173**, 71–77.

Deacon, J. W. 2005. *Fungal biology*. John Wiley Sons.

Deijns, A. J., Egmond, H. P., Speijers, G. A. J., Loveren, H. V. 1997. *Immunotoxicity van natuurlijke toxinen: Een literatuuroverzicht*. Rijksinstituut voor Volksgezondheid en Milieu.

Del Palacio, A., Corallo, B., Simoens, M., Cea, J., De Aurrecoechea, I., Martinez, I., Pan, D. 2023. Major *Fusarium* species and mycotoxins associated with freshly harvested maize grain in Uruguay. **Mycotoxin Research, 39(4)**, 379–391.

Desjardins, A. E., Proctor, R. H. 2007. Molecular biology of *Fusarium* mycotoxins. **International Journal of Food Microbiology, 119(1–2)**, 47–50.

Dey, D. 2016. Role of secondary metabolites in plant defense. **Innovative Farming, 1(4)**, 115–118.

Dodd, J. G., Vegi, A., Vashisht, A., Tobias, D., Schwarz, P., Wolf-Hall, C. E. 2011. Effect of ozone treatment on the safety and quality of malting barley. **Journal of Food Protection, 74(12)**, 2134–2141.

Dong, T., Zhang, Y., Islam, M. S., Liu, Y., El-Din, M. G. 2015. Impact of ozone pretreatment doses on the performance of microbial communities for remediation of oil sands process-affected water. **International Biodeterioration Biodegradation, 100**, 17–28.

Du, W. L., Xu, Z. R., Han, X. Y., Xu, Y. L., Miao, Z. G. 2008. Preparation, characterization and adsorption properties of chitosan nanoparticles for eosin Y as a model anionic dye. **Journal of Hazardous Materials, 153(1–2)**, 152–156.

Dubey, N. K., Srivastava, B., Kumar, A. 2008. Current status of plant products as botanical pesticides in storage pest management. **Journal of Biopesticides, 1(2)**, 182–186.

Duraisamy, N., Dhayalan, S., Shaik, M. R., Shaik, A. H., Shaik, J. P., Shaik, B. 2022. Green synthesis of chitosan nanoparticles using *Martynia annua* leaf extract and their antibacterial activity. **Crystals, 12(11)**, 1550.

Durmaz, L. 2021. Antioxidant, antiepileptic, and anticholinergic properties of 4′,5,7-trihydroxy-3,6-dimethoxyflavone. **Toxin Reviews, 40(3)**, 292–299.

Dutt, Y., Pandey, R. P., Dutt, M., Gupta, A., Vibhuti, A., Priyadarshini, A. 2023. Therapeutic applications of nanobiotechnology. **Journal of Nanobiotechnology, 21(1)**, 148.

Dweba, C. C., Figlan, S., Shimelis, H. A., Motaung, T. E., Sydenham, S., Mwadzingeni, L., Tsilo, T. J. 2017. *Fusarium* head blight of wheat: Pathogenesis and control strategies. **Crop Protection, 91**, 114–122.

Ealia, S. A. M., Saravanakumar, M. P. 2017. A review on the classification, characterization, synthesis of nanoparticles and their application. **IOP Conference Series: Materials Science and Engineering, 263**, 032019.

Ehling, G., Cockburn, A., Snowdon, P., Buchhaus, H. 1997. The significance of the *Fusarium* toxin deoxynivalenol (DON) for human and animal health. **Cereal Research Communications, 25**, 443–447.

El-Desouky, T. A., Sharoba, A. M. A., El-Desouky, A. I., El-Mansy, H. A., Naguib, K. 2012. Effect of ozone gas on degradation of aflatoxin B1 and *Aspergillus flavus*. **Journal of Environmental Analytical Toxicology, 2(1)**, 128.

Elieh-Ali-Komi, D., Hamblin, M. R. 2016. Chitin and chitosan: Production and application of versatile biomedical nanomaterials. **International Journal of Advanced Research, 4(3)**, 411.

Elkeleny, S. S., Mohamed, A. A. 2023. Effect of some plant extracts on quality, storability and pathogenic fungi during cold storage of husk tomato. **Horticulture Research Journal, 1(Special Issue 1)**, 137–150.

El-Mohamedy, R. S., Abdalla, A. M. 2014. Evaluation of antifungal activity of *Moringa oleifera* extracts as natural fungicide against plant pathogenic fungi.

El-Naggar, N. E., Eltarahony, M., Hafez, E. E., Bashir, S. I. 2023. Green fabrication of chitosan nanoparticles using *Lavandula angustifolia*: Optimization,

characterization and antibiofilm activity. **Scientific Reports, 13(1)**. https://doi.org/10.1038/s41598-023-37660-6

Eriksen, G. S., Alexander, J. 1998. *Risk assessment*. Nordic Council of Ministers.

Eskola, M., Päivi, P., Aldo, R. 2001. Trichothecenes, ochratoxin A and zearalenone contamination and *Fusarium* infection in Finnish cereal samples in 1998. **Food Additives Contaminants, 18(8)**, 707–718.

Fang, Y., Hu, J., Xiong, S., Zhao, S. 2011. Effect of low-dose microwave radiation on *Aspergillus parasiticus*. **Food Control, 22(7)**, 1078–1084.

FAO. 2022. *Crop prospects and food situation – Quarterly global report No. 3*. Food and Agriculture Organization.

FAO. 2024. *World food and agriculture – Statistical yearbook 2023*. Food and Agriculture Organization.

FAO, Cephas, T., Danilo, M., Javier, S. A. 2014. *Appropriate seed and grain storage systems for small-scale farmers*. Food and Agriculture Organization.

Fauzi, N. I. M., Fen, Y. W., Omar, N. A. S., Saleviter, S., Ebtisyam, W. M., Daniyal, M. M., Hashim, H. S., Nasrullah, M. 2020. Nanostructured chitosan/maghemite composite thin film for optical detection of mercury ions. **Polymers, 12(7)**, 1497.

Fernandez, M. R., Conner, R. L. 2011. Root and crown rot of wheat. **Prairie Soils Crops Journal, 4**, 151–157.

Ferrigo, D., Raiola, A., Causin, R. 2016. *Fusarium* toxins in cereals: Occurrence, legislation, factors promoting appearance and management. **Molecules, 21(5)**, 627.

Fravel, D. R., Stosz, S. K., Larkin, R. P. 1996. Effect of temperature, soil type and matric potential on proliferation and survival of *Fusarium oxysporum*. **Phytopathology, 86**, 236–240.

Gnonlonfin, G. J. B., Hell, K., Adjovi, Y., Fandohan, P., Koudande, D. O., Mensah, G. A., Brimer, L. 2013. A review on aflatoxin contamination and its implications in the developing world. **Critical Reviews in Food Science and Nutrition, 53(4)**, 349–365.

Goliński, P., Kostecki, M., Kaptur, P., Wojciechowski, S., Kaczmarek, Z., Wiśniewska, H., Chełkowski, J. 1997. *Fusarium* head blight and moniliformin accumulation in winter wheat cultivars. **Cereal Research Communications, 25**, 673–675.

Gonçalves, C., Mischke, C., Stroka, J. 2020. Determination of deoxynivalenol and its conjugates in cereals using solvent-free extraction. **Food Additives Contaminants: Part A, 37(10)**, 1765–1776.

Gontero, D., Lessard-Viger, M., Brouard, D., Bracamonte, A. G., Boudreau, D., Veglia, A. V. 2017. Smart multifunctional nanoparticles as sensors and drug delivery systems. **Microchemical Journal, 130**, 316–328.

Gordon, T. R. 2017. *Fusarium oxysporum* and the Fusarium wilt syndrome. **Annual Review of Phytopathology, 55**, 23–39.

Gupta, S., Banerjee, A. B. 1970. A rapid method of screening antifungal antibiotic producing plants.

Gutiérrez-Grijalva, E. P., López-Martínez, L. X., Contreras-Angulo, L. A., Elizalde-Romero, C. A., Heredia, J. B. 2020. Plant alkaloids: Structures and bioactive properties. In *Plant-derived bioactives: Chemistry and mode of action*, 85–117.

Guzman, M. G., Dille, J., Godet, S. 2009. Synthesis of silver nanoparticles by chemical reduction method and their antibacterial activity. **International Journal of Chemical and Biomolecular Engineering**, 2(3), 104–111.

Güneşer, B. A., Zorba, N. D., Yılmaz, E. 2018. Antimicrobial activity of cold-pressed citrus seed oils, some citrus flavonoids and phenolic acids. **Journal of Food Science and Technology**, 95(2), 119–131.

Hamad, G. M., Mehany, T., Simal-Gandara, J., Abou-Alella, S., Esua, O. J., Abdel-Wahhab, M. A., Hafez, E. E. 2023. A review of recent innovative strategies for controlling mycotoxins in foods. **Food Control**, 144, 109350.

Hameed, I. H., Hussein, H. J., Kareem, M. A., Hamad, N. S. 2015. Identification of five newly described bioactive chemical compounds in methanolic extract of *Mentha viridis* by using gas chromatography-mass spectrometry (GC-MS). **Journal of Pharmacognosy and Phytotherapy**, 7(7), 107–125.

Hameed, M. A., Rana, R. M., Ali, Z. 2012. Identification and characterization of a novel Iraqi isolate of *Fusarium pseudograminearum* causing crown rot in wheat. **Genetics and Molecular Research**, 11(2), 1341–1348.

Harborne, J. B. 1973. *Photochemical methods*. Halsted Press, John Wiley Sons, New York.

Hassani, F., Zare, L., Khaledi, N. 2019. Evaluation of germination and vigor indices associated with Fusarium-infected seeds in pre-basic seeds wheat fields. **Journal of Plant Protection Research**, 59(1).

Hatem, M. W., Shukri, H. M., Rasheed, K. A., Nawar, M. H., Hasan, S. M., Adnan, R. 2020. The effect of magnetically treated water against Fusarium wilt disease in tomato caused by the fungus *Fusarium oxysporum* and its effect on production under fertilized farming conditions. **Plant Archives**, 20(1), 533–536.

Hodoroaba, V. 2019. Energy-dispersive X-ray spectroscopy (EDS). In *Elsevier eBooks*, 397–417. https://doi.org/10.1016/b978-0-12-814182-3.00021-3

Horky, P., Skalickova, S., Baholet, D., Skladanka, J. 2018. Nanoparticles as a solution for eliminating the risk of mycotoxins. **Nanomaterials**, 8(9), 727.

Hossain, M. A. 2018. Biological and phytochemicals review of Omani medicinal plant *Dodonaea viscosa*. **Journal of King Saud University – Science**, 31(4), 1089–1094. https://doi.org/10.1016/j.jksus.2018.09.012

HuiJia, W., Wu, X., Jie, L., Cheng-Hua, Z., Hai, Z. 2017. Role of glucagon-like peptide-1 and gastric inhibitory peptide in anorexia induction following oral exposure to the trichothecene mycotoxin deoxynivalenol (vomitoxin). **Toxicological Sciences**, 159(1), 6–24.

Ibanoglu, S. 2002. Wheat washing with ozonated water: Effects on selected flour properties. **International Journal of Food Science Technology**, 37, 579–584. https://doi.org/10.1046/j.1365-2621.2002.00593.x

Ibrahim, H. M., El-Zairy, E. M. R. 2015. Chitosan as a biomaterial—structure, properties, and electrospun nanofibers. In *Concepts, compounds and the alternatives of antibacterials*, 1(1), 81–101.

Ibrahim, I. K., Thalaj, K. M. 1998. *Mycotoxins and their effects and its risks*. Baghdad: Abaa Center for Agricultural Research.

Inamdar, A. A., Suresh, D. S. 2014. Application of color sorter in wheat milling. **International Food Research Journal**, 21(6), 2083.

Ing, L. Y., Zin, N. M., Sarwar, A., Katas, H. 2012. Antifungal activity of chitosan nanoparticles and correlation with their physical properties. **International Journal of Biomaterials**, 2012, 632698.

Iqbal, M. J., Shams, N., Fatima, K. 2022. Nutritional quality of wheat. In *Wheat – Recent Advances*. IntechOpen.

Ishtiaq, M. U. H., Hussain, T., Bhatti, K. H., Adesemoye, T. O. N., Maqbool, M. E. H., Azam, S. H., Ghani, A. B. 2019. Management of root rot diseases of eight wheat varieties using resistance and biological control agents techniques. **Pakistan Journal of Botany**, 51(1), 327–339.

Isikber, A. A., Athanassiou, C. G. 2015. The use of ozone gas for the control of insects and micro-organisms in stored products. **Journal of Stored Products Research**, 64, 139–145.

Ismail, A. N. 2014. *Mycotoxins, theory and general concept*. University of Baghdad, College of Agriculture, Department of Plant Protection.

Ivić, D., Domijan, A. M., Peraica, M., Miličević, T., Cvjetković, B. 2009. Fusarium spp. contamination of wheat, maize, soybean, and pea grain in Croatia. **Arhiv za Higijenu Rada i Toksikologiju**, 60(4), 435–441. https://doi.org/10.2478/10004-1254-60-2009-1963

Jestoi, M. 2008. Emerging *Fusarium* mycotoxins: Fusaproliferin, beauvericin, enniatins, and moniliformin—A review. **Critical Reviews in Food Science and Nutrition**, 48(1), 21–49.

Ji, F., He, D., Olaniran, A. O., Mokoena, M. P., Xu, J., Shi, J. 2019. Occurrence, toxicity, production and detection of *Fusarium* mycotoxin: A review. **Food Production, Processing and Nutrition**, 1(1), 1–14. https://doi.org/10.1186/s43014-019-0007-2

Jonsson, M. 2017. *The toxicity of Fusarium mycotoxins enniatin and moniliformin* (Doctoral dissertation, University of Helsinki).

Kahdestani, S. A., Shahriari, M. H., Abdouss, M. 2021. Synthesis and characterization of chitosan nanoparticles containing teicoplanin using sol–gel. **Polymer Bulletin**, 78(2), 1133–1148.

Kaltner, F., Rampl, C., Rychlik, M., Zimmermann, T., Rohe, A. 2017. Development and validation of a cost-effective HPLC-FLD method for routine analysis of fumonisins B1 and B2 in corn and corn products. **Food Analytical Methods**, 10(5), 1349–1358.

Karaca, H., Velioglu, Y. S. 2007. Ozone applications in fruit and vegetable processing. **Food Reviews International**, 23(1), 91–106.

Kashyap, P. L., Xiang, X., Heiden, P. 2015. Chitosan nanoparticle based delivery systems for sustainable agriculture. **International Journal of Biological Macromolecules**, 77, 36–51. https://doi.org/10.1016/j.ijbiomac.2015.02.039

Kasprowicz, M. J., Gorczyca, A., Szymocha, A. 2015. Physiological effects of nanosilver on vegetative mycelium, conidia and the development of the entomopathogenic fungus *Isaria fumosorosea*. **Biocontrol Science and Technology**, 25(8), 873–887.

Kaundal, B., Dalai, S., Choudhury, S. R. 2017. Nanomaterial toxicity in microbes, plants and animals. In *Nanoscience in Food and Agriculture 5*, 243–266.

Kaurinovic, B., Vastag, D. 2019. Flavonoids and phenolic acids as potential natural antioxidants. In *IntechOpen*, 1–20.

Kayıhan, C. 2014. *Physiological, biochemical and molecular analysis of wheat cultivars under boron treatments* (Doctoral dissertation, Middle East Technical University, Turkey).

Kayim, M., Nawaz, H., Alsalmo, A. 2022. Fungal diseases of wheat. In *Wheat – Recent Advances*. IntechOpen.

Khadre, M., Yousef, A. E., Kim, J. 2001. Microbiological aspects of ozone applications in food: A review. **Journal of Food Science**.

Khalid, A., Hameed, A., Tahir, M. F. 2023. Wheat quality: A review on chemical composition, nutritional attributes, grain anatomy, types, classification, and function of seed storage proteins in bread making quality. **Frontiers in Nutrition**, 10, 1053196.

Kim, D. I., Park, J. D., Kim, S. G., Kuk, H., Jang, M. S., Kim, S. S. 2005. Screening of some crude plant extracts for their acaricidal and insecticidal efficacies. **Journal of Asia-Pacific Entomology**, 8(1), 93–100. https://doi.org/10.1016/S1226-8615(08)60076-X

Knight, S. C., Anthony, V. M., Brady, A. M., Greenland, A. J., Heaney, S. P., Murray, D. C., Powell, K. A., Schulz, M. A., Spinks, C. A., Worthington, P. A., Youle, D. 1997. Rationale and perspectives on the development of fungicides. **Annual Review of Phytopathology**, 35, 349–372.

Kocaçalışkan, I., Talan, I., Terzi, I. 2006. Antimicrobial activity of catechol and pyrogallol as allelochemicals. **Zeitschrift für Naturforschung C**, 61(9–10), 639–642.

Korsten, L., De Jager, E. S. 1995. Mode of action of *Bacillus subtilis* for control of avocado postharvest pathogens. **South African Avocado Growers Association Yearbook**, 18, 124–130.

Kraft, J. M. 1994. Fusarium wilt of peas (a review). **Agronomie**, 14(9), 561–567.

Kregiel, D., Berlowska, J., Witonska, I., Antolak, H., Proestos, C., Babic, M., Zhang, B. 2017. Saponin-based biological-active surfactants from plants. **Application and Characterization of Surfactants**, 6(1), 184–205.

Kumar, G. V., Kumar, M. A., Kumar, G. R. 2010. Growth characteristics of *Fusarium* spp. causing wilt disease in *Psidium guajava* L. in India. **Journal of Plant Protection Research**, 50(4), 452–462.

Kumar, S., Stecher, G., Li, M., Knyaz, C., Tamura, K. 2018. MEGA X: Molecular evolutionary genetics analysis across computing platforms. **Molecular Biology and Evolution**, 35(6), 1547–1549.

Lacey, J., Bateman, G. L., Mirocha, C. J. 1999. Effects of infection time and moisture on development of ear blight and deoxynivalenol production by *Fusarium* spp. in wheat. **Annals of Applied Biology**, 134(3), 277–283. https://doi.org/10.1111/j.1744-7348.1999.tb05265.x

Lahlali, R., Ezrari, S., Radouane, N., Kenfaoui, J., Esmaeel, Q., El Hamss, H., Barka, E. A. 2022. Biological control of plant pathogens: A global perspective. **Microorganisms**, 10(3), 596.

Lai, X., Zhang, H., Liu, R., Liu, C. 2015. Potential for trichothecene production by *Fusarium* spp. strains isolated from rice samples. **Saudi Journal of Biological Sciences**, 22(2), 176–180.

Langseth, W., Stenwig, H., Sogn, L., Mo, E. 1993. Growth of moulds and production of mycotoxins in wheat during drying and storage. **Acta Agriculturae Scandinavica B – Plant Soil Sciences**, 43(1), 32–37.

Liu, C., Wang, C., Liu, Y., Huang, J., Xu, W., Li, J., Xu, H. 2024. Selenium nanoparticles/carboxymethyl chitosan/alginate antioxidant hydrogel for treating steroid-induced osteonecrosis of the femoral head. **International Journal of Pharmaceutics**, 653, 123929.

Luo, X. Y. 1988. Outbreaks of moldy cereals poisoning in China. In *Issues in Food Safety* (pp. 56–63). Washington DC: Toxicology Forum, Inc.

Luthfiyana, N., Bija, S., Nugraeni, C. D., Lembang, M. S., Anwar, E., Laksmitawati, D. R., Nusaibah, N., Ratrinia, P. W., Mukmainna, M. 2022. Characteristics and antibacterial activity of chitosan nanoparticles from mangrove crab shell (*Scylla* sp.) in Tarakan waters, North Kalimantan, Indonesia. **Biodiversitas Journal of Biological Diversity, 23**(8). https://doi.org/10.13057/biodiv/d230820

Maheshwari. 2018. Wheat cleaning. In *IAOM Inaugural South Asia Region Meetings*. Teutopolis, Illinois Delhi, India. https://www.iaom.info

Mahmoud, A. L. E., Kilany, A. H. M., Hassan, E. A. 2023. Antifungal activity of *Lysinibacillus macroides* against toxigenic *Aspergillus flavus* and *Fusarium proliferatum* and analysis of its mycotoxin minimization potential. **BMC Microbiology, 23**(1), 269.

Makhuvele, R., Naidu, K., Gbashi, S., Thipe, V. C., Adebo, O. A., Njobeh, P. B. 2020. The use of plant extracts and their phytochemicals for control of toxigenic fungi and mycotoxins. **Heliyon, 6**(10).

Maluin, F. N., Hussein, M. Z. 2020. Chitosan-based agronanochemicals as a sustainable alternative in crop protection. **Molecules, 25**(7), 1611.

Maresca, M., Mahfoud, R., Garmy, N., Fantini, J. 2002. The mycotoxin deoxynivalenol affects nutrient absorption in human intestinal epithelial cells. **The Journal of Nutrition, 132**(9), 2723–2731.

Manjulatha, K. A. 2012. *Comparative study of different parts of flavonoid rich plant, Dodonaea viscosa for antimicrobial and antioxidant potential*. LAP Lambert Academic Publishing.

Matny, O. N. 2014. *Mycotoxins: Theory and general concept*. AlSeemah Publisher. https://doi.org/10.13140/RG.2.2.19487.97443

Miller, C. 2019. Importance of grain cleaning for food production. Department of Grain Science and Industry, Kansas State University, Manhattan, United States.

Minati, M. H., Mohammed-Ameen, M. K. 2019. Novel report on six *Fusarium* species associated with head blight and crown rot of wheat in Basra province, Iraq. **Bulletin of the National Research Centre, 43**, 1–15.

Miraglia, M., Marvin, H. J. P., Kleter, G. A., Battilani, P., Brera, C., Coni, E., Vespermann, A. 2009. Climate change and food safety: An emerging issue with special focus on Europe. **Food and Chemical Toxicology, 47**(5), 1009–1021.

Mohammed, M. A., Syeda, J. T., Wasan, K. M., Wasan, E. K. 2017. An overview of chitosan nanoparticles and its application in non-parenteral drug delivery. **Pharmaceutics, 9**(4), 53.

Mohapatra, D., Kumar, S., Kotwaliwale, N., Singh, K. K. 2016. Strategies for control of fungal invasion in stored food grains. In *Proceedings of the 10th International Conference on Controlled Atmosphere and Fumigation in Stored Products* (pp. 37–43). Winnipeg, Canada.

Moretti, A. N. 2009. Taxonomy of *Fusarium* genus: A continuous fight between lumpers and splitters. **Zbornik Matice Srpske Za Prirodne Nauke**, (117), 7–13.

Morin-Crini, N., Lichtfouse, E., Torri, G., Crini, G. 2019. Applications of chitosan in food, pharmaceuticals, medicine, cosmetics, agriculture, textiles, pulp and paper, biotechnology, and environmental chemistry. **Environmental Chemistry Letters, 17**(4), 1667–1692.

Morones, J. R., Elechiguerra, J. L., Camacho, A., Holt, K., Kouri, J. B., Ramírez, J. T., Yacaman, M. J. 2005. The bactericidal effect of silver nanoparticles. **Nanotechnology, 16**(10), 2346.

Morton, V., Staub, T. 2008. A short history of fungicides. **APSnet Features, 308**, 1–12.

Moubark, M. Y., Abdel-Monaim, M. F. 2011. Effect of bio-control agents on yield, yield components and root rot control in two wheat cultivars at New Valley region. **Notulae Scientia Biologicae, 3**(4), 79–87.

Mrema, G. C., Gumbe, L. O., Chepete, H. J., Agullo, J. O. 2012. *Rural structures in the tropics: Design and development*. Food and Agriculture Organization of the United Nations.

Muhammed, S., Hussein, H. Z. 2022. Survey and morphological study of wheat root rot disease in some Iraqi governorates. **Indian Journal of Ecology, 49**, 109–113.

Mujumdar, A. S., Beke, J. 2003. Grain drying: Basic principles. In *Handbook of Postharvest Technology: Cereals, Fruits, Vegetables, Tea, and Spices* (pp. 119–139).

Muthomi, J. W., Lengai, G. M., Wagacha, M. J., Narla, R. D. 2017. *In vitro* activity of plant extracts against some important plant pathogenic fungi of tomato. **Australian Journal of Crop Science, 11**(6), 683–689.

Naseer, R., Sultana, B., Khan, M. Z., Naseer, D., Nigam, P. 2014. Utilization of waste fruit peels to inhibit aflatoxin synthesis by *Aspergillus flavus*: A biotreatment of rice for safer storage. **Bioresource Technology, 172**, 423–428.

Neal, A. L. 2008. What can be inferred from bacterium–nanoparticle interactions about the potential consequences of environmental exposure to nanoparticles? **Ecotoxicology, 17**, 362–371.

Nur, M., Kusdiyantini, E., Wuryanti, W., Winarni, T. A., Widyanto, S. A., Muharam, H. 2015. Development of ozone technology rice storage systems for quality improvement of rice production. **Journal of Physics: Conference Series, 622**(1), 012029.

Nwankiti, A. O., Gwa, V. I. 2018. Evaluation of antagonistic effect of *Trichoderma harzianum* against *Fusarium oxysporum* causal agent of white yam (*Dioscorea rotundata*). **Trends in Technical Scientific Research, 1**(1), 12–18.

Oadi, M. 2020. Mycotoxin: Global risk and silent killer in our food. **International Journal of Agricultural Science and Veterinary Medicine, 8**(1), 26–32.

Ogbonna, I. O., Amai, I. U., Aguoru, C. U., Amai, D. C. 2021. Occurrence, molecular characterization and phylogenetic relationship of *Aspergillus* species isolated from garri sold in Benue State, Nigeria. **American Journal of Molecular Biology, 11**(4), 100–115.

Olivier, C., Halseth, D. E., Mizubuti, E. S., Loria, R. 1998. Postharvest application of organic and inorganic salts for suppression of silver scurf on potato tubers. **Plant Disease, 82**(2), 213–217.

Omosa, L. K., Amugune, B., Ndunda, B., Milugo, T. K., Heydenreich, M., Yenesew, A., Midiwo, J. O. 2014. Antimicrobial flavonoids and diterpenoids from *Dodonaea angustifolia*. **South African Journal of Botany, 91**, 58–62.

Özeren, P. 2022. *Determination of aflatoxin, ochratoxin, zearalenone and deoxynivalenol levels in fodder corn and relationships between toxin production and Aspergillus, Penicillium and Fusarium species*. PhD Thesis, Ankara University.

Pal, M. 2017. Are mycotoxins silent killers of humans and animals? **Journal of Experimental Food Chemistry, 3**, e110.

Palazzini, J., Fumero, V., Yerkovich, N., Barros, G., Cuniberti, M., Chulze, S. 2015. Correlation between *Fusarium graminearum* and deoxynivalenol during the

2012/13 wheat Fusarium head blight outbreak in Argentina. **Cereal Research Communications, 43**(4), 627–637.

Panche, A. N., Diwan, A. D., Chandra, S. R. 2016. Flavonoids: An overview. **Journal of Nutritional Science, 5**, e47.

Pandey, A. K., Dinesh, K., Nirmala, N. S., Dutta, P. 2024. Fusarium wilt of tomato: Past, present, and future. In *Plant Pathogen Interaction* (pp. 55–87). Springer Nature Singapore.

Panth, M., Hassler, S. C., Baysal-Gurel, F. 2020. Methods for management of soilborne diseases in crop production. **Agriculture, 10**(16), 1–22.

Pérez-Narváez, O. A., Castillo Hernández, S. L., Leos-Rivas, C., Pérez-Hernández, R. A., Chávez-Montes, A., Verduzco-Martínez, J. A., Sánchez-García, E. 2023. Antibacterial effect of ethanolic extracts of *Dodonaea viscosa* and *Mammea americana* against staphylococci isolated from skin lesions. **BioMed Research International, 2023**, 5584412.

Peters, R., Brandhoff, P., Weigel, S., Marvin, H., Bouwmeester, H., Aschberger, K., Rauscher, H., Amenta, V., Arena, M., Botelho Moniz, F., Gottardo, S. 2014. Inventory of nanotechnology applications in the agricultural, feed and food sector. **EFSA Supporting Publications, 11**(7), 621E. https://doi.org/10.2903/sp.efsa.2014.EN-621

Piemontese, L., Messia, M. C., Marconi, E., Falasca, L., Zivoli, R., Gambacorta, L., Solfrizzo, M. 2018. Effect of gaseous ozone treatments on DON, microbial contaminants and technological parameters of wheat and semolina. **Food Additives Contaminants: Part A, 35**(4), 761–772.

Pitt, J. I. 2000. Toxigenic fungi: Which are important? **Sabouraudia, 38**(Supplement 1), 17–22.

Pitt, J. I., Hocking, A. D. 2009. *Fungi and food spoilage*. Springer.

Popovski, S., Celar, F. A. 2013. The impact of environmental factors on the infection of cereals with *Fusarium* species and mycotoxin production: A review. **Acta Agriculturae Slovenica, 101**(1), 105–116.

Pratama, O. A., Tunjung, W. A. S., Sutikno, S., Daryono, B. S. 2019. Bioactive compound profile of melon leaf extract (*Cucumis melo*) infected by downy mildew. **Biodiversitas, 20**(11), 3448–3453.

Pronyk, C., Cenkowski, S., Abramson, D. 2006. Superheated steam reduction of deoxynivalenol in naturally contaminated wheat kernels. **Food Control, 17**(10), 789–796.

Punn, M., Bhalla, N. 2013. Classification of wheat grains using machine algorithms. **International Journal of Science and Research, 2**(8), 363–366.

Quevedo, A. C., Guggenheim, E., Briffa, S. M., Adams, J., Lofts, S., Kwak, M., Lee, T. G., Johnston, C., Wagner, S., Holbrook, T. R., Hachenberger, Y. U., Tentschert, J., Davidson, N., Valsami-Jones, E. 2021. UV-Vis spectroscopic characterization of nanomaterials in aqueous media. **Journal of Visualized Experiments, 176**, e61764. https://doi.org/10.3791/61764

Rabie, C. J., Marasas, W. F. O., Thiel, P. G., Lübben, A., Vleggaar, R. 1982. Moniliformin production and toxicity of different *Fusarium* species from Southern Africa. **Applied and Environmental Microbiology, 43**(3), 517–521.

Radić, B. Đ., Kos, J. J., Tanackov, S. D. K., Hajnal, E. P. J., Mandić, A. I. 2019. Occurrence of moniliformin in cereals. **Food and Feed Research, 46**(2), 149–160. https://doi.org/10.5937/FFR1902149R

Rai, M. K., Bonde, S. R., Ingle, A. P., Gade, A. K. 2012. Mycotoxin: Rapid detection, differentiation and safety. **Journal of Pharmaceutical Education Research, 3**(1).

Raila, A., Lugauskas, A., Steponavicius, D., Railiene, M., Stepanoviciene, A., Zvicevicius, E. 2006. Application of ozone for reduction of mycological infection in wheat grain. **Annals of Agricultural and Environmental Medicine, 13**(2).

Rajendran, S. 2003. Grain storage: Perspectives and problems. In *Handbook of Post-Harvest Technology* (pp. 183–214). Marcel Dekker, USA.

Ramires, F. A., Masiello, M., Somma, S., Villani, A., Susca, A., Logrieco, A. F., Moretti, A. 2018. Phylogeny and mycotoxin characterization of *Alternaria* species isolated from wheat grown in Tuscany, Italy. **Toxins, 10**(11), 472.

Rampersad, S. N. 2020. Pathogenomics and management of *Fusarium* diseases in plants. **Pathogens, 9**(5), 340.

Rauscher, H., Rasmussen, K., Sokull-Klüttgen, B. 2017. Regulatory aspects of nanomaterials in the EU. **Chemie Ingenieur Technik, 89**(3), 224–231.

Rheeder, J. P., Marasas, W. F. O., Van Wyk, P. S. 1990. Fungal associations in corn kernels and effects on germination. **Phytopathology, 80**(2), 131–134.

Rico, C. M., Majumdar, S., Duarte-Gardea, M., Peralta-Videa, J. R., Gardea-Torresdey, J. L. 2011. Interaction of nanoparticles with edible plants and their possible implications in the food chain. **Journal of Agricultural and Food Chemistry, 59**(8), 3485–3498.

Rotter, B. A., Prelusky, D. B., Pestka, J. J. 1996. Toxicology of deoxynivalenol (vomitoxin). **Journal of Toxicology and Environmental Health, 48**, 1–34.

Salman, A. S., Alkhatib, S. N., Ahmed, F. M., Hamouda, R. A. 2023. Chitosan nanoparticles loaded with *Capparis cartilaginea* extract: Insights into characterization and antigenotoxicity in vivo. **Pharmaceutics, 15**(11), 2551. https://doi.org/10.3390/pharmaceutics15112551

Saranya, K., Divyabharathi, U. 2019. Gas chromatography and mass spectroscopic analysis of phytocompounds in *Dodonaea viscosa* leaf extract. **Pramana Research Journal, 9**(9), 26–35.

Sardjono, N. A., Yamashita, A., Yoshizawa, T. 1998. Natural co-occurrence of aflatoxins and *Fusarium* mycotoxins in corn from Indonesia. **Food Additives and Contaminants, 15**(4), 377–387.

Sassolas, A., Blum, L. J., Leca-Bouvier, B. D. 2012. Immobilization strategies to develop enzymatic biosensors. **Biotechnology Advances, 30**(3), 489–511.

Savi, G. D., Piacentini, K. C., Bittencourt, K. O., Scussel, V. M. 2014. Ozone treatment efficiency on *Fusarium graminearum* and deoxynivalenol degradation and its effects on whole wheat grains quality and germination. **Journal of Stored Products Research, 59**, 245–253.

Sathiyabama, M. S., Boomija, R. V., Muthukumar, S., Gandhi, M., Salma, S., Kokila Prinsha, T., Rengasamy, B. 2024. Green synthesis of chitosan nanoparticles using tea extract and its antimicrobial activity against phytopathogens of rice. **Scientific Reports, 14**, 7381–7391.

Schütt, F., Nirenberg, H. I., Demi, G. 1998. Moniliformin production in the genus *Fusarium*. **Mycotoxin Research, 14**(1), 35–40.

Scimeca, M., Bischetti, S., Lamsira, H. K., Bonfiglio, R., Bonanno, E. 2018. Energy dispersive X-ray (EDX) microanalysis: A powerful tool in biomedical research and diagnosis. **European Journal of Histochemistry, 62**(1), 89–99.

Seeck, O. H., Murphy, B. M. 2015. *X-ray diffraction*. https://doi.org/10.1201/b15674

Seifert, K. 1996. *Fuskey (Fusarium interactive key)*. Agriculture and Agri-Food Canada.

Semple, R. L., Frio, A. S., Hicks, P. A., Lozare, J. V. 1989. *Mycotoxin prevention and control in food grains*. Bangkok, Thailand.

Shaghati, H. A. 2022. *Characterization of chitosan nanoparticles coated with Syzygium aromaticum extract and evaluation of their inhibitory activity against Klebsiella pneumoniae* (Master's thesis, University of Baghdad).

Shaghati, H. A., Jassim, E. H. 2023. Antibacterial activity of chitosan nanoparticles loaded with *Syzygium aromaticum* extract against *Klebsiella pneumoniae*. **Iraqi Journal of Biotechnology, 22**(1).

Sharmin, S., Rahaman, M. M., Sarkar, C., Atolani, O., Islam, M. T., Adeyemi, O. S. 2021. Nanoparticles as antimicrobial and antiviral agents: A literature-based perspective study. **Heliyon, 7**(3).

Shen, D., Song, H., Zou, T., Raza, A., Li, P., Li, K., Xiong, J. 2022. Reduction of sodium chloride: A review. **Journal of the Science of Food and Agriculture, 102**(10), 3931–3939.

Shephard, G. S., Van Der Westhuizen, L., Gatyeni, P. M., Katerere, D. R., Marasas, W. F. O. 2005. Do fumonisin mycotoxins occur in wheat? **Journal of Agricultural and Food Chemistry, 53**(23), 9293–9296.

Shewry, P. R. 2009. Wheat. **Journal of Experimental Botany, 60**(6), 1537–1553.

Shotwell, O. L., Hesseltine, C. W., Stubblefield, R. D., Sorenson, W. G. 1966. Production of aflatoxin on rice. **Applied Microbiology, 14**(3), 425–428.

Shrestha, S., Wang, B., Dutta, P. 2020. Nanoparticle processing: Understanding and controlling aggregation. **Advances in Colloid and Interface Science, 279**, 102162. https://doi.org/10.1016/j.cis.2020.102162

Siddiqui, M. 2021. Phytochemical analysis of some medicinal plants. **Liaquat Medical Research Journal, 3**(8), 1–5.

Singh, A. P., Kumar, S. 2020. Applications of tannins in industry. In *Tannins: Structural Properties, Biological Properties and Current Knowledge* (pp. 1–13).

Slinski, S. L., Zakharov, F., Gordon, T. R. 2015. The effect of resin and monoterpenes on spore germination and growth in *Fusarium circinatum*. **Phytopathology, 105**(1), 119–125.

Sopher, C. D., Graham, D. M., Rice, R. G., Strasser, J. H. 2002. Studies on the use of ozone in production agriculture and food processing. In *Proceedings of the International Ozone Association* (pp. 1–15).

IBM Corp. 2019. *IBM SPSS Statistics 26 step by step: A simple guide and reference* (16th ed.). https://doi.org/10.4324/9780429056765

Stakheev, A. A., Samokhvalova, L. V., Ryazantsev, D. Y., Zavriev, S. K. 2016. Molecular genetic approaches for identification of toxin-producing *Fusarium* species. **Sel'skokhozyaistvennaya Biologiya, 51**(3), 275–284.

Steponavičienė, A., Steponavičius, D., Raila, A., Kemzūraitė, A. 2012. Modelling the ozone penetration in a grain layer. **Journal of Environmental Engineering and Landscape Management, 20**(4), 292–300.

Sundram, S., Naidu, Y., Mohamed-Azni, I. N. A., Aripin, S. M. S., Ramli, N. R., Mohamed, M. S., Rusli, M. H. 2023. Fungi in biological management of plant diseases: Current and future perspective. **Journal of Oil Palm Research, 35**(3), 375–390.

Kareem, T. A. S., Al-Hiti, A. W., Al-Karbouli, H. H. 2009. Testing the effectiveness of plant extracts against *Pythium aphanidermatum* causing damping-off disease in cucumbers. **Diyala Journal of Agricultural Sciences, 1**, 320–334.

Thanaboripat, D., Ramunsri, W., Apintanapong, M., Chusanatasana, U. 1992. Effects of sodium chloride, propionic acid and ammonium hydroxide on growth of *Aspergillus flavus* and aflatoxin production.

Thanaboripat, D., Ruangrattanametee, V., Srikitkasemwat, K. 2010. Control of growth and aflatoxin production of aflatoxin-producing fungi in corn by salts. In *8th International Symposium on Biocontrol and Biotechnology* (pp. 283–289).

Thippeswamy, S., Mohana, D. C., Abhishek, R. U., Manjunath, K. 2013. Effect of plant extracts on inhibition of *Fusarium verticillioides* growth and fumonisin B1 production.

Tiwari, B. K., Brennan, C. S., Curran, T., Gallagher, E., Cullen, P. J., O'Donnell, C. P. 2010. Application of ozone in grain processing. **Journal of Cereal Science, 51**(3), 248–255.

Topi, D., Babič, J., Pavšič-Vrtač, K., Tavčar-Kalcher, G., Jakovac-Strajn, B. 2020. Incidence of *Fusarium* mycotoxins in wheat and maize from Albania. **Molecules, 26**(1), 172.

Türkkan, M. 2013. Antifungal effect of various salts against *Fusarium oxysporum* f. sp. *cepae*. **Journal of Agricultural Sciences, 19**(3), 178–187.

Ugwu, O., Wokocha, T., Akani, I. J., Braide, W. 2021. Mycotoxins and mycotoxicoses: Detection and analysis.

Elmer, W. H., McGovern, R. J., Geiser, D. M., Harbaugh, B. K. 2000. Biology, epidemiology and integrated management of diseases caused by *Fusarium* in potted ornamentals. University of Florida.

Waheed, A. A., Dahham, A. A., Azra, E. K., Kamal, J. A., Khaeim, H. M. 2019. Concentration effects of salts on growth of *Aspergillus niger* and *Penicillium oxalicum*. **Plant Archives, 19**(2), 310–312.

Wang, L., Hu, C., Shao, L. 2017. The antimicrobial activity of nanoparticles: Present situation and prospects for the future. **International Journal of Nanomedicine, 12**, 1227–1249.

Wang, L., Shao, H., Luo, X., Wang, R., Li, Y., Li, Y., Chen, Z. 2016. Effect of ozone treatment on deoxynivalenol and wheat quality. **PLOS ONE, 11**(1), e0147613.

Wani, S., Maker, J. K., Thompson, J. R., Barnes, J., Singleton, I. 2015. Effect of ozone treatment on inactivation of *Escherichia coli* and *Listeria* spp. on spinach. **Agriculture, 5**(2), 155–169.

Walsh, N. G., Entwisle, T. J. 1996. *Flora of Victoria* (Vol. 3). Inkata Press, Melbourne.

White, T. J., Bruns, T., Lee, S., Taylor, J. 1990. Amplification and direct sequencing of fungal ribosomal RNA genes for phylogenetics. In *PCR Protocols: A Guide to Methods and Applications* (pp. 315–322).

Wolf-Hall, C. E., Milford, A. H., Bullerman, L. B. 1999. Stability of deoxynivalenol in heat-treated foods. **Journal of Food Protection, 62**, 962–966.

World Health Organization. 2018. Aflatoxins. Department of Food Safety and Zoonoses.

Wu, J., Doan, H., Cuenca, M. A. 2006. Investigation of gaseous ozone as an antifungal fumigant for stored wheat. **Journal of Chemical Technology and Biotechnology, 81**(7), 1288–1293.

Xu, F., Shi, R., Liu, L., Li, S., Wang, J., Han, Z., Xu, X. 2024. *Fusarium pseudograminearum* biomass and toxin accumulation in wheat tissues. **Frontiers in Plant Science, 15**, 1356723.

Yamanaka, M., Hara, K., Kudo, J. 2005. Bactericidal actions of a silver ion solution on *Escherichia coli*. **Applied and Environmental Microbiology, 71**(11), 7589–7593.

Yanat, M., Schroën, K. 2021. Preparation methods and applications of chitosan nanoparticles with an outlook toward biodegradable packaging. **Reactive and Functional Polymers, 161**, 104849.

Yazid, S. N. E., Tajudin, N. I., Razman, N. A. A., Selamat, J., Ismail, S. I., Sanny, M., Samsudin, N. I. P. 2023. Mycotoxigenic fungal growth inhibition and multi-mycotoxin reduction by biological control agents. **Mycotoxin Research, 39**(3), 177–192.

Yousaf, Z., Saleh, N., Ramazan, A., Aftab, A. 2016. Postharvesting techniques and maintenance of seed quality. In *New Challenges in Seed Biology* (p. 113).

Zada, A. K. 2018. The geographical names of provinces in Iraq. **Polytechnic Journal, 8**(3), 9.

Zeller, K. A., Bowden, R. L., Leslie, J. F. 2003. Diversity of epidemic populations of *Gibberella zeae*. **Phytopathology, 93**(7), 874–880.

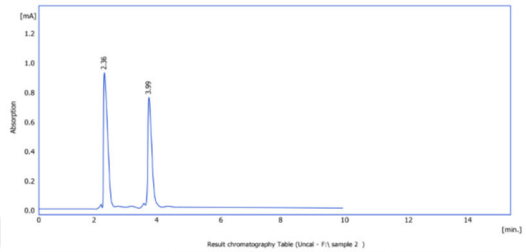
Zhang, X., Davenport, K. W., Gu, W., Daligault, H. E., Munk, A. C., Tashima, H., Han, C. S. 2012. Improving genome assemblies by sequencing PCR products with PacBio. **BioTechniques, 53**(1), 61–62.

Zhu, F. 2018. Effect of ozone treatment on the quality of grain products. **Food Chemistry, 264**, 358–366.

APPENDICES

Chromatography Laboratory
HPLC

Sample Info:
Sample ID : sample 2
Sample : sample 2
Inj. Volume [mL] : 0.1
Amount 0
ISTD Amount 0
Dilution 1
Autostop : 20.00 min
Detector 1 : Detector 3
Subtraction Chromatogram : (None)
External Start : Start - Restart, Down
Range 1 : Bipolar, 2000 mAU, 10 Samp. per Sec.
Matching : No Change



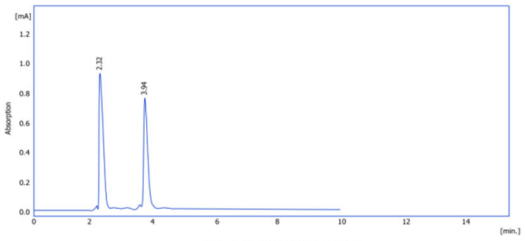
Result chromatography Table (Uncal - F:\ sample 2)

No	Reten. Time [min]	Area [mAU.s]	Height [mAU]	Area [%]	Height [%]	W05 [min]	Compound Name
1	2.36	15214.99	982.90	55.00	55.00	0.25	
2	3.99	31223.65	801.40	45.00	45.00	0.20	
	Total	46435.98	1784.30	100.00	100.00		

sample 2 before treatment

Chromatography Laboratory
HPLC

Sample Info:
Sample ID : sample 3
Sample : sample 3
Inj. Volume [mL] : 0.1
Amount 0
ISTD Amount 0
Dilution 1
Autostop : 20.00 min
Detector 1 : Detector 3
Subtraction Chromatogram : (None)
External Start : Start - Restart, Down
Range 1 : Bipolar, 2000 mAU, 10 Samp. per Sec.
Matching : No Change



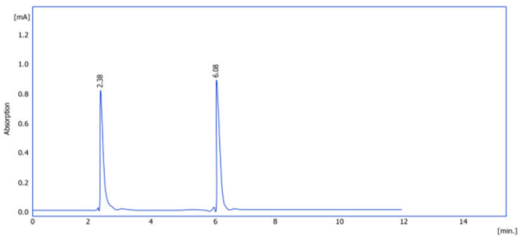
Result chromatography Table (Uncal - F:\ sample 3)

No	Reten. Time [min]	Area [mAU.s]	Height [mAU]	Area [%]	Height [%]	W05 [min]	Compound Name
1	2.32	16552.08	981.50	55.00	55.00	0.25	
2	3.94	33660.50	802.11	45.00	45.00	0.20	
	Total	50212.49	1783.61	100.00	100.00		

sample 3 before treatment

Chromatography Laboratory
HPLC

Sample Info:
Sample ID : sample 4
Sample : sample 4
Inj. Volume [mL] : 0.1
Amount 0
ISTD Amount 0
Dilution 1
Autostop : 20.00 min
Detector 1 : Detector 3
Subtraction Chromatogram : (None)
External Start : Start - Restart, Down
Range 1 : Bipolar, 2000 mAU, 10 Samp. per Sec.
Matching : No Change



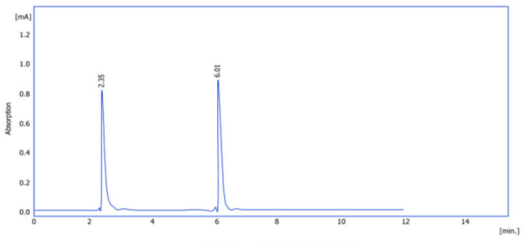
Result chromatography Table (Uncal - F:\ sample 4)

No	Reten. Time [min]	Area [mAU.s]	Height [mAU]	Area [%]	Height [%]	W05 [min]	Compound Name
1	2.38	17841.58	804.11	50.00	50.00	0.20	
2	6.08	38957.90	810.12	50.00	50.00	0.20	
	Total	56799.88	1614.23	100.00	100.00		

sample 4 before treatment

Chromatography Laboratory
HPLC

Sample Info:
Sample ID : sample 5
Sample : sample 5
Inj. Volume [mL] : 0.1
Amount 0
ISTD Amount 0
Dilution 1
Autostop : 20.00 min
Detector 1 : Detector 3
Subtraction Chromatogram : (None)
External Start : Start - Restart, Down
Range 1 : Bipolar, 2000 mAU, 10 Samp. per Sec.
Matching : No Change



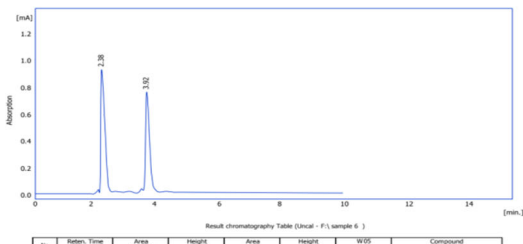
Result chromatography Table (Uncal - F:\ sample 5)

No	Reten. Time [min]	Area [mAU.s]	Height [mAU]	Area [%]	Height [%]	W05 [min]	Compound Name
1	2.35	18952.14	803.65	50.00	50.00	0.20	
2	6.01	39852.14	812.11	50.00	50.00	0.20	
	Total	58804.28	1615.76	100.00	100.00		

sample 5 before treatment

Chromatography Laboratory
HPLC

Sample Info:
Sample ID : sample 6
Sample : sample 6
Inj. Volume [mL] : 0.1
Amount 0
ISTD Amount 0
Dilution 1
Autostop : 20.00 min
Detector 1 : Detector 3
Subtraction Chromatogram : (None)
External Start : Start - Restart, Down
Range 1 : Bipolar, 2000 mAU, 10 Samp. per Sec.
Matching : No Change



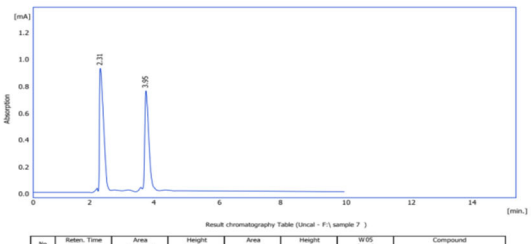
Result chromatography Table (Uncal - F:\ sample 6)

No	Reten. Time [min]	Area [mAU.s]	Height [mAU]	Area [%]	Height [%]	W05 [min]	Compound Name
1	2.38	16251.45	983.65	55.00	55.00	0.25	
2	3.92	31256.98	801.08	45.00	45.00	0.20	
	Total	47508.74	1788.90	100.00	100.00		

sample 6 before treatment

Chromatography Laboratory
HPLC

Sample Info:
Sample ID : sample 7
Sample : sample 7
Inj. Volume [mL] : 0.1
Amount 0
ISTD Amount 0
Dilution 1
Autostop : 20.00 min
Detector 1 : Detector 3
Subtraction Chromatogram : (None)
External Start : Start - Restart, Down
Range 1 : Bipolar, 2000 mAU, 10 Samp. per Sec.
Matching : No Change



Result chromatography Table (Uncal - F:\ sample 7)

No	Reten. Time [min]	Area [mAU.s]	Height [mAU]	Area [%]	Height [%]	W05 [min]	Compound Name
1	2.31	15246.80	985.45	55.00	55.00	0.25	
2	3.95	33652.98	800.14	45.00	45.00	0.20	
	Total	48899.78	1785.59	100.00	100.00		

sample 7 before treatment

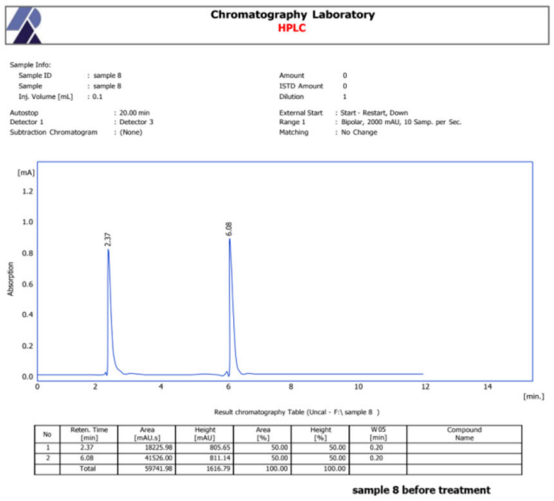


Figure S1. Chromatograms of deoxynivalenol and moniliformin before treatment by HPLC chromatography analysis. (sample 2) *F. pseudograminearum* strain 2, (sample 3) *F. pseudograminearum* strain 3, (sample 4) *F. oxysporum* strain 4, (sample 5) *F. oxysporum* strain 5, (sample 6) *F. pseudograminearum* strain 6, (sample 7) *F. pseudograminearum* strain 7, (sample 8) *F. chlamydosporum* strain 8.

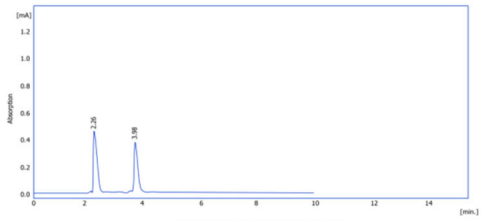
Chromatography Laboratory
HPLC

Sample Info:
Sample ID : sample 2 (Extract)
Sample : sample 2 (Extract)
Inj. Volume [mL] : 0.1

Amount 0
ISTD Amount 0
Dilution 1

Autostop : 20.00 min
Detector 1 : Detector 3
Subtraction Chromatogram : (None)

External Start : Start - Restart, Down
Range 1 : Bipolar, 2000 mAU, 10 Samp. per Sec.
Matching : No Change



Result chromatography Table (Uncal - F:\ sample 2 (Extract)

No	Reten. Time [min]	Area [mAU.s]	Height [mAU]	Area [%]	Height [%]	W05 [min]	Compound Name
1	2.26	9854.11	432.65	55.00	55.00	0.25	
2	3.98	8985.08	401.11	45.00	45.00	0.20	
	Total	18839.98	833.76	100.00	100.00		

sample 2 DVE TREATMENT

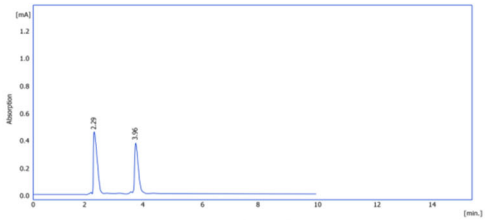
Chromatography Laboratory
HPLC

Sample Info:
Sample ID : sample 3 (extract)
Sample : sample 3 (extract)
Inj. Volume [mL] : 0.1

Amount 0
ISTD Amount 0
Dilution 1

Autostop : 20.00 min
Detector 1 : Detector 3
Subtraction Chromatogram : (None)

External Start : Start - Restart, Down
Range 1 : Bipolar, 2000 mAU, 10 Samp. per Sec.
Matching : No Change



Result chromatography Table (Uncal - F:\ sample 3 (extract)

No	Reten. Time [min]	Area [mAU.s]	Height [mAU]	Area [%]	Height [%]	W05 [min]	Compound Name
1	2.29	10102.65	431.40	55.00	55.00	0.25	
2	3.96	9365.90	402.00	45.00	45.00	0.20	
	Total	19468.55	833.40	100.00	100.00		

SAMPLE 3 DVE TREATMENT

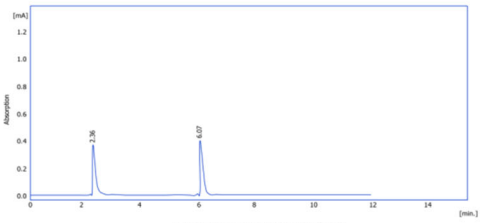
Chromatography Laboratory
HPLC

Sample Info:
Sample ID : sample 4 (extract)
Sample : sample 4 (extract)
Inj. Volume [mL] : 0.1

Amount 0
ISTD Amount 0
Dilution 1

Autostop : 20.00 min
Detector 1 : Detector 3
Subtraction Chromatogram : (None)

External Start : Start - Restart, Down
Range 1 : Bipolar, 2000 mAU, 10 Samp. per Sec.
Matching : No Change



Result chromatography Table (Uncal - F:\ sample 4 (extract)

No	Reten. Time [min]	Area [mAU.s]	Height [mAU]	Area [%]	Height [%]	W05 [min]	Compound Name
1	2.36	8745.00	394.77	50.00	50.00	0.20	
2	6.07	9355.80	400.12	50.00	50.00	0.20	
	Total	18100.80	794.89	100.00	100.00		

SAMPLE 4 DVE TREATMENT

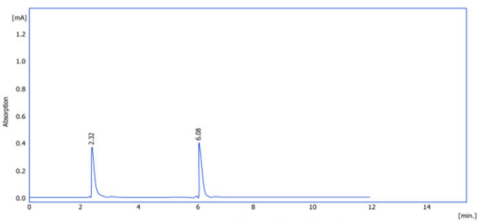
Chromatography Laboratory
HPLC

Sample Info:
Sample ID : sample 5 (extract)
Sample : sample 5 (extract)
Inj. Volume [mL] : 0.1

Amount 0
ISTD Amount 0
Dilution 1

Autostop : 20.00 min
Detector 1 : Detector 3
Subtraction Chromatogram : (None)

External Start : Start - Restart, Down
Range 1 : Bipolar, 2000 mAU, 10 Samp. per Sec.
Matching : No Change



Result chromatography Table (Uncal - F:\ sample 5 (extract)

No	Reten. Time [min]	Area [mAU.s]	Height [mAU]	Area [%]	Height [%]	W05 [min]	Compound Name
1	2.32	9652.14	395.11	50.00	50.00	0.20	
2	6.08	7044.90	404.12	50.00	50.00	0.20	
	Total	16697.04	799.23	100.00	100.00		

SAMPLE 5 DVE TREATMENT

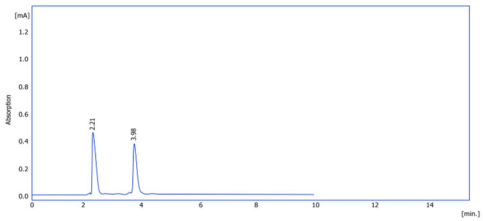
Chromatography Laboratory
HPLC

Sample Info:
Sample ID : sample 6 (extract)
Sample : sample 6 (extract)
Inj. Volume [mL] : 0.1

Amount 0
ISTD Amount 0
Dilution 1

Autostop : 20.00 min
Detector 1 : Detector 3
Subtraction Chromatogram : (None)

External Start : Start - Restart, Down
Range 1 : Bipolar, 2000 mAU, 10 Samp. per Sec.
Matching : No Change



Result chromatography Table (Uncal - F:\ sample 6 (extract)

No	Reten. Time [min]	Area [mAU.s]	Height [mAU]	Area [%]	Height [%]	W05 [min]	Compound Name
1	2.21	11542.00	432.00	55.00	55.00	0.25	
2	3.98	9521.40	403.12	45.00	45.00	0.20	
	Total	20063.40	835.12	100.00	100.00		

SAMPLE 6 DVE TREATMENT

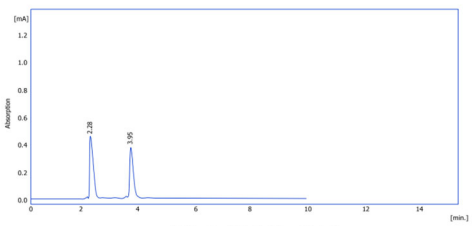
Chromatography Laboratory
HPLC

Sample Info:
Sample ID : sample 7 (extract)
Sample : sample 7 (extract)
Inj. Volume [mL] : 0.1

Amount 0
ISTD Amount 0
Dilution 1

Autostop : 20.00 min
Detector 1 : Detector 3
Subtraction Chromatogram : (None)

External Start : Start - Restart, Down
Range 1 : Bipolar, 2000 mAU, 10 Samp. per Sec.
Matching : No Change



Result chromatography Table (Uncal - F:\ sample 7 (extract)

No	Reten. Time [min]	Area [mAU.s]	Height [mAU]	Area [%]	Height [%]	W05 [min]	Compound Name
1	2.28	9856.90	432.11	55.00	55.00	0.25	
2	3.95	8574.00	405.25	45.00	45.00	0.20	
	Total	18430.90	837.36	100.00	100.00		

SAMPLE 7 DVE TREATMENT

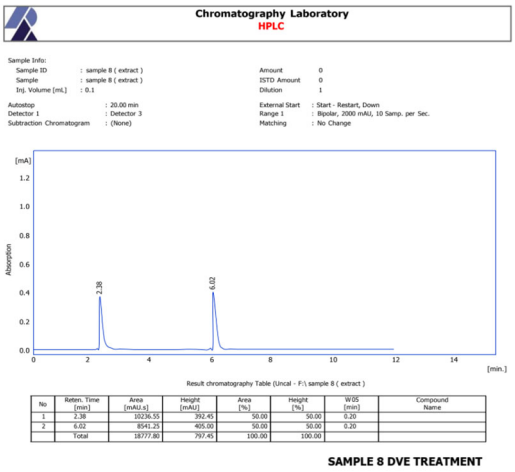
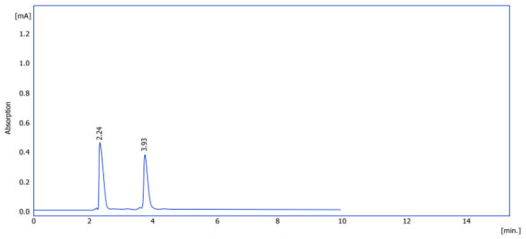


Figure S2. Chromatograms of deoxynivalenol and moniliformin after treatment of *D. viscosa* extract (DVE) by HPLC chromatography analysis (sample 2) *F. pseudograminearum* strain 2, (sample 3) *F. pseudograminearum* strain 3, (sample 4) *F. oxysporum* strain 4, (sample 5) *F. oxysporum* strain 5, (sample 6) *F. pseudograminearum* strain 6, (sample 7) *F. pseudograminearum* strain 7, (sample 8) *F. chlamydosporum* strain 8.

Chromatography Laboratory
HPLC

Sample Info:
Sample ID : sample 2 (nano)
Sample : sample 2 (nano)
Inj. Volume [mL] : 0.1
Amount 0
ISTD Amount 0
Dilution 1
Autostop : 20.00 min
Detector 1 : Detector 3
Subtraction Chromatogram : (None)
External Start : Start - Restart, Down
Range 1 : Bipolar, 2000 mAU, 10 Samp. per Sec.
Matching : No Change



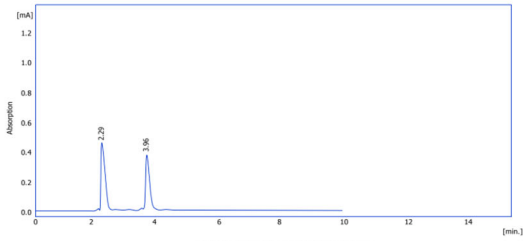
Result chromatography Table (Uncal - F:\ sample 2 (nano)

No	Reten. Time [min]	Area [mAU.s]	Height [mAU]	Area [%]	Height [%]	W05 [min]	Compound Name
1	2.24	10245.98	431.44	55.00	55.00	0.25	
2	3.93	8521.49	405.12	45.00	45.00	0.20	
	Total	18767.47	836.56	100.00	100.00		

SAMPLE 2 CHITOSAN NPs LOADED DVE

Chromatography Laboratory
HPLC

Sample Info:
Sample ID : sample 3 (nano)
Sample : sample 3 (nano)
Inj. Volume [mL] : 0.1
Amount 0
ISTD Amount 0
Dilution 1
Autostop : 20.00 min
Detector 1 : Detector 3
Subtraction Chromatogram : (None)
External Start : Start - Restart, Down
Range 1 : Bipolar, 2000 mAU, 10 Samp. per Sec.
Matching : No Change



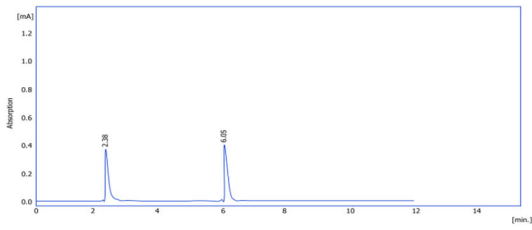
Result chromatography Table (Uncal - F:\ sample 3 (nano)

No	Reten. Time [min]	Area [mAU.s]	Height [mAU]	Area [%]	Height [%]	W05 [min]	Compound Name
1	2.29	11854.70	432.11	55.00	55.00	0.25	
2	3.96	8759.80	405.10	45.00	45.00	0.20	
	Total	20614.50	837.21	100.00	100.00		

SAMPLE 3 CHITOSAN NPs LOADED DVE

Chromatography Laboratory
HPLC

Sample Info:
Sample ID : sample 4 (nano)
Sample : sample 4 (nano)
Inj. Volume [mL] : 0.1
Amount 0
ISTD Amount 0
Dilution 1
Autostop : 20.00 min
Detector 1 : Detector 3
Subtraction Chromatogram : (None)
External Start : Start - Restart, Down
Range 1 : Bipolar, 2000 mAU, 10 Samp. per Sec.
Matching : No Change



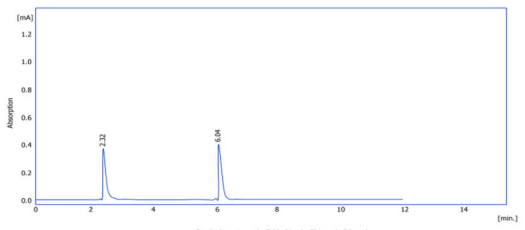
Result chromatography Table (Uncal - F:\ sample 4 (nano)

No	Reten. Time [min]	Area [mAU.s]	Height [mAU]	Area [%]	Height [%]	W05 [min]	Compound Name
1	2.38	8541.25	392.55	50.00	50.00	0.20	
2	6.05	9102.65	402.12	50.00	50.00	0.20	
	Total	17643.90	793.67	100.00	100.00		

SAMPLE 4 CHITOSAN NPs LOADED DVE

Chromatography Laboratory
HPLC

Sample Info:
Sample ID : sample 5 (nano)
Sample : sample 5 (nano)
Inj. Volume [mL] : 0.1
Amount 0
ISTD Amount 0
Dilution 1
Autostop : 20.00 min
Detector 1 : Detector 3
Subtraction Chromatogram : (None)
External Start : Start - Restart, Down
Range 1 : Bipolar, 2000 mAU, 10 Samp. per Sec.
Matching : No Change



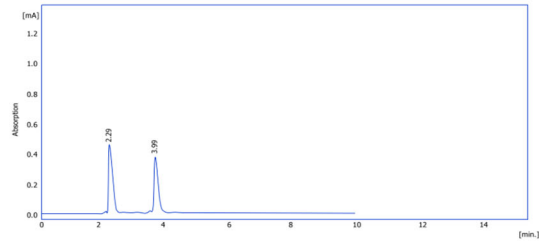
Result chromatography Table (Uncal - F:\ sample 5 (nano)

No	Reten. Time [min]	Area [mAU.s]	Height [mAU]	Area [%]	Height [%]	W05 [min]	Compound Name
1	2.32	8952.14	392.15	50.00	50.00	0.20	
2	6.04	8053.65	402.00	50.00	50.00	0.20	
	Total	17005.79	794.15	100.00	100.00		

SAMPLE 5 CHITOSAN NPs LOADED DVE

Chromatography Laboratory
HPLC

Sample Info:
Sample ID : sample 6 (nano)
Sample : sample 6 (nano)
Inj. Volume [mL] : 0.1
Amount 0
ISTD Amount 0
Dilution 1
Autostop : 20.00 min
Detector 1 : Detector 3
Subtraction Chromatogram : (None)
External Start : Start - Restart, Down
Range 1 : Bipolar, 2000 mAU, 10 Samp. per Sec.
Matching : No Change



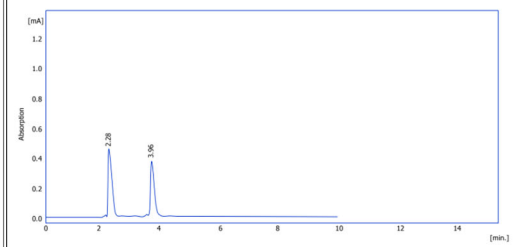
Result chromatography Table (Uncal - F:\ sample 6 (nano)

No	Reten. Time [min]	Area [mAU.s]	Height [mAU]	Area [%]	Height [%]	W05 [min]	Compound Name
1	2.29	10887.49	432.00	55.00	55.00	0.25	
2	3.99	8745.00	403.12	45.00	45.00	0.20	
	Total	19632.49	835.12	100.00	100.00		

SAMPLE 6 CHITOSAN NPs LOADED DVE

Chromatography Laboratory
HPLC

Sample Info:
Sample ID : sample 7 (nano)
Sample : sample 7 (nano)
Inj. Volume [mL] : 0.1
Amount 0
ISTD Amount 0
Dilution 1
Autostop : 20.00 min
Detector 1 : Detector 3
Subtraction Chromatogram : (None)
External Start : Start - Restart, Down
Range 1 : Bipolar, 2000 mAU, 10 Samp. per Sec.
Matching : No Change



Result chromatography Table (Uncal - F:\ sample 7 (nano)

No	Reten. Time [min]	Area [mAU.s]	Height [mAU]	Area [%]	Height [%]	W05 [min]	Compound Name
1	2.28	9854.47	430.11	55.00	55.00	0.25	
2	3.96	8012.65	402.12	45.00	45.00	0.20	
	Total	17678.12	832.23	100.00	100.00		

SAMPLE 7 CHITOSAN NPs LOADED DVE

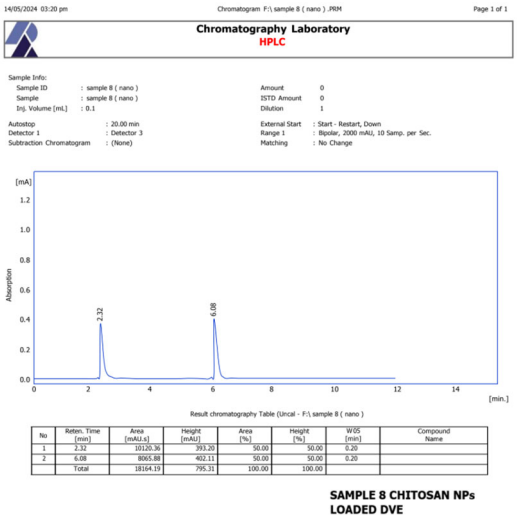


Figure S3. Chromatograms of deoxynivalenol and moniliformin after treatment of chitosan NPs loaded DVE by HPLC chromatography analysis (sample 2) *F. pseudograminearum* strain 2, (sample 3) *F. pseudograminearum* strain 3, (sample 4) *F. oxysporum* strain 4, (sample 5) *F. oxysporum* strain 5, (sample 6) *F. pseudograminearum* strain 6, (sample 7) *F. pseudograminearum* strain 7, (sample 8) *F. chlamydosporum* strain 8.

15/05/2024 03:20 pm Chromatogram F:\ sample 2 (Ozone) .PRM Page 1 of 1

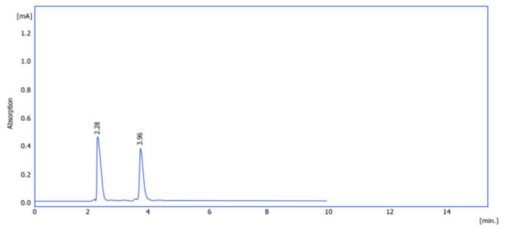
Chromatography Laboratory
HPLC

Sample Info:
Sample ID : sample 2 (Ozone)
Sample : sample 2 (Ozone)
Inj. Volume [mL] : 0.1

Amount 0
ISTD Amount 0
Dilution 1

Autostop : 20.00 min
Detector 1 : Detector 3
Subtraction Chromatogram : (None)

External Start : Start - Restart, Down
Range 1 : Bipolar, 2000 mAU, 10 Samp. per Sec.
Matching : No Change



Result chromatography Table (Uncal - F:\ sample 2 (Ozone)

No	Reten. Time [min]	Area [mAU.s]	Height [mAU]	Area [%]	Height [%]	W05 [min]	Compound Name
1	2.28	13201.45	433.05	55.00	55.00	0.25	
2	3.96	9854.00	402.41	45.00	45.00	0.20	
	Total	23055.45	835.46	100.00	100.00		

sample 2 after ozone treatment

15/05/2024 03:20 pm Chromatogram F:\ sample 3 (Ozone) .PRM Page 1 of 1

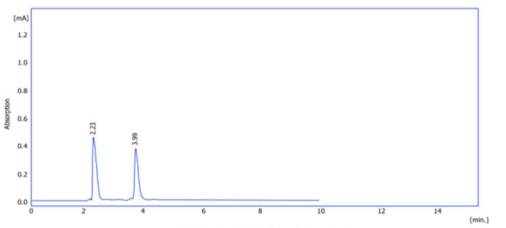
Chromatography Laboratory
HPLC

Sample Info:
Sample ID : sample 3 (Ozone)
Sample : sample 3 (Ozone)
Inj. Volume [mL] : 0.1

Amount 0
ISTD Amount 0
Dilution 1

Autostop : 20.00 min
Detector 1 : Detector 3
Subtraction Chromatogram : (None)

External Start : Start - Restart, Down
Range 1 : Bipolar, 2000 mAU, 10 Samp. per Sec.
Matching : No Change



Result chromatography Table (Uncal - F:\ sample 3 (Ozone)

No	Reten. Time [min]	Area [mAU.s]	Height [mAU]	Area [%]	Height [%]	W05 [min]	Compound Name
1	2.23	12918.80	431.45	55.00	55.00	0.25	
2	3.99	9214.80	402.14	45.00	45.00	0.20	
	Total	22133.60	833.59	100.00	100.00		

sample 3 after ozone treatment

14/05/2024 03:20 pm Chromatogram F:\ sample 4 (ozone) .PRM Page 1 of 1

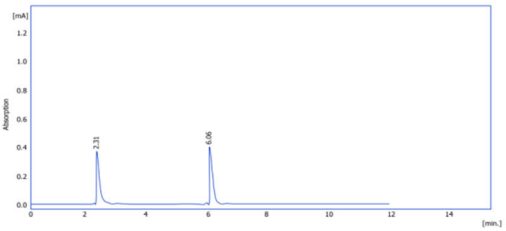
Chromatography Laboratory
HPLC

Sample Info:
Sample ID : sample 4 (ozone)
Sample : sample 4 (ozone)
Inj. Volume [mL] : 0.1

Amount 0
ISTD Amount 0
Dilution 1

Autostop : 20.00 min
Detector 1 : Detector 3
Subtraction Chromatogram : (None)

External Start : Start - Restart, Down
Range 1 : Bipolar, 2000 mAU, 10 Samp. per Sec.
Matching : No Change



Result chromatography Table (Uncal - F:\ sample 4 (ozone)

No	Reten. Time [min]	Area [mAU.s]	Height [mAU]	Area [%]	Height [%]	W05 [min]	Compound Name
1	2.31	8621.14	395.14	50.00	50.00	0.20	
2	6.06	9201.55	403.25	50.00	50.00	0.20	
	Total	17822.69	798.39	100.00	100.00		

sample 4 after ozone treatment

14/05/2024 03:20 pm Chromatogram F:\ sample 5 (ozone) .PRM Page 1 of 1

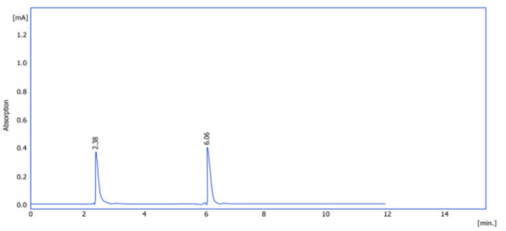
Chromatography Laboratory
HPLC

Sample Info:
Sample ID : sample 5 (ozone)
Sample : sample 5 (ozone)
Inj. Volume [mL] : 0.1

Amount 0
ISTD Amount 0
Dilution 1

Autostop : 20.00 min
Detector 1 : Detector 3
Subtraction Chromatogram : (None)

External Start : Start - Restart, Down
Range 1 : Bipolar, 2000 mAU, 10 Samp. per Sec.
Matching : No Change



Result chromatography Table (Uncal - F:\ sample 5 (ozone)

No	Reten. Time [min]	Area [mAU.s]	Height [mAU]	Area [%]	Height [%]	W05 [min]	Compound Name
1	2.38	8795.14	398.00	50.00	50.00	0.20	
2	6.06	9365.99	400.36	50.00	50.00	0.20	
	Total	18161.47	798.36	100.00	100.00		

sample 5 after ozone treatment

15/05/2024 03:20 pm Chromatogram F:\ sample 6 (ozone) .PRM Page 1 of 1

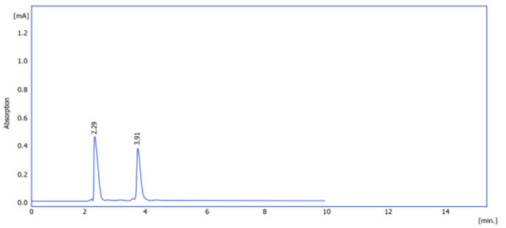
Chromatography Laboratory
HPLC

Sample Info:
Sample ID : sample 6 (ozone)
Sample : sample 6 (ozone)
Inj. Volume [mL] : 0.1

Amount 0
ISTD Amount 0
Dilution 1

Autostop : 20.00 min
Detector 1 : Detector 3
Subtraction Chromatogram : (None)

External Start : Start - Restart, Down
Range 1 : Bipolar, 2000 mAU, 10 Samp. per Sec.
Matching : No Change



Result chromatography Table (Uncal - F:\ sample 6 (ozone)

No	Reten. Time [min]	Area [mAU.s]	Height [mAU]	Area [%]	Height [%]	W05 [min]	Compound Name
1	2.29	11248.91	431.50	55.00	55.00	0.25	
2	3.91	9856.80	402.22	45.00	45.00	0.20	
	Total	21105.49	833.72	100.00	100.00		

sample 6 after ozone treatment

15/05/2024 03:20 pm Chromatogram F:\ sample 7 (ozone) .PRM Page 1 of 1

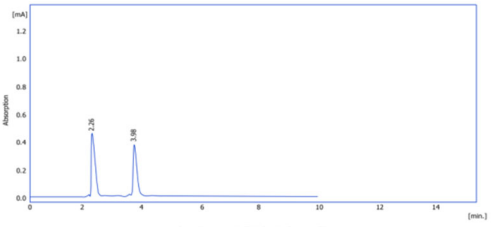
Chromatography Laboratory
HPLC

Sample Info:
Sample ID : sample 7 (ozone)
Sample : sample 7 (ozone)
Inj. Volume [mL] : 0.1

Amount 0
ISTD Amount 0
Dilution 1

Autostop : 20.00 min
Detector 1 : Detector 3
Subtraction Chromatogram : (None)

External Start : Start - Restart, Down
Range 1 : Bipolar, 2000 mAU, 10 Samp. per Sec.
Matching : No Change



Result chromatography Table (Uncal - F:\ sample 7 (ozone)

No	Reten. Time [min]	Area [mAU.s]	Height [mAU]	Area [%]	Height [%]	W05 [min]	Compound Name
1	2.26	10548.00	432.65	55.00	55.00	0.25	
2	3.98	9690.14	405.11	45.00	45.00	0.20	
	Total	20238.14	837.76	100.00	100.00		

sample 7 after ozone treatment

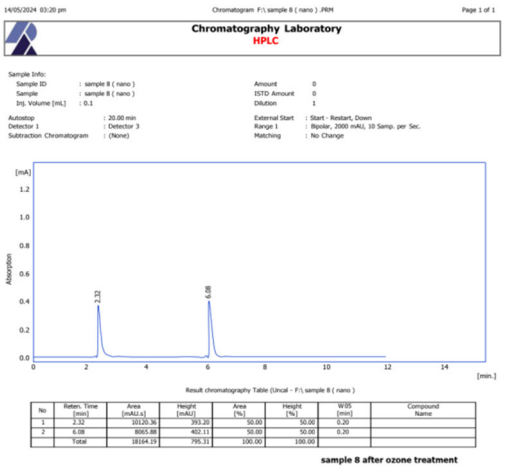


Figure S4. Chromatograms of deoxynivalenol and moniliformin after treatment of ozone gas by HPLC chromatography analysis (sample 2) *F. pseudograminearum* strain 2, (sample 3) *F. pseudograminearum* strain 3, (sample 4) *F. oxysporum* strain 4, (sample 5) *F. oxysporum* strain 5, (sample 6) *F. pseudograminearum* strain 6, (sample 7) *F. pseudograminearum* strain 7, (sample 8) *F. chlamydosporum* strain 8.

15/05/2024 03:20 pm Chromatogram F:\ sample 2 (salt) .PRM Page 1 of 1

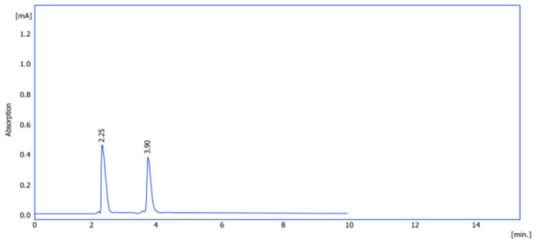
Chromatography Laboratory
HPLC

Sample Info:
Sample ID : sample 2 (salt)
Sample : sample 2 (salt)
Inj. Volume [mL] : 0.1

Amount 0
ISTD Amount 0
Dilution 1

Autostop : 20.00 min
Detector 1 : Detector 3
Subtraction Chromatogram : (None)

External Start : Start - Restart, Down
Range 1 : Bipolar, 2000 mAU, 10 Samp. per Sec.
Matching : No Change



Result chromatography Table (Uncal - F:\ sample 2 (salt)

No	Reten. Time [min]	Area [mAU.s]	Height [mAU]	Area [%]	Height [%]	W05 [min]	Compound Name
1	2.25	9365.11	433.65	55.00	55.00	0.25	
2	3.90	8521.45	400.01	45.00	45.00	0.20	
	Total	17884.49	833.66	100.00	100.00		

sample 2 after nano salt treatment

15/05/2024 03:20 pm Chromatogram F:\ sample 3 (salt) .PRM Page 1 of 1

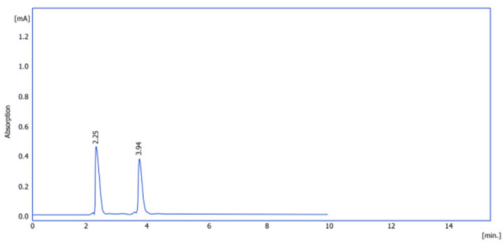
Chromatography Laboratory
HPLC

Sample Info:
Sample ID : sample 3 (salt)
Sample : sample 3 (salt)
Inj. Volume [mL] : 0.1

Amount 0
ISTD Amount 0
Dilution 1

Autostop : 20.00 min
Detector 1 : Detector 3
Subtraction Chromatogram : (None)

External Start : Start - Restart, Down
Range 1 : Bipolar, 2000 mAU, 10 Samp. per Sec.
Matching : No Change



Result chromatography Table (Uncal - F:\ sample 3 (salt)

No	Reten. Time [min]	Area [mAU.s]	Height [mAU]	Area [%]	Height [%]	W05 [min]	Compound Name
1	2.25	9852.14	430.55	55.00	55.00	0.25	
2	3.94	7845.98	401.23	45.00	45.00	0.20	
	Total	17698.92	831.78	100.00	100.00		

sample 3 after nano salt treatment

14/05/2024 03:20 pm Chromatogram F:\ sample 4 (salt) .PRM Page 1 of 1

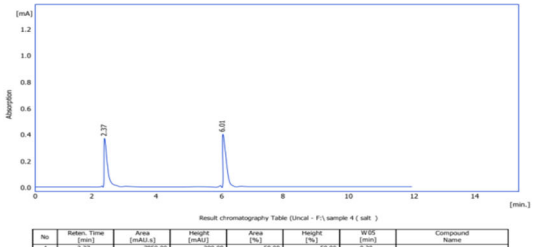
Chromatography Laboratory
HPLC

Sample Info:
Sample ID : sample 4 (salt)
Sample : sample 4 (salt)
Inj. Volume [mL] : 0.1

Amount 0
ISTD Amount 0
Dilution 1

Autostop : 20.00 min
Detector 1 : Detector 3
Subtraction Chromatogram : (None)

External Start : Start - Restart, Down
Range 1 : Bipolar, 2000 mAU, 10 Samp. per Sec.
Matching : No Change



Result chromatography Table (Uncal - F:\ sample 4 (salt)

No	Reten. Time [min]	Area [mAU.s]	Height [mAU]	Area [%]	Height [%]	W05 [min]	Compound Name
1	2.37	7859.90	399.08	50.00	50.00	0.20	
2	6.01	8215.65	400.15	50.00	50.00	0.20	
	Total	16075.55	799.23	100.00	100.00		

sample 4 after nano salt treatment

14/05/2024 03:20 pm Chromatogram F:\ sample 5 (salt) .PRM Page 1 of 1

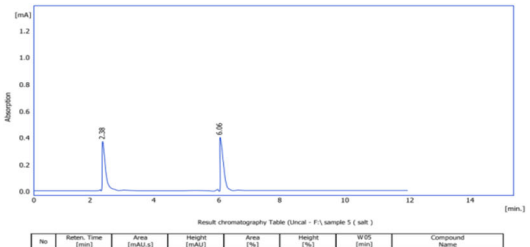
Chromatography Laboratory
HPLC

Sample Info:
Sample ID : sample 5 (salt)
Sample : sample 5 (salt)
Inj. Volume [mL] : 0.1

Amount 0
ISTD Amount 0
Dilution 1

Autostop : 20.00 min
Detector 1 : Detector 3
Subtraction Chromatogram : (None)

External Start : Start - Restart, Down
Range 1 : Bipolar, 2000 mAU, 10 Samp. per Sec.
Matching : No Change



Result chromatography Table (Uncal - F:\ sample 5 (salt)

No	Reten. Time [min]	Area [mAU.s]	Height [mAU]	Area [%]	Height [%]	W05 [min]	Compound Name
1	2.38	9541.08	393.22	50.00	50.00	0.20	
2	6.06	8521.49	400.41	50.00	50.00	0.20	
	Total	16062.71	793.63	100.00	100.00		

sample 5 after nano salt treatment

15/05/2024 03:20 pm Chromatogram F:\ sample 6 (salt) .PRM Page 1 of 1

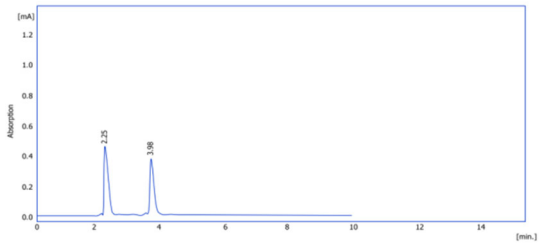
Chromatography Laboratory
HPLC

Sample Info:
Sample ID : sample 6 (salt)
Sample : sample 6 (salt)
Inj. Volume [mL] : 0.1

Amount 0
ISTD Amount 0
Dilution 1

Autostop : 20.00 min
Detector 1 : Detector 3
Subtraction Chromatogram : (None)

External Start : Start - Restart, Down
Range 1 : Bipolar, 2000 mAU, 10 Samp. per Sec.
Matching : No Change



Result chromatography Table (Uncal - F:\ sample 6 (salt)

No	Reten. Time [min]	Area [mAU.s]	Height [mAU]	Area [%]	Height [%]	W05 [min]	Compound Name
1	2.25	9856.08	433.00	55.00	55.00	0.25	
2	3.98	7412.65	401.45	45.00	45.00	0.20	
	Total	17268.98	834.45	100.00	100.00		

sample 6 after nano salt treatment

15/05/2024 03:20 pm Chromatogram F:\ sample 7 (salt) .PRM Page 1 of 1

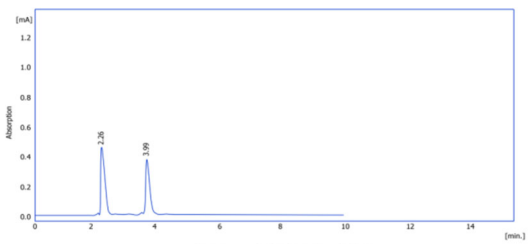
Chromatography Laboratory
HPLC

Sample Info:
Sample ID : sample 7 (salt)
Sample : sample 7 (salt)
Inj. Volume [mL] : 0.1

Amount 0
ISTD Amount 0
Dilution 1

Autostop : 20.00 min
Detector 1 : Detector 3
Subtraction Chromatogram : (None)

External Start : Start - Restart, Down
Range 1 : Bipolar, 2000 mAU, 10 Samp. per Sec.
Matching : No Change



Result chromatography Table (Uncal - F:\ sample 7 (salt)

No	Reten. Time [min]	Area [mAU.s]	Height [mAU]	Area [%]	Height [%]	W05 [min]	Compound Name
1	2.26	8547.00	431.50	55.00	55.00	0.25	
2	3.99	7841.14	403.11	45.00	45.00	0.20	
	Total	16388.49	834.61	100.00	100.00		

sample 7 after nano salt treatment

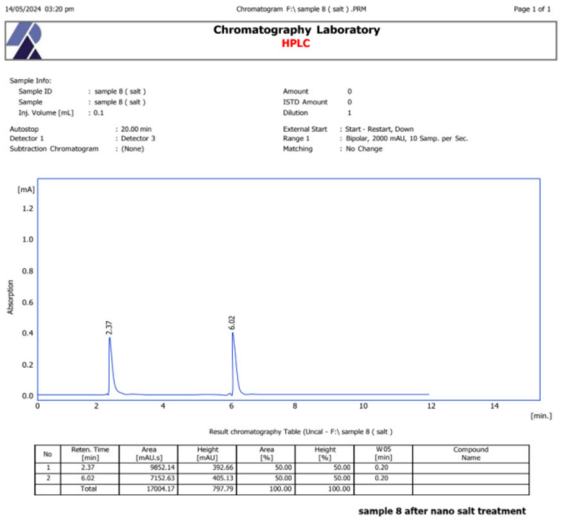


Figure S5. Chromatograms of deoxynivalenol and moniliformin after treatment of nano sea salt by HPLC chromatography analysis (sample 2) *F. pseudograminearum* strain 2, (sample 3) *F. pseudograminearum* strain 3, (sample 4) *F. oxysporum* strain 4, (sample 5) *F. oxysporum* strain 5, (sample 6) *F. pseudograminearum* strain 6, (sample 7) *F. pseudograminearum* strain 7, (sample 8) *F. chlamydosporum* strain 8.

CURRICULUM VITAE

PERSONAL INFORMATION

Name Surname:	Hussein Al-SAHHO
Nationality	Iraqi
Date and Place of Birth:	
Marital Status:	
E-mail:	

EDUCATION

Degree	Institution	Graduation Year
Master′s	Suleyman Demirel University Food Engineering Department	2020
Bachelor′s	College of Agricultural Engineering Sciences, University of Baghdad, Food Science and Biotechnology, Iraq	1999
High School	Al-Amiriya Secondary School, Baghdad, Iraq	1995

PROFESSIONAL EXPERIENCE

Years	Institution	Position
2001-2026	General Company for Grain Trade, Iraqi Ministry of Trade	Laboratory Supervisor

FOREIGN LANGUAGE

English, Arabic

Salman Alsahho, H. A., Horuz, S., & Karaman, K. (2025). Efficacy of *Dodonaea viscosa* extract and its chitosan-based nanoparticle formulation on the growth of *Fusarium* strains and the production of Deoxynivalenol and Moniliformin in stored wheat. Toxins, 17(11), 551.